UNIVERSITÀ DEGLI STUDI DI MILANO

PhD course in Environmental Sciences
XXXV cycle

Clinical Sciences and Community Health department,
and Environmental Sciences and Politics department

Epidemiological and functional approaches to evaluate the effects of Particulate Matter exposure in infants with viral bronchiolitis

Scientific disciplinary sector:

MED44 – Medicina del Lavoro

PhD candidate: Dr. **Marco Cafora**

Tutor:
Prof. **Valentina Bollati**

Head of the doctoral course:

Prof. Francesco Ficetola

Academic year 2021/2022

ABSTRACT

According to the World Health Organization (WHO), environmental air pollution is currently among the leading causes of death and disease globally. Particulate matter (PM) exposure has been linked to the exacerbation of acute respiratory diseases, especially in the most susceptible population's subgroups, such as infants and chil\dren. Acute bronchiolitis, a common clinical condition characterized by inflammation and obstruction of bronchioles, is generally caused by a viral infection of the lower airways and is estimated to be the leading cause of hospitalization of infants worldwide. At present, the severity of the disease is only partially explained by current known predisposing risk factors but recent evidence suggests that short-term exposure to PM causing airway inflammation, might result in increased susceptibility to viral infections and bronchiolitis severity.

Due to its anatomical location, the upper respiratory tract (URT) is persistently exposed to PM, which affects the airway microbiome: recent evidence has linked the effects of PM_{10} and $PM_{2.5}$ to microbiota structure and composition. In this context, innate immunity plays a fundamental role in the first response to both exogenous agents and commensal/pathobionts components of microbiota. In particular, bacterial-derived Extracellular vesicles (bEVs) are emerging as essential interregnum messengers that could play a crucial role in communication with mammalian cells, by modulating the host immune system.

The main aim of the work is to investigate how PM exposure might modulate the relation that occurs between the severity of acute bronchiolitis, the respiratory microbiota, and the host immune response mediated by bEVs. First, we showed that the exposure to $PM_{2.5}$ from the Milan metropolitan area impaired the innate immunity response following an acute infectious stimulus in a zebrafish (*Danio* rerio) embryo model. In particular, PM induced a pro-inflammatory effect, which leads to a dampened leukocytic response to a subsequent inflammatory stimulus. In the second part of the thesis, we investigated the relationship between short-term exposure to PM ($PM_{2.5}$ and PM_{10}) and the severity of viral bronchiolitis through a population study involving infants with bronchiolitis (with and without Respiratory Syncytial Virus, RSV, infection) aged less than one year living in the area of Milan. A positive association was observed between the severity of the disease and $PM_{2.5}$ and PM_{10} exposure levels in the third week before the bronchiolitis peak. Moreover, we performed a metataxonomic analysis, comparing the composition of the bacterial portion of the nasal

microbiome (bNM) of infants with bronchiolitis and matched it to healthy controls, to unveil a plausible interplay of the URT microbiota in this framework. We observed a respiratory dysbiosis in bNM of infants with bronchiolitis. Furthermore, *Haemophilus influenzae* (*Hi*) was predicted as the most represented species and also positively modulated by PM exposure during bronchiolitis. Last, the immunomodulatory potential of *Hi*-deriving bEVs was investigated using the zebrafish embryo. With this model, we showed that *Hi*-bEVs promote a pro-inflammatory response by altering leukocyte trafficking in particular in the neutrophil population.

Overall, our data support the role of PM exposure in influencing the interplay between respiratory viruses, such as RSV, and specific microbiota components of the URT, such as *Hi,* in modulating the host immune response, potentially determining the pathogenesis and severity of acute bronchiolitis.

INTRODUCTION

-State of the art

1. Air pollution and Particulate matter (PM)

Air pollution is the contamination of the environment by any chemical, physical or biological agent that modifies the natural characteristics of the atmosphere, as defined by the World Health Organization (WHO, www.who.int/health-topics/air-pollution#tab=tab_1). Air pollution is the leading environmental risk factor to health globally. Currently, the joint effects of household and ambient air pollution are estimated to cause around 7 million deaths, mainly from noncommunicable diseases, and millions of lost years of healthy life annually (WHO, 2021 [1]). Air pollutants are usually classified according to their physical state, as well as they can also be distinguished between air pollutants in indoor and outdoor environments, as shown in **Table 1**.

Table 1. *Classification of air pollutants by physical state and environment (adapted from Bernstein et al., 2004)* [2].

Physical state	Gaseous/ vapours	Carbon oxides (CO, CO_2), nitrogen oxides (NO_x), sulphur dioxides (SO_2), ozone (O_3), semi-volatile and volatile organic compounds (SVOC and VOC, aldehydes, alcohols, benzene, polycyclic aromatic hydrocarbons (PAHs) etc.)
	Particulate	Particulate matter (aerodynamic diameter ≤10 μm, PM10), coarse particulate (<10μm and >2,5 μm, PM10-2.5), PM fine (≤2,5 μm, PM2.5), PM ultrafine (≤0,1 μm, PM0.1, UFP).
Environment	Indoor	CO, CO2, radon, biologic agents, SVOC
	Outdoor	Particulate matter, SO_2, ozone, NO_x, CO, PM, SVOC

Exposure to air pollutants is heavily dependent on their ambient concentration and in particular atmospheric particulate matter (PM) concentrations vary consistently both between and within regions across the world. According to the WHO, by reducing air pollution levels, countries can reduce the burden of different kinds of diseases, in particular chronic and acute respiratory diseases. Nevertheless, in 2019 it is estimated that more than 90% of the global population lived in areas in which the concentration levels of PM surpassed the air quality guideline thresholds established by the 2005 WHO guidelines. This situation is particularly problematic in northern Italy which is depicted in the European framework as one of the most polluted areas (**Figure 1**):

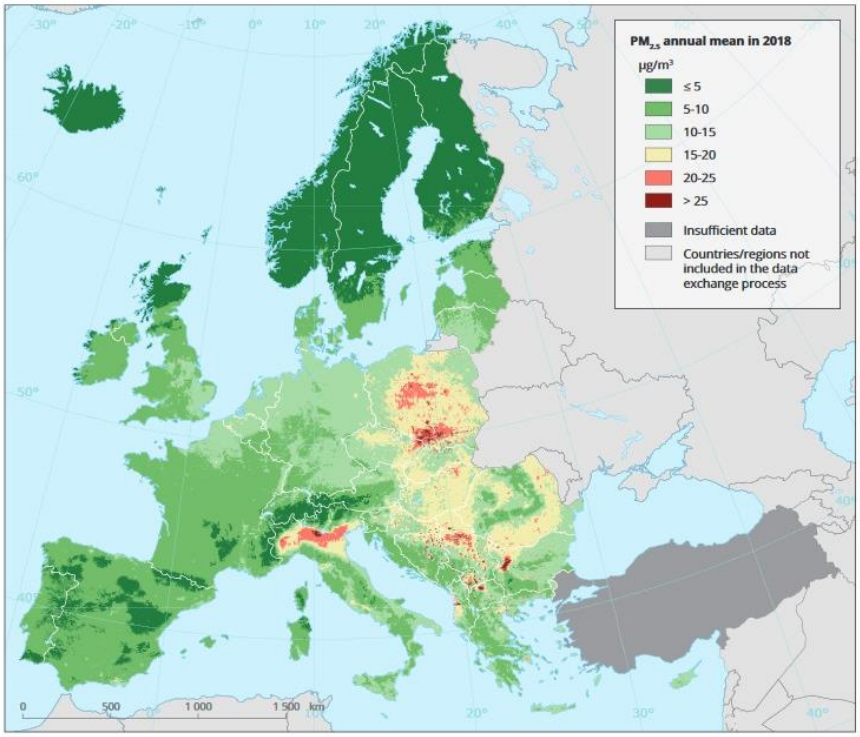

***Figure 1**. Average concentration of $PM_{2.5}$ in Europe for 2018. Annual mean µg/m^3 (EEA, 2020* [3]*)*

In **table 2** are reported the recommended standards levels of air quality for the main air pollutants, as suggested by the European environment agency (EEA) and WHO.

***Table 2.** Standards for Air quality in EU and WHO 2021 guideline thresholds.*

	EU	WHO
NO_2	200 µg/m³ (1h mean, 18 times/year) 40 µg/m³ (annual mean)	25 µg/m³ (1-day mean) 10 µg/m³ (annual mean)
PM_{10}	50 µg/m³ (1-day mean, 35 days/year)	45 µg/ m³ (1-day mean) 15 µg/m³ (annual mean)
$PM_{2.5}$	25 µg/m³ (annual mean)	15 µg/m3 (1-day mean) 5 µg/m3 (annual mean)
SO_2	350 µg/m³ (1h mean, 24 days/year)	40 µg/ m³ (1-day mean)
O_3	120 µg/m³ (8h mean, 25 days/year)	100 µg/ m³ (daily 8h mean)
CO	10 mg/m³ (daily 8h mean)	4 mg/ m³ (1-day mean)

Among the others, over the past few decades, PM, especially its fine fraction known as $PM_{2.5}$, has emerged as a significant contributor to atmospheric pollution, by causing a wide range of harmful effects, including those on human health. PM is a combination of solid pollutants and liquid droplets that occur naturally or due to anthropogenic activity and can be observed at various dimensions

ranging from nanoscale to a maximum of 100 µm. A major source of PM is related to anthropogenic processes. In general, diesel usage, industrial activity, and road and agricultural-derived dust are considered among the main sources of PM [4–6]. In addition, natural phenomena must also be considered, especially in Italy where wildfires (both natural and human-caused) are frequent in the summer season [7] and where dust from the Saharan-Sahelian region is carried by winds [8]. In regions where the combustion of fossil fuels and biomasses is prevalent, the fine fraction of PM tends to be predominant. Overall, PM is defined as a complex mixture comprising chemical and biological elements, such as heavy metals, carbonaceous materials, aromatic hydrocarbons, and volatile compounds [9].

Among all of the pollutants, exposure to PM_{10} and $PM_{2.5}$ (with a diameter less than or equal to 10 and 2.5 µm, respectively) is the primary cause of premature mortality and increase morbidity, particularly related to cardiovascular [10,11] and respiratory diseases [12–14]. For these latter, an example is reported by the study of Burnett and colleagues which analyzed data from 41 cohort studies, showing an association between $PM_{2.5}$ exposure and respiratory diseases (**Figure 2**).

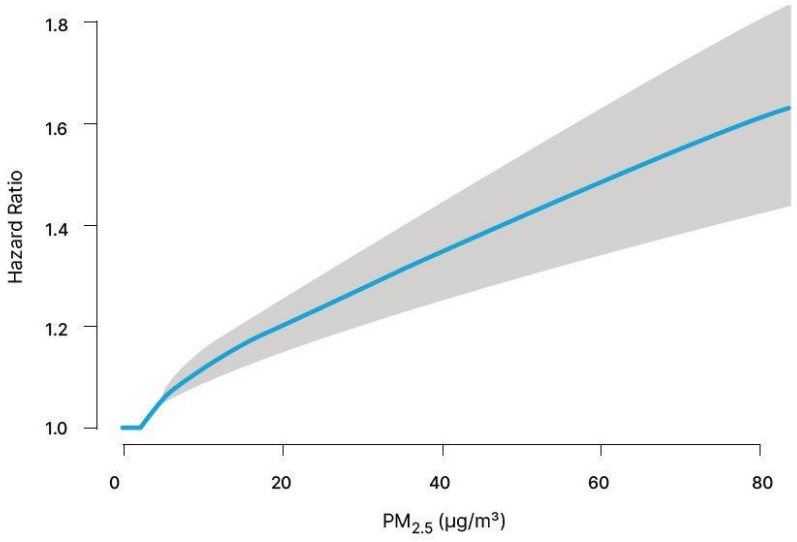

Figure 2. *Association between mean $PM_{2.5}$ exposure (µg/m^3) and mortality from noncommunicable diseases and lower respiratory illness. Data derived from an analysis of 41 cohort studies* [14].

Exposure to $PM_{2.5}$ can determine a short-term impact on health. There is a broader consensus that breathing this type of pollutant increases the risk of contracting and/or exacerbating acute respiratory diseases, particularly in the most susceptible subgroups of the population as infants and children [15,16]. Indeed, PM particles can access different locations within the respiratory system

based on their size. While PM_{10} particles can reach only the upper airways, conversely finer particles ($\leq PM_{2.5}$) can enter the terminal bronchioles and alveoli, triggering an immune response, and PM_1 are moreover sufficiently small to penetrate the bloodstream [5,17] (**Figure 3**).

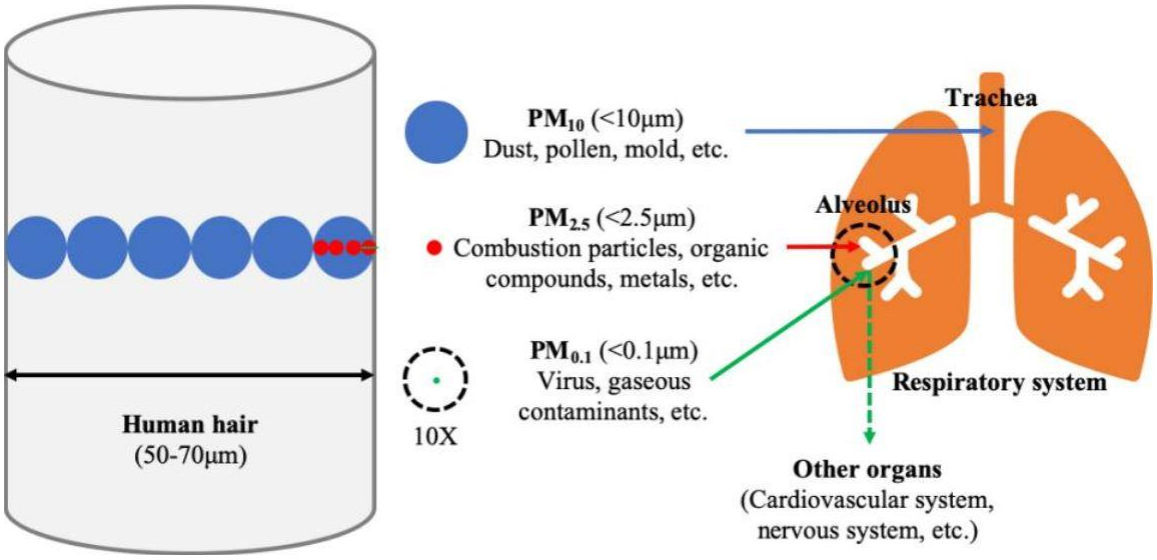

***Figure 3**. Size, primary composition, and deposition location of PM. PM_{10} is mainly deposited on the upper airways, until the trachea. PM less than 2.5 μm in diameter can get deep into the terminal bronchioles and alveoli, and some with a diameter less than 0.1 μm can potentially enter the bloodstream, leading to systemic effects on other organs. (Adapted from Yang et al. 2020* [5]*)*

PM can damage the respiratory system by reducing airway epithelial defense and by altering the host's immune response [18,19]. Indeed, among the other components of PM, some of the organic compounds, such as plant pollen, microorganisms, mold, spores, and microbial components (e.g., lipopolysaccharides (LPS)), confer an inflammatory potential [20–22]. How $PM_{2.5}$ exposure can shape the inflammatory status in acute respiratory diseases represent a poorly understood topic, as well as its influence on the response to the occurrence of a respiratory infectious agent (e.g. bacterial or viral infections). Some studies in the last decade have focused on elucidating the potential role of PM in this framework, in particular on children's diseases [9]. Evidence from different studies on large population cohorts of infants and children indicated that PM exposure triggers a potent systemic inflammatory reaction, leading to higher hospitalization rates due to higher susceptibility to pulmonary conditions like influenza [23] and pneumonia [24] as well as for viral bronchiolitis in infants, for which associations have been reported [16,25]. Several *in vitro* and

in vivo studies pointed out that exposure to $PM_{2.5}$ and PM_{10} is capable to induce high levels of pro-inflammatory markers such as IL-1β, IL-6, cxcl-8, MIP-1α/β, TNF-α, and Cox-2 [19,26–28], as well as it resulted potent activator of inflammasome complex [9,29,30]. Also, lung's immune response is affected by PM, leading to oxidative stress and systemic inflammation [31,32]. This effect is mainly due to reactive oxygen species (ROS) overproduction, that in turn, through the activation of Toll-like receptors (TLRs) (especially TLR4), can result in cellular and tissue damage [33,34] (**Figure 4**). Consistently, PM exposure could lead to airway inflammation [9,35]. Alveolar macrophages (AM) play an important role in response to PM trigger, aiding in clearing inhaled particles. *In vivo* and *in vitro* studies have shown that $PM_{2.5}$ can interfere with AM physiological functions, by impairing phagocytic capacity and in some cases inducing M2 profile [36,37]. Moreover, PM can alter the function of other critical immune cells as neutrophils [38]. Overall, this scenario promotes a strong recruitment of leukocytes to the airways with impaired functionality (e.g. altered phagocytic ability) [27,39], thus resulting in an increased susceptibility to bacterial and viral infections due to a dampened immune response, especially in infants [18,40]. Consistently, it has been reported that PM exposure is associated to an increased rate of bacterial/viral replication and with more severe infection of respiratory tract [41,42]. Among them, an increased susceptibility was described also for respiratory syncytial virus (RSV) in infants [43,44], and confirmed by *in vivo* studies on mice [45], thus implying that there might exist potential synergistic effects between PM exposure and respiratory viral infections that may exacerbate inflammation. However, the precise mechanisms underlying the pathophysiology due to PM exposure on acute lung inflammation are yet to be clearly understood.

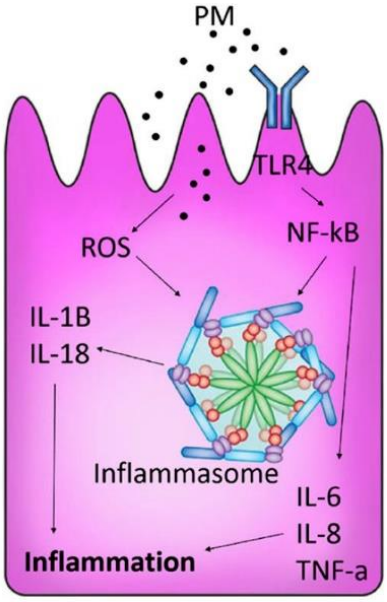

Figure 4. *Overview of inflammatory effects elicited by PM in the respiratory system. Adapted from Arias et al., 2020* [9].

2. Zebrafish (*Danio rerio)* as a model to study the innate immunity

Zebrafish (*Danio rerio*) is a small freshwater teleost fish originally from South Asia and belonging to the *Cyprinidae* family. Over the last decades, it has emerged as a powerful and versatile model system for studying a multitude of processes in biomedical research. Among them, the function of innate immune cells and pathways can be studied in isolation in larval stage zebrafish, since the lack of an adaptive immune response until 3-4 weeks after fertilization (**Figure 5**) [46]. Zebrafish represents an ideal model for studying different aspects of innate immunity since its immune system remarkably resembles that of mammals [47]. Indeed, the inflammation response occurs similarly to mammals, with a conserved population of immune cells [48]. In addition, pro and anti-inflammatory cytokines are evolutionary conserved between human and zebrafish, thus providing an excellent system for modeling various molecular and cellular elements of inflammation such as pathogen effects during infections and immune cell migration to inflamed or wound sites [49–51].

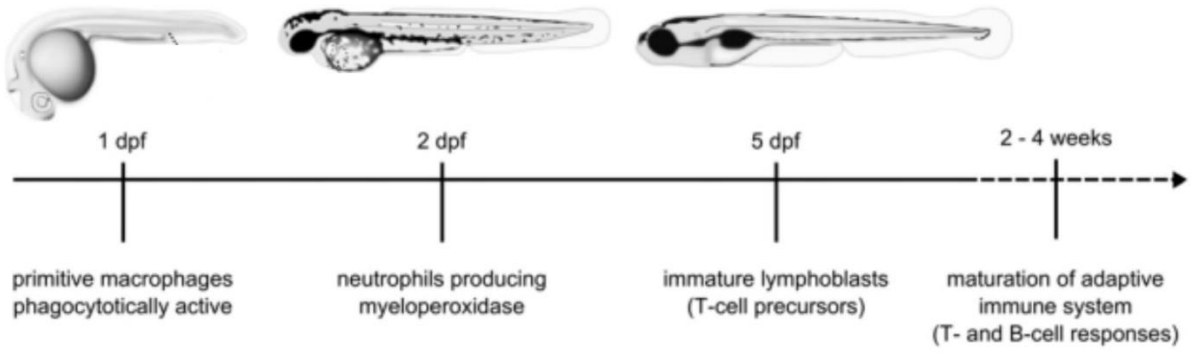

Figure 5*. Overview of the development of the immune system in zebrafish. Dpf: days post fertilization (Modified from Mejer et al., 2011* [52]*).*

Neutrophils and macrophages are the most important cell types of the innate immune system, and their primary function is to activate a response to exogenous stimuli, such as pathogens or environmental elements. Both zebrafish neutrophils [53] and macrophages [54] are similar to their mammals' equivalents. Functional leukocytes are already present in embryos by 30 hours post fertilization (hpf) [55,56]. Zebrafish macrophages can carry out phagocytosis, express pro-inflammatory genes and undergo polarization, as well as form granulomas [57,58]. While neutrophils have conserved motility mechanisms and are capable of phagocytosis and of generating

neutrophil extracellular traps (NETs) and reactive oxygen species (ROS) [55,59–61]. To study the behavior of these cell populations, it is largely diffuse the use of well-established reporters that utilize cell-specific promoters: macrophages are commonly marked by the *mpeg1.1* gene [62], while the neutrophil population is typically marked by *myeloperoxidase* (*mpx*) gene [63], one of the principal enzymes expressed by these cells upon activation [64]. At last, the optical transparency of zebrafish embryo and larva allow for monitoring *in vivo* leukocyte response to exogenous stimuli (**Figure 6**).

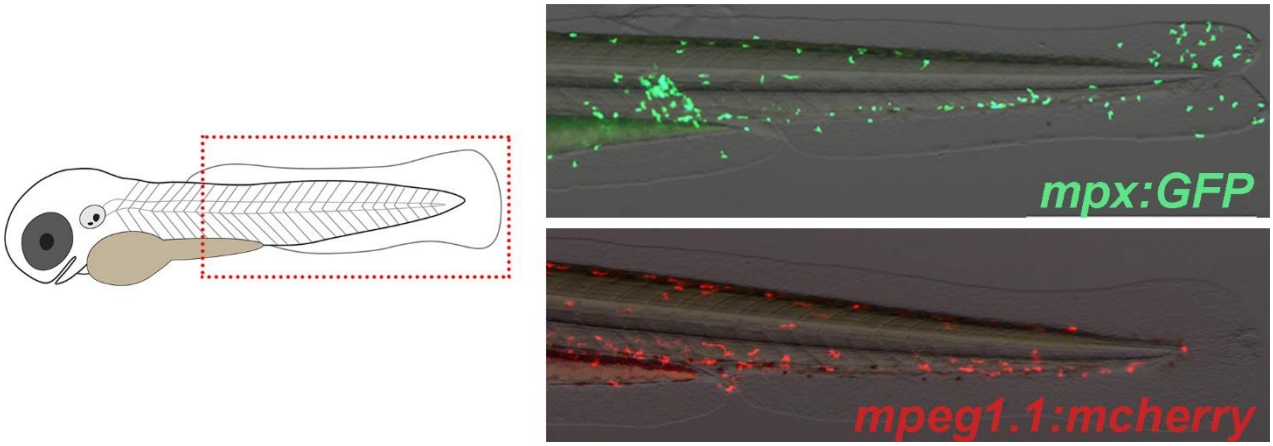

Figure 6. *Zebrafish transgenic lines, specific reporter for neutrophil (mpx:GFP) and for macrophage (mpeg1.1:mcherry) cell populations. Caudal region of 3 dpf larvae is shown.*

Zebrafish model for toxicological studies

In this framework, zebrafish has emerged as a powerful animal model for environmental and toxicological studies [65–67]. Compared to higher vertebrates, zebrafish at the embryonic or larval stage offers numerous advantages as an intermediate model. The most emphasized feature of embryos is their relatively small size (around 4 millimeters at the embryonic stage) that together with the ability to produce hundreds of offspring every week and their optical transparency, make the zebrafish a reliable model for routine toxicity screening. Moreover, due to the chemical permeability of its skin, small molecules and particles, such as liposomes or nanoparticles, are well absorbed throughout the embryo and therefore the effects can be studied by simply adding them to the larval medium (i.e. by immersion assay) [68–70]. Alternatively, it is possible to investigate the effects by directly microinjecting the element of interest (e.g., suspension of pollutants) into different sites of the embryos, thus evaluating the immune response elicited (**Figure 7**).

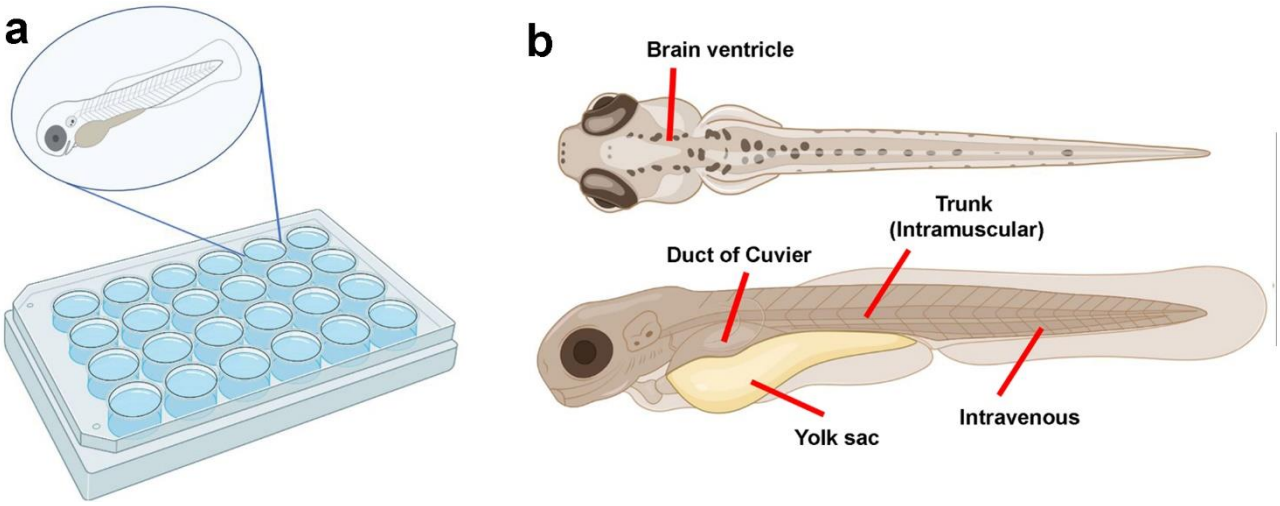

Figure 7. *Different ways to perform a toxicity assay on zebrafish. (a) Immersion assay, to directly expose embryo/larvae to the component under study (e.g. pollutants suspension); (b) Schematic representation of the different routes of microinjection in zebrafish larva (dorsal and lateral view); local injection in brain ventricle, intramuscular or into the yolk sac and systemic injection in the duct of Cuvier or intravenous (into the blood circulation).*

Zebrafish embryo has been widely used to evaluate the toxicity of nanoparticles and environmental pollutants [69,71], with the benefit of reducing time and costs of the mammalian models, and in accordance with the 3Rs principle [72]. Recently, it emerged as a model to study the effects of air pollutants and in particular of PM. As reviewed by Smoot *et al.,* only in the last years (i.e., from 2015) some studies concerning investigations of the harmful effects of PM exposure using zebrafish as an alternative model have been published [71]. In almost all of them, the effects of PM derived from different sources (e.g., urban/rural areas, diesel exhaust) were assessed by immersion assay, in which embryos/larvae were exposed to PM directly in the growth medium. Most of the studies are based on the investigation of large-scale effects on multi-organs or developmental toxicity caused by PM exposure [66,73,74]. Few studies have analyzed the inflammatory effects of PM. For example, PM_{10} collected in Shandong (China) has been shown to induce an increase in ROS production and to elicit endoplasmic reticulum stress in embryos expose at an early stage [75]. In another work, authors have pointed out that urban $PM_{2.5}$ (from Jinan area, China) exposure impaired embryo locomotion and caused developmental toxicity due to alterations in inflammation and autophagy pathways [76]. Moreover, exposure to hydrophobic components of PM, such as polycyclic aromatic hydrocarbons (PAH) has been shown to trigger inflammatory responses when absorbed in zebrafish

embryos [77]. However, no studies have directly investigated the effects on innate immunity and the functional mechanisms underlying the toxic outcomes of PM.

3. RSV bronchiolitis in infants

Acute bronchiolitis is a common condition that is diagnosed based on clinical symptoms, and it is identified by the presence of wheezing illness along with an upper respiratory tract infection. Usually, the disease begins with symptoms of coryza and a mild fever but then develops into coughing, tachypnea, hyperinflation, retractions in the chest wall between the ribs, grunting, and flaring of the nostrils [78]. Acute bronchiolitis is characterized by inflammation and edema of the airways, that together with an increased mucus production and necrosis of the airway epithelial cells, lead to obstruction of the bronchioles [79]. This syndrome affects mainly infants younger than 12 months of age, due to the small size of their lower respiratory tract (i.e., bronchioles) (**Figure 8**).

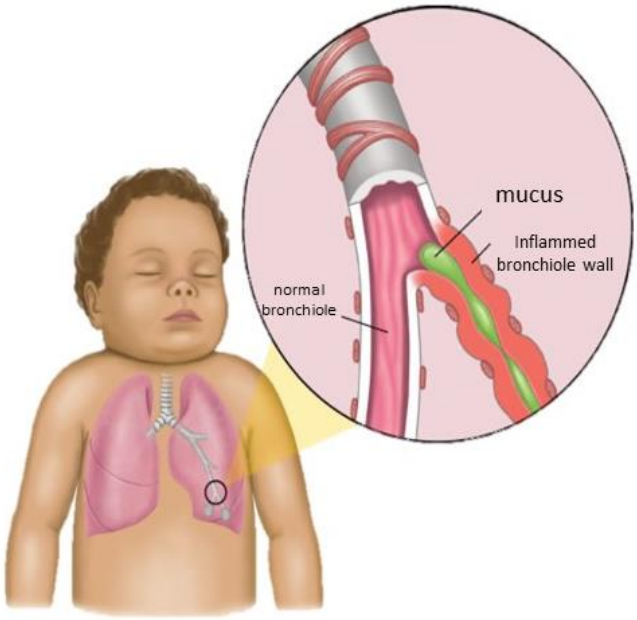

***Figure 8**. Bronchiolitis in infants is typically characterized by inflammation of bronchioles and mucus hyperproduction, with the consequent obstruction of the airways.*

In the vast majority of cases, the respiratory disease is caused by a viral infection of the lower airways, and respiratory syncytial virus (RSV) is the most prevalent viral agent for bronchiolitis in infants, causing about 70% of the cases (estimates are variable between 40 and 80% of incidence, depending on the region) [80–82]. However, other viral agents are associated with bronchiolitis, including rhinovirus, influenza, and parainfluenza viruses, as well as metapneumovirus, human bocavirus, and adenovirus [80,83,84]. Among infants, it is one of the most prevalent respiratory

tract diseases globally. Bronchiolitis is defined by a seasonal infection, typically starting in the latter part of October in the temperate northern hemisphere, reaching its highest incidence in January/ February, and concluding in April [85]. To date, the fundament of bronchiolitis treatment remains supportive care, with infants presenting moderate to severe respiratory distress often hospitalized (about 1% to 3% of total cases). The clinical approach to this common life-threatening condition exhibits significant variability, ranging from anti-inflammatory (e.g., corticosteroids) and antiviral therapies to respiratory support with high-flow oxygen systems and antibiotics treatments (for the concerns of bacterial superinfection) [79,80].

Focusing on RSV, the most common infecting agent involved in bronchiolitis, is a single-stranded RNA virus of the *Paramyxoviridae* family [86]. The attachment of the virus to the host cell and subsequent fusion with the cell involves two specific glycoproteins known as G (large glycoprotein) and F (fusion glycoprotein) [87]. The mechanism through which the virus binds to epithelial cells is not clear. Toll-like-receptor-4 (TLR-4) [79,88] and Annexin II [86] are two potential receptors for G and F glycoproteins. After entering, it replicates within the cells, causing both direct ciliary destruction and epithelial necrosis [79,89]. The cell destruction triggers a strong inflammatory response (mainly through TLRs and retinoic acid-inducible gene (RIG)-I signaling) with the activation of lymphocytes and polymorphonuclear leukocytes (PMNs). Moreover, neutrophil infiltration occurs and leads to edematous tissue with an increased mucus secretion, resulting in bronchiolar obstruction [86,89] (**Figure 9**).

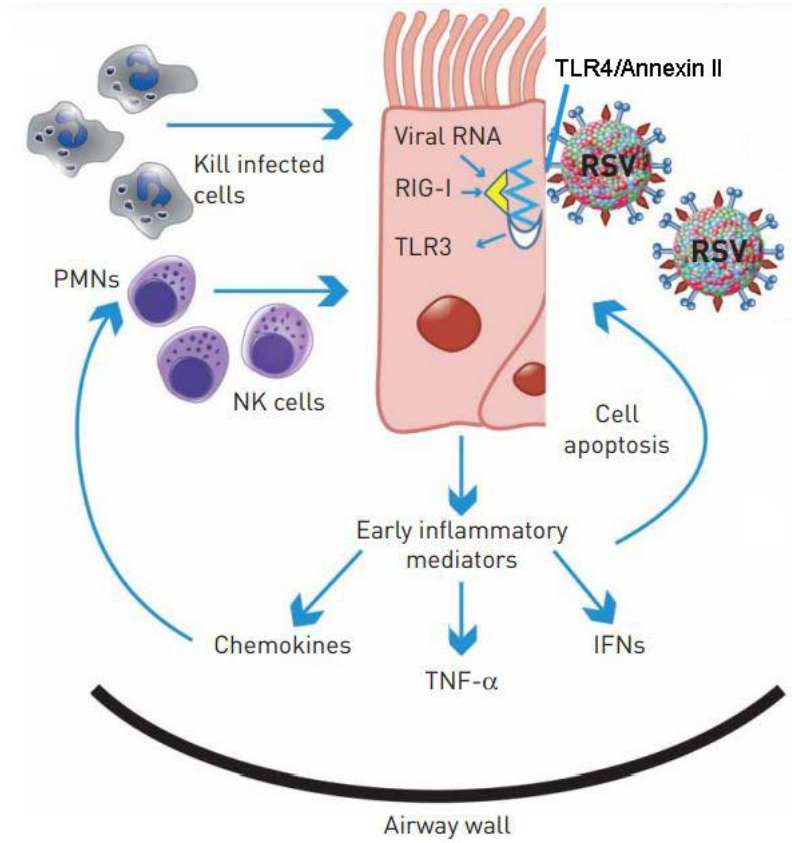

Figure 9*. Host's response to respiratory syncytial virus (RSV) infection. During viral replication, arising viral RNA, is recognized through Toll-like receptor 3 (TLR-3) and retinoic acid-inducible gene (RIG)-I-like receptors. The cellular infection induces the secretion of early inflammatory mediators, such as interferons (IFNs) and TNF-α, as well as chemokines like IL-8. Type I interferons induce an increase in pro-apoptotic elements within epithelial cells, whereas TNF-α and chemokines promote the recruitment of natural killer (NK) cells and polymorphonuclear leukocytes (PMNs) that possess the capability to eliminate infected cells, thus limiting the viral replication and spread to neighboring cells in the beginning of infection. Modified from Rossi et al. 2015* [86].

Some risk factors have been diffusely recognized for viral acute bronchiolitis, such as premature birth, young age, and pre-existing pulmonary diseases [90,91]. However, most cases of illness occur without any prior predisposing risk factors in infants [80]. Some evidence suggests that environmental factors such as air pollution (e.g., PM) are related to the worsening of respiratory diseases in young children [13,92]. In addition, studies reported that exposure to PM might influence the inflammatory cascade that brings to RSV infection, disease development, and exacerbation in infants [25,93]. *In vivo* and *in vitro* studies found associations between exposure to PM and accelerated viral replication and more severe infections of the respiratory tract, essentially sustaining an increased susceptibility to RSV infection upon PM exposure, which in principle alter

the host's inflammatory response [9,43,45]. Several retrospective studies on large cohorts of infants were carried out investigating a link between PM exposure and the risk of hospitalization and exacerbation due to viral bronchiolitis, but with inconsistent results [25,94–99]. Therefore, a full understanding of the role of air pollution (especially of the PM component) in disease onset and exacerbation is still lacking.

4. The nasal and upper respiratory tract (URT) microbiota

The respiratory system is a complex organ system, which can be categorized into two distinct sections: the upper respiratory tract (URT) and the lower respiratory tract (LRT). In particular, the URT comprises the anterior nostrils, nasal cavity, paranasal sinuses, nasopharynx, and oropharynx. The entire surface of the respiratory system is inhabited by niche-specific bacterial communities and the URT is where the highest bacterial densities are typically found [100] (**Figure 10**).

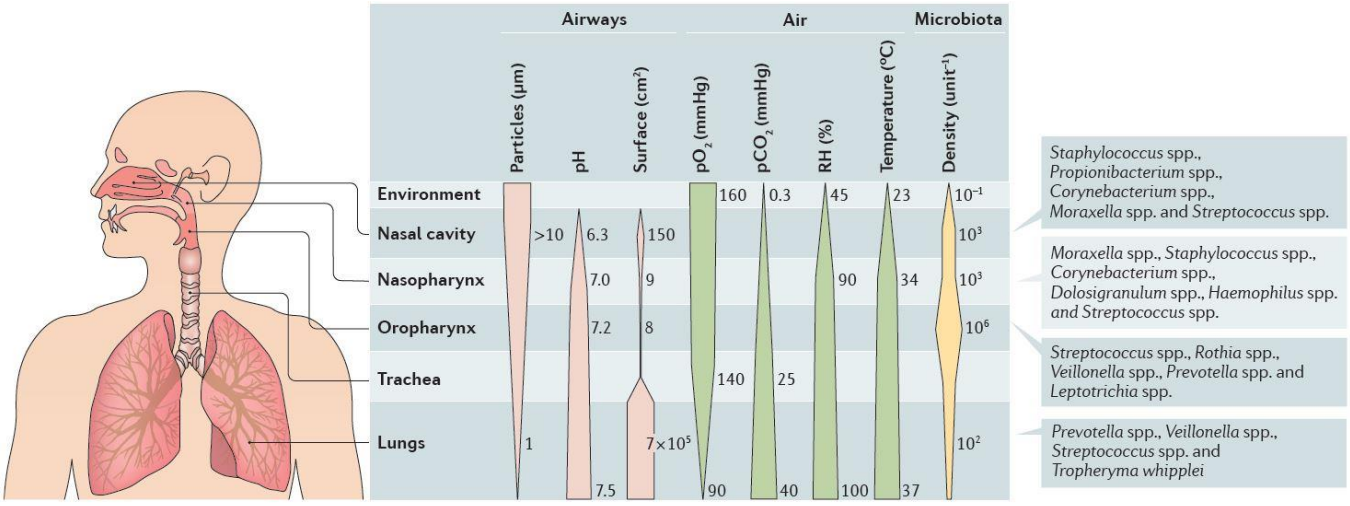

Figure 10. *Particles deposition and physiological and microbial gradients along the respiratory tract. Inhaled particles of diameter ≥ 10 µm are deposited in the URT, whereas particles with diameter < than 1 µm can reach the lungs. The indicated physiological parameters define the selective growth conditions that are optimal for the different bacterial niches, ultimately shaping the microbial communities throughout the respiratory tract. Adapted from Wing Ho et al., 2017* [100].

The overall microbiota of the URT and in particular the bacterial nasal microbiota (bNM) can play a significant role in various physiological and pathological processes. Associations have been demonstrated between the composition of the microbiota and the onset and progression of such conditions [100]. bNM is typically composed of both resident and transient microorganisms and is characterized by the presence of commensal microbes and pathobionts that constitute

Actinobacteria, Firmicutes, and Proteobacteria as the most represented phyla [101]. Several studies have dedicated their efforts to identifying the composition of the bNM, establishing that it is largely composed of *Corynebacterium spp., Moraxella spp., Dolosigranulum spp., Cutibacterium spp., Streptococcus spp., Staphylococcus spp*. Genera [100,102]. However, the composition of bNM is plastic and can vary over stages of life [101] (**Figure 11**).

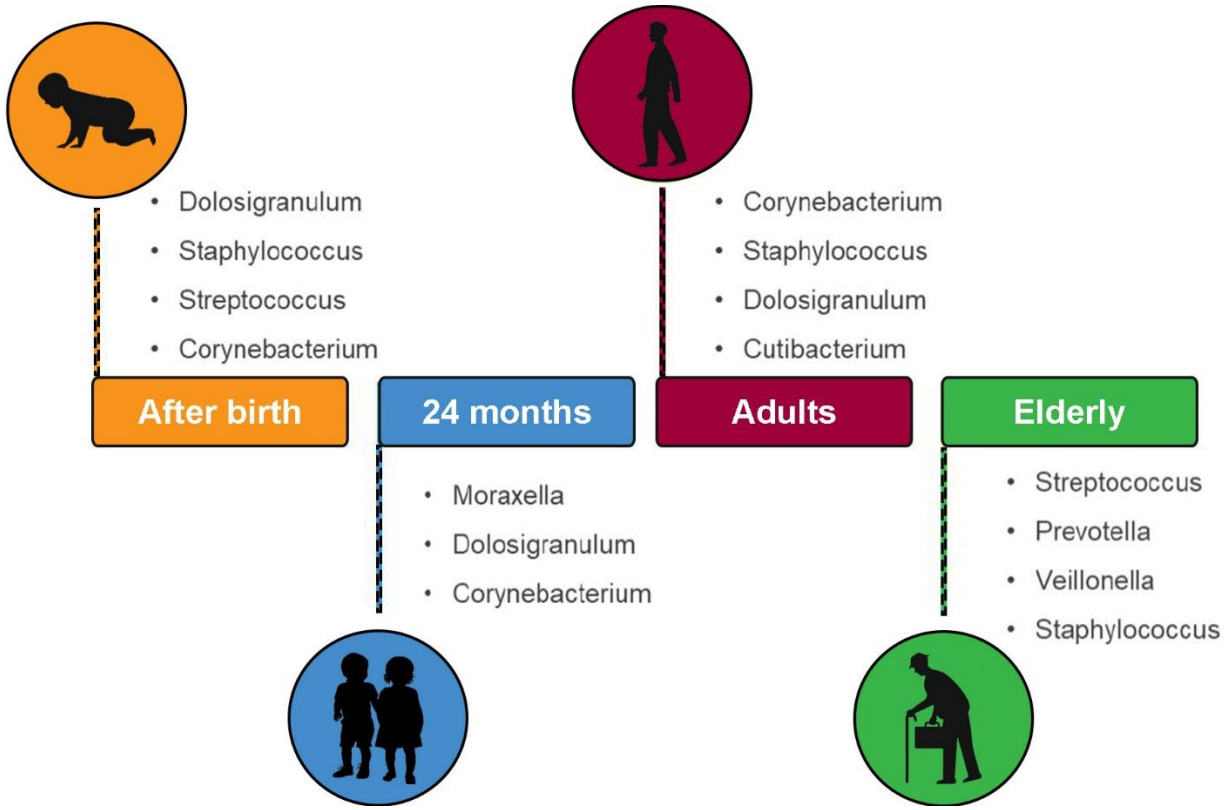

Figure 11. *Composition of bacterial nasal microbiota (bNM) at the different life-stages, from infancy to old age. Bacterial genera given in the figure were found during the specified time points or intervals of life stages by molecular methods (16S rRNA sequencing). Based on references in Kumpitsch et al., 2019.* [101]

Examining bNM of infants, studies have shown a transition in its composition during the first two years of life. Specifically, the microbiota shifts from a community that is more similar to the maternal skin or vaginal microbiota to one that is dominated by the *Dolosigranulum*, *Moraxella*, and *Corynebacterium* genera [101,103]. Generally, the bacterial communities belonging to other URT niches such as *Moraxella spp. and Streptococcus spp.,* are frequently detected and recognized within the bNM community [100,104]. Similar to the other URT residential communities, the main function of bNM consists in enhancing the resistance against the colonization of pathogens, through competitive exclusion activity [100,103,105]. Studies have documented that the *Corynebacterium spp*. and *Dolosigranulum spp*. are capable of regulating the growth rate of common respiratory

pathobionts such as *S. pneumoniae, H. influenzae, and S. aureus* in URT, especially among younger individuals [106], thus maintaining a fragile balance between commensal and pathobiont bacteria inhabiting the respiratory mucosa. However, if any changes in the functional or compositional settlement of the bacterial membership occur, the functions that are provided to the host may be affected or even disrupted. This can result in a state of dysbiosis, which is often associated with various pathological conditions [100,101]. In turn, dysbiosis in the residential communities can be linked to infections of the URT, due to the loss of the beneficial and commensal part of the community [101,107,108]. The URT is persistently exposed to chemical and biological particulates, that can shape its environment and leads to dysbiosis [103]. Due to its anatomical location, the nasal cavity is the first structure interacting with exogenous elements and air pollutants such as PM, which can elicit a host immune response and activate nasal epithelium [101]. Both coarse and fine PM can penetrate and deposit in anterior nasal passages, thus interacting with bNM [100]. To date, the relation between bNM and PM exposure has been poorly investigated, however, some recent evidence has linked the effects of PM_{10} and $PM_{2.5}$ to bNM structure and composition, both in healthy adults and subjects with allergic rhinitis, showing a positive association in particular with *Moraxella* taxa [102,109].

5. Immunomodulatory properties of Extracellular vesicles of Gram-negative bacteria

Extracellular vesicles (EVs) are microscopic membranous structures secreted by most types of both eukaryotic and prokaryotic cells. They have emerged as essential intercellular messengers, implicated moreover in interregnum communication, and can modulate the host's immune system [110–112]. Both Gram-negative and Gram-positive bacteria produce EVs ranging from 10 to 300 nm in diameter [113], that are involved in different key functions, including bacterial biofilm formation and quorum sensing [114,115]. In particular, Gram-negative bacteria-derived EVs originate from controlled blebbing of the outer membrane, for this reason, called outer membrane vesicles (OMVs) [116]. Therefore, they are enriched of outer-membrane proteins, as well as lipopolysaccharide (LPS), have specific lipid compositions and the cargo molecules can vary in both quantity and composition, depending on the growing conditions [117–120]. In general, they can transport periplasmatic and cytosolic proteins, nucleic acids (both DNA and RNA), and virulence factors [116,121–123]. Furthermore, OMVs have been detected in human nasal samples during the occurrence of infections, thus highlighting their possible significance in the pathogenesis and development of

infective diseases [124,125]. Given that OMVs transport virulence factors and can play a role in pathogenesis, it is reasonable to expect that host cells have evolved mechanisms to trigger an immune response when they meet OMVs. In particular, innate immunity plays a key role in response to OMVs, and neutrophil and macrophage cell populations are the main players involved (**Figure 12**).

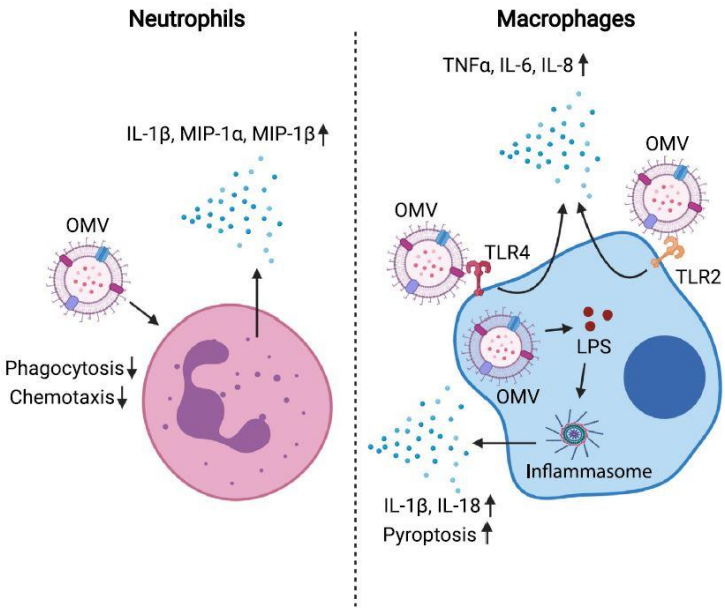

Figure 12. *Innate immunity response elicited on leukocytes by outer membrane vesicles (OMVs). OMVs comprise some danger-associated molecular patterns (DAMPs) which are like those of their parent bacteria, including outer membrane proteins, LPS, and DNA. DAMPs are recognized by host-pathogen recognition receptors (PRRs) on the membrane, such as the TLR-2 and TLR-4, which rise a downstream immune response by activating NF-κB signaling, thus leading to the production of pro-inflammatory agents. Modified from Tiku et al.,2021* [125].

Typically, neutrophils are the initial responders to an infection site and their significant impact on OMV challenge has been recently demonstrated through *in vitro* and *in vivo* studies. When stimulated *in vitro* with OMVs derived from *N. meningitidis,* human neutrophils were induced in the production of pro-inflammatory cytokines including TNFα, IL-1β, and macrophage inflammatory protein (MIP)-α and -β, as well as chemokines [126]. In addition, the injection of *E. coli* OMVs into mice's peritoneal cavity resulted in the production of CXCL1/IL-8 by endothelial cells, which then recruited neutrophils, thus reinforcing the proinflammatory consequences on neutrophils upon exposure to OMVs [127]. Nevertheless, further investigations are needed to assess whether neutrophils are capable to engulf and clearing OMVs as well as to determine whether bacteria employ virulence factors, that are released via OMVs, to interact with neutrophils and modulate the immune response.

OMVs can also affect macrophage response by binding to their cell surface pattern recognition receptors (PRRs). For instance, *in vitro* treatment of THP1 human macrophages with OMVs isolated from *Legionella pneumophila,* induced a strong pro-inflammatory response driven by TLR2 leading to overproduction of IL-8, IL-6, IL-1β, and TNF-α [128]. Similarly, *E. coli* OMVs were able *in vitro* to engage TLR4 in human epithelial cells through the LPS, eliciting a downstream production of IL-8 [129]. Moreover, since OMVs are readily phagocyted by macrophages, can trigger intracellular PRRs. Consistently, some studies have shown that OMVs derived from different bacteria are capable to activate inflammasome-related pathways both *in vitro* and in *in vivo* mouse models [130,131].

On the other hand, it has been reported that, besides their pro-inflammatory potential, OMVs can also elicit immune escape effects, by inhibiting the function of leukocytes, thus assisting bacteria in evading macrophages and neutrophils defense. For example, *in vitro* studies demonstrated the ability of *E. coli* OMVs in reducing the phagocytic ability of murine neutrophils, dampening their response [132]. Moreover, *P. gingivalis* OMVs have the potential to abrogate the expression of TNFα in human macrophages, thus attenuating the response against the bacterium [133]. Hence, it will be crucial to elucidate these findings through *in vivo* studies, to better understand the underlying mechanisms. For this purpose, new models to study EVs biology have been developed in the last years, such as the zebrafish embryo model [134,135].

Aims and rationale of the thesis

The research of my PhD thesis is based on the study of the harmful effects of airborne particulate matter (PM) exposure on the alteration of the immune response, with the purpose of investigating its impacts on the onset and severity of viral bronchiolitis in infants. To address the present study, I carried out *in vivo* analyses, setting up a zebrafish model to study the immunomodulatory effects of PM on the response to an infectious inflammatory stimulus. In the second part of the thesis, a population study involving infants with viral bronchiolitis was also performed to define a possible link between PM and bronchiolitis severity. Moreover, metataxonomic analysis on the population was carried out to explore a plausible interplay of the upper respiratory tract microbiome in this framework. Finally, the immunomodulatory potential of bacterial extracellular vesicles (EVs) of a bacterial species resulted involved in the aforementioned interplay was investigated *in vivo* in a newly set zebrafish model.

The main starting hypothesis of the present thesis is illustrated in **figure 13**:
The dysbiosis of the respiratory tract microbiota due to PM exposure could play a key role in promoting the onset and development of viral bronchiolitis in infants, by modulating host immune response also through bacterial EVs. This interplay is mediated by the effects of PM on the host response to viral infections.

To test this hypothesis, my PhD project has followed four specific aims. An overview of the main study aims with the experimental design is described in **figure 14.**

AIM 1. To examine *in vivo* the effects of PM exposure on the host innate immune response against an infectious inflammatory stimulus. For this study, a new zebrafish model of PM exposure is set up to elucidate the functional mechanisms underlying the immunomodulatory effects of PM exposure, and to model the specific effects of the exposure to a PM collected in the Milan metropolitan area on the innate immune response following a subsequent infectious acute inflammatory trigger.

AIM 2. To investigate the relationship between short-term $PM_{2.5}$ and PM_{10} exposure and severity of bronchiolitis in infants. This objective is addressed through a population study involving infants with viral bronchiolitis living in Milan. The PM analyzed in the aim 1 is similar in terms of chemical composition to the PM of Milan, potentially leading to comparable effects and thus allowing parallel considerations of outcomes.

AIM 3. To assess the composition of the upper respiratory tract microbial community of infants with bronchiolitis and to evaluate its association with PM exposure. For this purpose, 16S analysis is exploited to describe and compared the nasal microbiome of infants with bronchiolitis enrolled in the framework of the AIM 2, and matched healthy controls. Respiratory dysbiosis is investigated to identify bacterial taxa differentially expressed.

AIM 4. To evaluate *in vivo* the immunomodulatory potential of bacterial EVs derived from the bacterial species emerged in aim 3 (i.e., *Haemophilus influenzae*). To verify this feature, a new zebrafish model is set up to study effects of EVs derived from different biological sources. Using this model, functional analysis is performed on bacterial EVs to unveil a potential link with RSV infection and acute bronchiolitis.

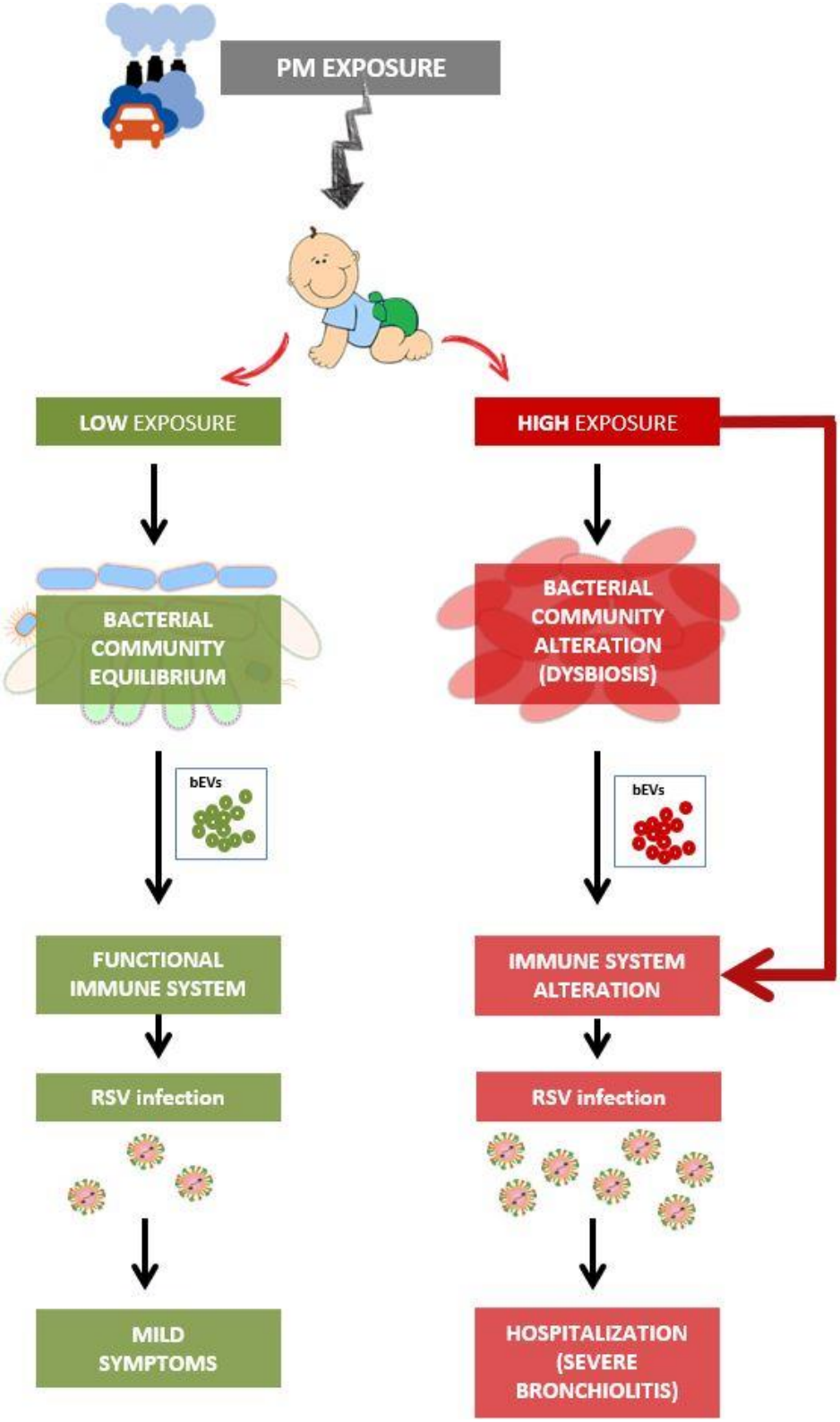

***Figure 13**. Graphic synthesis of the central hypothesis of the thesis*

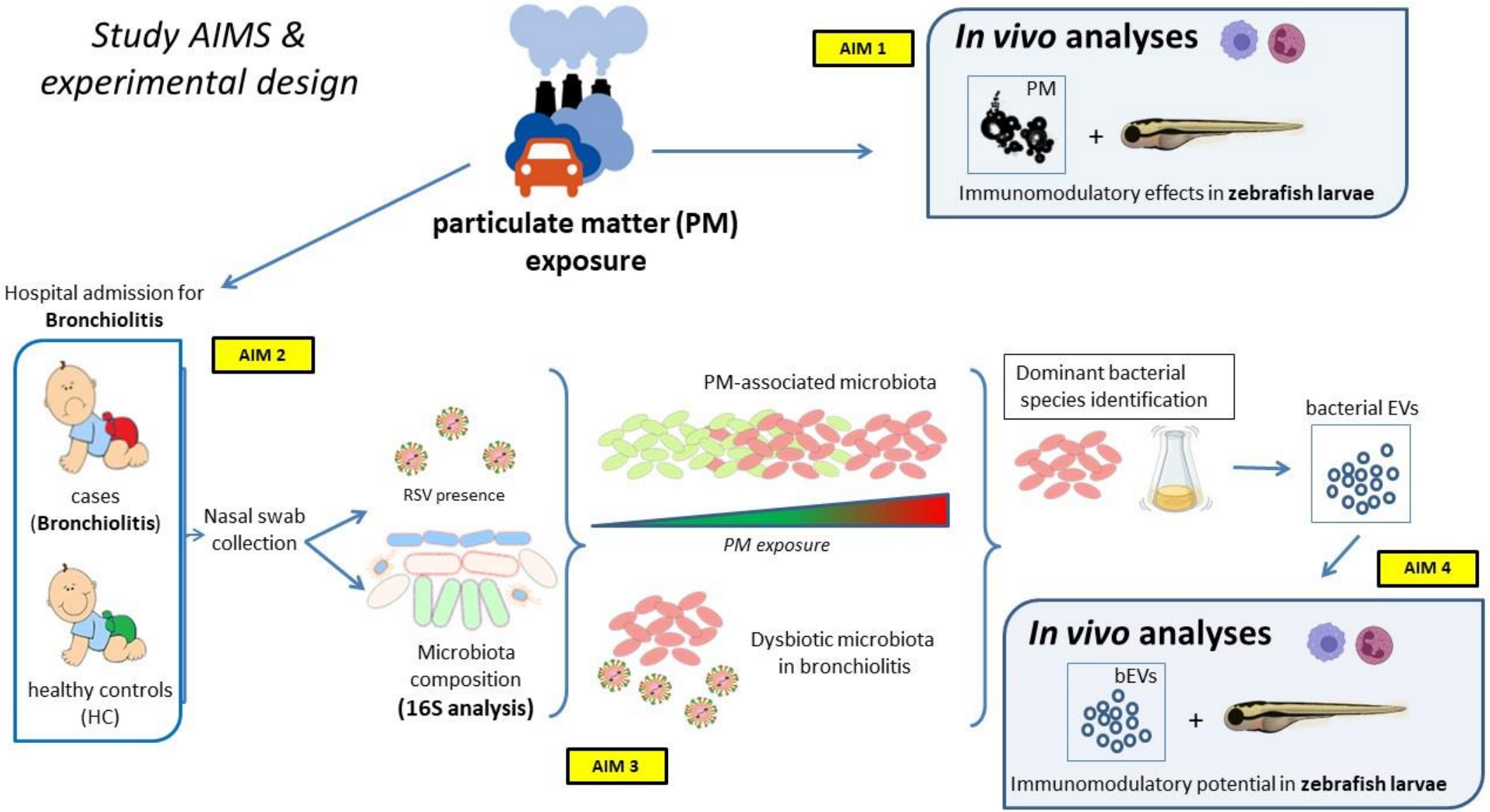

Figure 14. *Graphical summary of the specific aims and experimental design of the thesis.*

NOTE:

Part of the results presented are published in international peer-reviewed journal articles, as indicated in the summary of each chapter.

This contribution is in part related to the BUG project, “Nasal microbiota, bronchiolitis and air pollution: the Good, the Bad and the Ugly”, supported by PRIN “progetti di ricerca di rilevante interesse nazionale” 2017 [grant number 2017HWPZZZ].

Chapter 1

in vivo study of the immunomodulatory effects of Particulate Matter on the zebrafish model

1.1 Summary

This part of the dissertation will focus on the investigation of how exposure to PM influences the response of the innate immune system. For this purpose, the effects of fine PM of Milan metropolitan area were analyzed. The analyses were conducted by taking advantage of the *in vivo* zebrafish embryo model, which is largely used in toxicological studies and is suitable to study innate immunity response. Indeed, zebrafish shares the main immune cell populations with higher vertebrates, including mammals, and, during the larval stage, the adaptive immune system is not yet developed, allowing for the study of innate responses in isolation.

The main goals of the present chapter are *i*) to generate a new *in vivo* model that recapitulates the immunomodulatory effects of PM exposure observed in human, in order to study the underlying functional mechanisms; *ii)* to set a screening platform for the rapid assessment of the potentially harmful effects of PM and *iii*) to model the specific effects of PM exposure on the innate immunity response to an infectious inflammatory stimulus.

1.2 Materials and Methods

1.2.1 Zebrafish husbandry

Zebrafish (*Danio rerio*) strains AB (Wild type, Wilson lab, University College London, UK), *Tg BAC(mpx :EGFP)^{i114}* (known as *Tg(mpx:EGFP)*) [63] and *Tg(mpeg1:mcherry)* strains [62] were maintained according to international (EU Directive 2010/63/EU) and national guidelines (Italian decree No 26 of the 4th of March 2014) and raised at 28,5°C on a 14 h light/10 h dark cycle, in the fish facility at the University of Milan, Via Celoria 26, 20133 Milan, Italy (Aut. Prot. n. 295/2012-A – December 20, 2012). Embryos were collected by natural spawning, staged according to Kimmel *et al.* [136] and raised at 28,5°C in E3 embryo/larvae growth medium (E3; Instant Ocean, 0,1% Methylene Blue) in Petri dishes, according to established techniques. Embryonic ages are expressed in hours post fertilization (hpf) and days post fertilization (dpf). In this work were used exclusively embryos/larvae up to 120 hpf. When necessary, from 24 hpf, 0,003% 1-phenyl-2-thiourea (PTU, Sigma Aldrich) was added to the E3 to prevent pigmentation (this solution will be cited as "PTU" in the text). Embryos were washed, dechorionated and anaesthetized with 0.016% tricaine (Ethyl 3- aminobenzoate methanesulfonate salt; Sigma Aldrich) in E3, before observations, microinjection, tailfin amputation and image acquisitions. For imaging analysis, unless otherwise stated, embryos were fixed for 2 hours in 4% paraformaldehyde (PFA) in Phosphate Buffer Saline (PBS) at RT, then rinsed twice in PBS solution.

1.2.2 Collection and preparation of $PM_{2.5}$ samples

$PM_{2.5}$ samples were provided by Professor Andrea Cattaneo (University of Insubria). Fine particulate matter ($PM_{2.5}$) was collected during different sampling campaigns over two months (within February and March 2019) in an outdoor urban background site in Como, a medium-sized town of Lombardy region (Northern Italy) belonging to the metropolitan area of Milan, and subsequently characterized, as described in Rovelli *et al.* [137]. 34.0% of the fine PM mass is composed by anions and 17.4% by cations (NO_3^- (21.8%) and SO_4^{2-} (10.8%) are the main inorganic ionic components), which represent the major contribution, followed by organic (14.1%) and elemental (0.5%) carbon. The elemental content is less than 0.5% and Zn and Fe are the most abundant elements (87% of the total amount). Dried $PM_{2.5}$ samples were weighted and aliquoted in 4 mL glass vials containing 0.7-1.2 mg of dried material (**Figure 16a**) and stored at 4°C until use for the *in vivo* experiments. Just before use, the

whole sample was dissolved in the E3 embryo medium to reach a stock concentration of 700 µg/mL. To further dissolve completely the dried material, after the addition of the E3 medium, the glass vial was vortexed 2 times for 30'' and then the resulting PM suspension was subjected to two sequential sonication processes at 30 kHz (30'' each) to obtain a clean homogeneous suspension of straw-yellow color ($PM_{2.5}$ suspension) (**Figure 16b**). Stereomicroscopic observation of the suspension was performed to ruled out aggregates or undissolved sample.

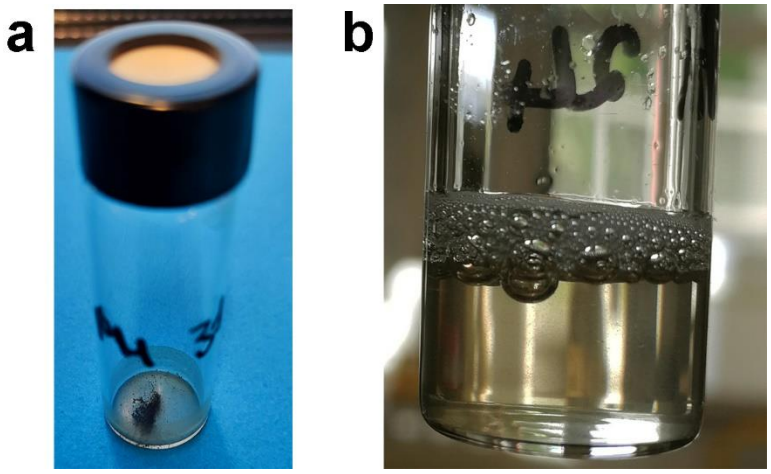

Figure 16. *$PM_{2.5}$ sample.* ***(a)*** *Dried PM sample in glass vial;* ***(b)*** *PM suspension (700 µg/mL) in E3 embryo medium (straw-yellow color).*

1.2.3 Exposure of zebrafish embryos to $PM_{2.5}$

Embryos at 30 hpf were manually decohorionated, if necessary, and divided into groups of 30-35. Each group was transferred into a 6-well plate in a total volume of 4 mL of PTU added with $PM_{2.5}$ suspension at a final concentration of 15, 30, 45, 75 or 100 µg/mL per well. Control unexposed embryos were kept in PTU without addition of $PM_{2.5}$ suspension. To avoid particles precipitation, immediately after the addition of $PM_{2.5}$ suspension, the plate was shaked for 1', then the embryos were incubated at 28,5°C for the indicated time. At 18 hours post-exposure (hpe) (2 dpf) embryos were observed under stereomicroscope to assessed mortality rate and to check for the precipitation of PM inside the well. For short exposure setting (SES) experiments, embryos were thoroughly washed three times with PTU, transferred into clean Petri dishes and incubated at 28,5°C in PTU. For long-exposure setting (LES) experiments, dead embryos were removed from wells with fine pipette tips (negligibly altering the volume) and live embryos were kept exposed to $PM_{2.5}$ under same conditions until 42 hpe. At 42 hpe (3dpf) larvae were observed and washed as stated above and

live/dead and morphological analyzesis were performed under stereomicroscope. For survival rate analysis, larvae were scored as dead when heartbeat was absent, necrosis effects were present and movement in response to touch was absent, as previously described [138].

1.2.4 Acute infectious inflammatory stimuli in zebrafish larvae

To generate zebrafish acute inflammation models, 3 dpf larvae (exposed or not to $PM_{2.5}$) were microinjected systemically or locally with 5 mg/mL of *Pseudomonas aeruginosa* lipopolysaccharide suspension (*Pa*-LPS) (derived from strain ATCC 27316, Sigma Aldrich), a dose able to elicit a strong inflammatory response. For gene expression experiments, to obtain systemic delivery, 2 nL of *Pa*-LPS were microinjected into the duct of Cuvier (therefore into the circulation) of larvae (**Figure 17a**), as described in [138]. At least 15 larvae were injected for each condition and after 8 hpi total RNA was extracted from them for mRNA levels analysis. For leukocyte recruitment experiments, *Tg(mpx:EGFP)* and *Tg(mpeg1:mcherry)* larvae were locally injected with 1 nL of *Pa*-LPS suspension intramuscularly (**Figure 17b**) or in the hindbrain ventricle (**Figure 17c**), as previously described [59,139]. For intra-muscle injection, *Pa*-LPS was delivered into the skeletal muscle of the trunk region, in the area within the second and the fifth somite before the yolk extension. 10-12 larvae were injected for each condition. As control, larvae were systemically/locally injected with physiological solution. Systemically/locally injected larvae were incubated at 28,5°C in PTU for the indicated time until the downstream immune response analysis. Each experiment was conducted at least in biological duplicate.

1.2.5 Acute sterile inflammatory stimulus in zebrafish larvae (tailfin amputation model)

To generate zebrafish sterile local inflammatory stimulus, 3 dpf larvae (exposed or not to $PM_{2.5}$) were amputated of a portion of the tailfin with the use of a sterile scalpel blade, without damaging circulatory loop (**Figure 17d**) , as described [51,141]. The properly amputated larvae were selected for the assay and incubated at 28,5°C in PTU. After 6 hours post-amputation (hpa) leukocyte recruitment in the caudal area of the tailfin was assessed.

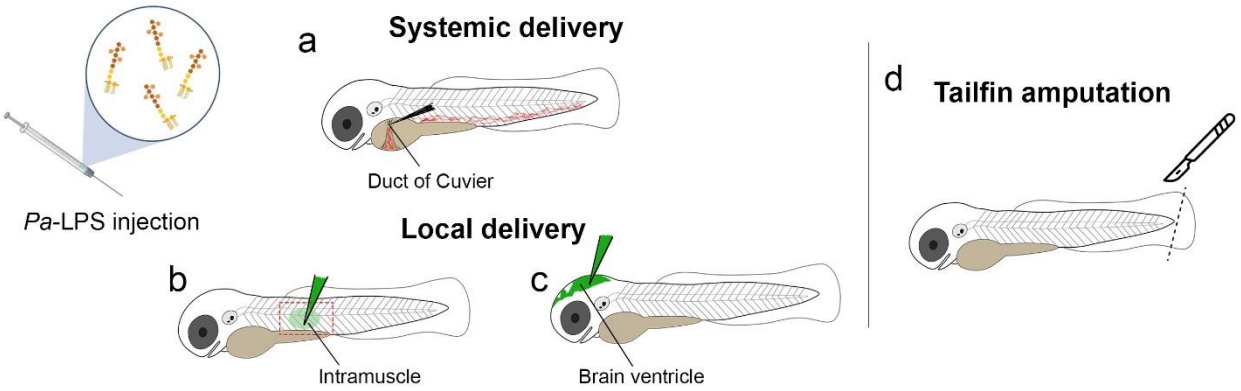

Figure 17. *Acute inflammatory stimuli in zebrafish larvae.* ***(a-c)*** *Schematic representation of the different routes of Pseudomonas aeruginosa LPS (Pa-LPS) microinjection: systemic delivery into the blood circulation* ***(a)*** *and local delivery intramuscular* ***(b)*** *or into the brain ventricle* ***(c). (d)*** *Schematic representation of tailfin amputation model.*

1.2.6 Image acquisition and quantification of total/local leukocytes

To study leukocytes activation, *Tg(mpx:GFP)* and *Tg(mpeg1:mcherry)* zebrafish transgenic reporter lines were used to follow the behaviour of neutrophils and macrophages, respectively. After $PM_{2.5}$ exposure and/or post-inflammatory trigger, embryos/larvae were fixed in 4% PFA in PBS for 2 hours at RT, then washed three times in PBS and analysed. Single slice bright-field and fluorescent images of lateral/dorsal side of larvae were sequentially acquired using an epi-fluorescence stereomicroscope (M205FA, Leica, Germany) equipped with a fluorescent lamp and a digital camera and mounting mcherry-filter (excitation 587 nm) and GFP-filter (excitation of 488 nm). Images were processed using Adobe software, merging different focal planes when necessary. Neutrophils and macrophages were quantified as mpx^+ and $mpeg1^+$ cell count, respectively. For $PM_{2.5}$-exposure experiments, quantification analysis was performed on whole embryo (total leukocytes count) and on head region (dashed box) at 18 and 42 hpe. For the acute inflammation trigger experiments, leukocytes recruitment was measured in the defined region of interest (brain ventricle, trunk region or caudal fin region; dashed boxes) and was assessed at 6 hpi in brain ventricle injection model, at 4 hpi in intramuscular injection model or at 6 hpa in tailfin amputation model. For both experimental settings, cell count was performed by computation using of Fiji (ImageJ software, developer: Wayne Rasband) as already described [140,142]: i) manually selecting of the region of interest for the analysis with “polygon selection” tool (e.g. head area or whole body of the embryo/larva); ii) using of “subtract background” command, to avoid interference by the autofluorescence of the yolk sac; iii) running of the “Find maxima” function to detect single fluorescent cells. Alternatively, in tailfin

amputation model, macrophages were quantified as mpeg1$^+$ signal area in the tailfin region (dashed box), by modified the protocol of the above Fiji analysis from step iii onwards, as described also by Phan and colleagues [59]: iii) running of "make binary" function to convert the image to B&W; iiii) setting of a common threshold level; iiiii) running of "measure area" tool to determine the area of fluorescent pixels within the selected region of interest. Mean and SEM of cell count of at least two independent experiments are reported on graphs.

1.2.7 Analysis of Reactive oxygen species (ROS) production in zebrafish larvae

Live 3 dpf *Tg(mpx:GFP)* larvae exposed or not to $PM_{2.5}$ and stimulated by intramuscular injection of *Pa*-LPS were assessed at 4 hpi for ROS production. ROS analysis was performed by using the commercial kit DHE (dihydroethidium, Santa Cruz biotechnology, US): 30 mM DHE stock solution was diluted in PTU to obtain a final concentration of 5 µM. Live Larvae were incubated for 15 minutes with DHE 5 µM in the dark (DHE is photosensitive) at 28.5°C, then washed three times in PTU and trunk region was immediately imaged using an epifluorescence stereomicroscope as described above. ROS production at the region of inflammation was measured in terms of DHE$^+$ cell count as described by Phan *et al.* [59]. Whole body and local neutrophil migration at the injection site was measured through mpx$^+$ cell count, as described above. Quantification of neutrophils actively producing ROS (mpx$^+$ DHE$^+$ cell count) was extrapolated as co-localization signal between red cells (ROS producers) related to green cells (neutrophils) through computation using of Fiji as follows: i) merging of different colour channels of the image; ii) using of "subtract background" function; iii) adjusting of brightness/contrast parameters for better visualization of overlapped signals; iiii) setting of a "colour threshold"; iiiii) using of "measure area" function to determine overlapped fluorescent pixels of the image to extrapolate mpx$^+$ DHE$^+$ cells. Relative percent of neutrophils actively producing ROS was extrapolated by considering the ratio of mpx$^+$ DHE$^+$ cells and local neutrophil count (mpx$^+$ DHE$^+$/local mpx$^+$).

1.2.8 Determination of the expression level of inflammation mediator genes

mRNA expression levels of inflammatory genes were assessed by reverse transcription-PCR and real-time quantitative-PCR (RT-qPCR) assays. Total RNA was extracted from groups of 15-20 zebrafish larvae/condition using NucleoZOL reagent (Macherey-Nagel, Germany) according to the manufacturer's instructions. Concentration and purity of RNA were measured using the Nanodrop spectrophotometer. RNA was treated with DNase I RNase-free (Roche Diagnostics, Switzerland) to

avoid possible genomic contamination. 1 µg of RNA was reverse-transcribed using the "ImProm II™ Reverse Transcription System" (Promega) using a mixture of oligo(dT) and random primers, according to manufacturer's instructions. qPCRs were carried out in a total volume of 10 µl containing 1X iQ SYBR Green Super Mix (Promega), using proper amount of synthesized cDNA. qPCRs were performed using the QuantStudio 5 Real-Time PCR System (Applied Biosystems, ThermoFisher Scientific) following the manufacturer's guidelines. Thermocycling conditions were 95°C for 10', 95°C for 10'', 55°C for 30''. All reactions were performed at least in triplicate for 40 cycles. The relative expression level of each gene was calculated according to the $2^{-\Delta\Delta Ct}$ method [143]. For normalization purposes, *rpl8* and *β-actin* genes were used as internal reference genes. Primers used in the analyses are listed in **Table 3**. Mean and SEM of at least three independent experiments were reported on graphs.

***Table 3**. qPCR primer list*

Gene	Primer ff (5'- 3')	Primer rev (5'- 3')	Reference
rpl8	CTCCGTCTTCAAAGCCCATGT	TCCTTCACGATCCCCTTGATG	Mazzola *et al.*, *Hematol*, 2019
β-actin	GCACGAGAGATCTTCACTCC	GCAGCGATTTCCTCATCCAT	Cafora *et al.*, *Front. Microbiol*, 2022
il-10	TTCAGGAACTCAAGCGGGAT	GACCCCCTTTTCCTTCATCTTT	Ferrari *et al. J. Mol. Sci*, 2019
il-1β	TGGACTTCGCAGCACAAAATG	CGTTCACTTCACGCTCTTGGATG	Cafora *et al.*, *Sci rep*, 2019
tnf-α	CTTCACGCTCCATAAGACCC	GCCTTGGAAGTGAAATTGCC	Cafora *et al.*, *Front. Microbiol*, 2022
il-6	TCAGAGACGAGCAGTTTGAG	GAGAGGAGTGCTGATCCTGA	Cafora *et al. J. Mol. Sci*, 2021
cxcl8	CGACGCATTGGAAAACACAT	TGTCATCAAGGTGGCAATGA	Cafora *et al. J. Mol. Sci*, 2021
sele	CAGGACCACTGCAGAACAT	CTGCATCTCCATAAGTTTAGCG	Unpublished, designed with the Primer Blast tool (NCBI)
edn1	GACCATGCTGACATCTGGATT	CTTATTCCTGGAGTGACGTGC	Unpublished, designed with the Primer Blast tool (NCBI)
eng	GATACGCACAGGGCATCC	GCATCCGGATATGGAGAGGA	Unpublished, designed with the Primer Blast tool (NCBI)
icam1	CACCGCTGCAAACTATCTGG	ACGAGACAAACGTGGATGGA	Unpublished, designed with the Primer Blast tool (NCBI)
vcam1a	TGACATTGGGATTGAGCGAAG	GCAGGTATTATGGCTACAGGC	Unpublished, designed with the Primer Blast tool (NCBI)
cox2a	ATCCTGTTGTCAAGGTCCCA	CAAGGGTGCGGGTGTAAT	Unpublished, designed with the Primer Blast tool (NCBI)
cox2b	AATGCGATACGTGCTGACAT	GCTTCCCAGCTTTTGTAACCA	Unpublished, designed with the Primer Blast tool (NCBI)

1.2.9 Statistical analysis

The statistical analyses carried out on zebrafish experiments were performed using GraphPad (Prism) software version 8.0.2 for Windows. The normal distribution of all datasets, when necessary, was

guaranteed by Kolmogorov-Smirnov or Shapiro-Wilk normality test. Outliers' data were excluded from analyses. Specific statistical tests were used to evaluate the significance of differences between experimental groups, as reported in the corresponding figure legend: unpaired two-tailed *Student's t-test* with Welch correction when comparing two groups, One-sample *t-test* when comparing a group with an hypothetical value (when control group=1) or ordinary one-way analysis of variance (ANOVA) followed by Tukey post hoc correction for multiple comparisons. The results represent data derived from at least two (for cell count and area measurement analyses) or three (for qPCR molecular analyses) independent experiments and mean ± SEM were reported in the graphs. P-value<0.05 was defined to indicate statistically significant differences.

1.3 Results

1.3.1 Effects of PM exposure on innate immune response of zebrafish

In the present paragraph of the results, the direct effects triggered by $PM_{2.5}$ suspension on the innate immune system of zebrafish embryo were assessed. An adequate PM concentration was first set for the analyses and then the effects on leukocyte populations and inflammatory gene expression were investigated.

1.3.1.1 Impact of $PM_{2.5}$ on mortality rate and morphology of larvae

Based on the scarce literature in the field [71,73,76], the effects of a range of $PM_{2.5}$ concentrations between 15 and 100 µg/mL (15, 30, 45, 75, 100 µg/mL) were tested in the zebrafish model. Embryos were exposed to $PM_{2.5}$ dissolved directly in the E3 medium + PTU (PTU) to prevent pigmentation, in plastic multi-well plates and incubated at the optimal growth temperature (28,5°C) for different periods. A non-negligible precipitation of black powder, deposited on the bottom of the plastic well, was observed under stereomicroscope after exposure to concentration equal or greater than 75 µg/mL. Therefore, only the treatments with a concentration equal to or less than 45 µg/mL represent reliable amounts of exposure and were used for the following experiments. Embryos were exposed to $PM_{2.5}$ from 30 hours post-fertilization (hpf), a developmental stage in which active innate immunity cell populations and blood circulation are already present [50]. In the first set of experiments, effects of the exposure to $PM_{2.5}$ were compared in 30 hpf embryos with or without the chorion, (i.e. the acellular proteinaceous envelope surrounding the embryo until 72 hpf), can be manually removed at earlier stages. On the surface of the chorion of exposed not-dechorionated embryos a black powder was deposited, avoiding the direct contact with the embryo. Although embryo mortality was not observed, it was not possible to determine whether $PM_{2.5}$ got in touch with the embryo. Hence, manually dechorionated embryos were used for the following exposure experiments. To mimic $PM_{2.5}$ exposure two exposure settings were tested (**Figure 18**): in the long exposure setting (LES), embryos were exposed for 42 hours to $PM_{2.5}$ (from 30 hpf to 72 hpf), while in the short exposure setting (SES) for 18 hours (from 30 hpf to 48 hpf). Embryo mortality and morphology were analyzed at 48 hpf (18 hours post-exposure start (hpe)) and at 72 hpf (42 hpe) (**Figure 19**). At 18 hpe no significant differences in embryo mortality were observed in comparison to the untreated controls, while at 42 hpe LES resulted in high embryo toxicity, reaching 100% mortality already at the lowest $PM_{2.5}$

concentration tested (i.e., 15 µg/mL) (**Figure 19a**). In comparison to not-exposed control embryos, SES did not increase the embryo mortality rate with concentration of 15, 30 and 45 µg/mL, while the exposure to concentrations equal or greater than 75 µg/mL resulted in high mortality rate (**Figure 19b**). Larvae that survived after 75 µg/mL SES generally exhibited morphological alterations, with diffuse necrosis, yolk sac and pericardial edema and muscle fiber disorganization (**Figure 19c**), in line with the toxic effects observed with exposure to high concentrations of PM by other authors [66,73,76]. Accordingly, 45 µg/mL in SES were set as concentration and exposure-time limits for the following innate immune response analyses.

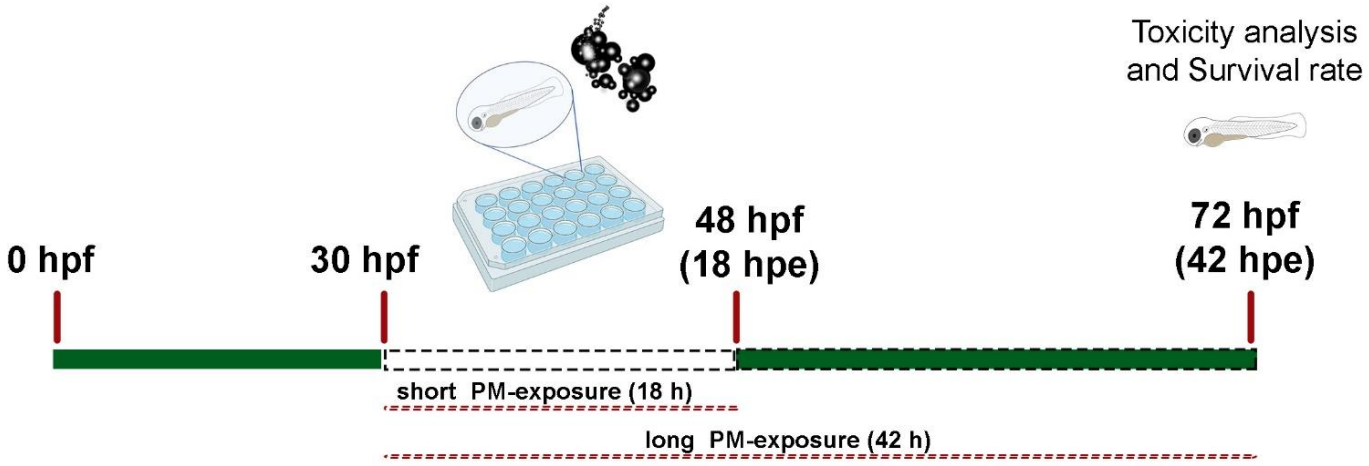

***Figure 18**. Schematic representation of the two tested PM exposure settings: in long exposure setting (LES) embryos were exposed for 42 hours while in short exposure setting (SES) embryos were exposed for 18 hours.*

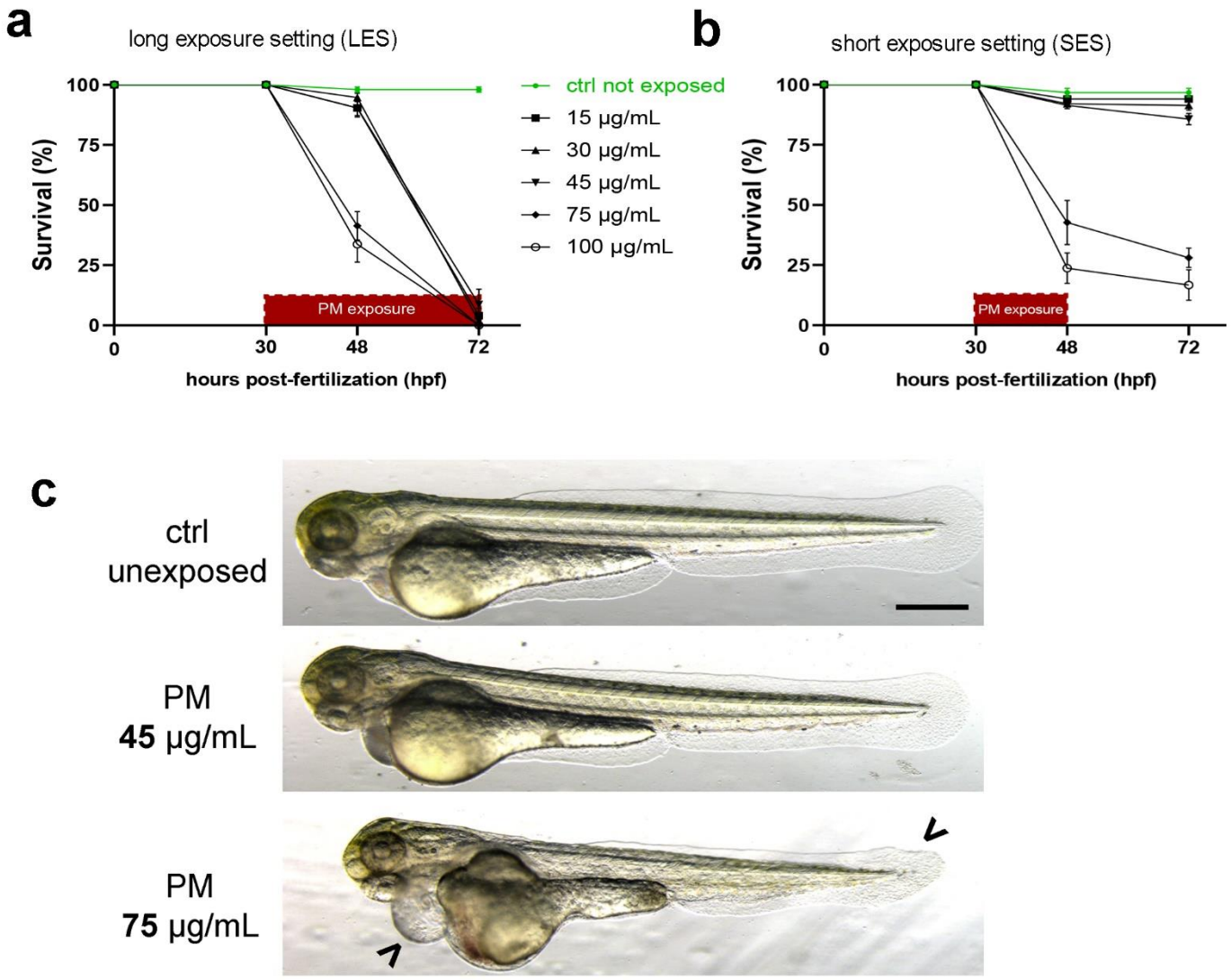

***Figure 19**. Effects of PM in LES and SES on survival rate and morphology of embryos/larvae. (**a-b**) survival rate at 48 and 72 hpf is reported for LES (**a**) and SES (**b**) with different concentrations of $PM_{2.5}$. (**c**) Representative 72 hpf larvae after SES to different concentrations of PM; black arrowhead indicate morphological alterations of pericardial edema and tailfin. Scale bar=400µm.*

1.3.1.2 Effects of $PM_{2.5}$ exposure on leukocyte activation

To investigate the role of leukocyte populations in response to $PM_{2.5}$ acute inflammatory stimulus, neutrophils and macrophages activation and recruitment was assessed. *Tg*(*mpx*:*EGFP)* and *Tg*(*mpeg1*:mcherry) zebrafish transgenic reporter lines, with green fluorescent neutrophils and red fluorescent macrophages respectively, were used to dissect the response of the two myeloid populations. In 30 hpf embryos, leukocytes are already mature and represent the main players in response to inflammatory stimuli active [50]. Embryos exposed to $PM_{2.5}$ in SES were analyzed and

imaged under fluorescence stereomicroscope and leukocyte count was assessed (**Figure 20**). Both whole embryo and head region quantifications were performed (**Figures 21a and 21b**). The whole embryo average number of mpx^+ neutrophils/embryo increased at 18 hpe (48 hpf) in the embryos exposed to the highest concentration of $PM_{2.5}$ (45 µg/mL) (i.e., 73.0 vs 93.4, *p-value 0.0018*), while no difference was observed for 15 and 30 µg/mL (**Figure 21b**). An even more marked effect was observed at 42 hpe (in 72 hpf larvae), where the average number of activated neutrophils/embryo increased in embryos treated with all the $PM_{2.5}$ in a concentration-dependent manner (i.e., controls, 87.1 ; 15 µg/mL, 110.7, *p-value 0.0145*; 30 µg/mL, 111.0, *p-value 0.0128*; 45 µg/mL, 119.9, *p-value< 0.0001*), suggesting that inflammatory effect of $PM_{2.5}$ had not been resolved yet, being maintained even after the end of exposure window (SES, 30 – 48 hpf) (**Figure 21c**). As neutrophils are the first immune cells to be recruited toward a site of acute inflammation [50,51], we investigated their migration by measuring their recruitment to the head region of the larva after 48 hpe. Interestingly, an increase of neutrophils concentration in the head region was observed in larvae exposed to the higher concentration of $PM_{2.5}$ with respect to control embryos (*p-value 0.0004*). Although not significant, an increase in neutrophil concentration in the head region was also observed for 15 and 30 µg/mL PM exposure concentrations (**Figure 21d**). However, the ratio of the neutrophil count in the head over the whole embryo (i.e., head/total, %) did not show differences in larvae exposed with all concentrations of PM (**Figure 21e**). Considering macrophages activation, $mpeg^+$ macrophages were quantified in *Tg*(*mpeg1*:*mcherry)* larvae (**Figure 22a)**. No differences were observed in whole embryo count assay after exposure to 45 µg/mL of $PM_{2.5}$ (**Figure 22b**). On the other hand, unlike the effect observed on the neutrophil population, the presence of macrophages in the head region increased in larvae exposed to 45 µg/mL of $PM_{2.5}$ compared with controls (i.e., 33.17 vs 39.40, *p-value* 0.463), and, consequently, their relative percentage (i.e., 32.8% vs 36.8%, *p-value* 0.361) (**Figure 22c-d**).

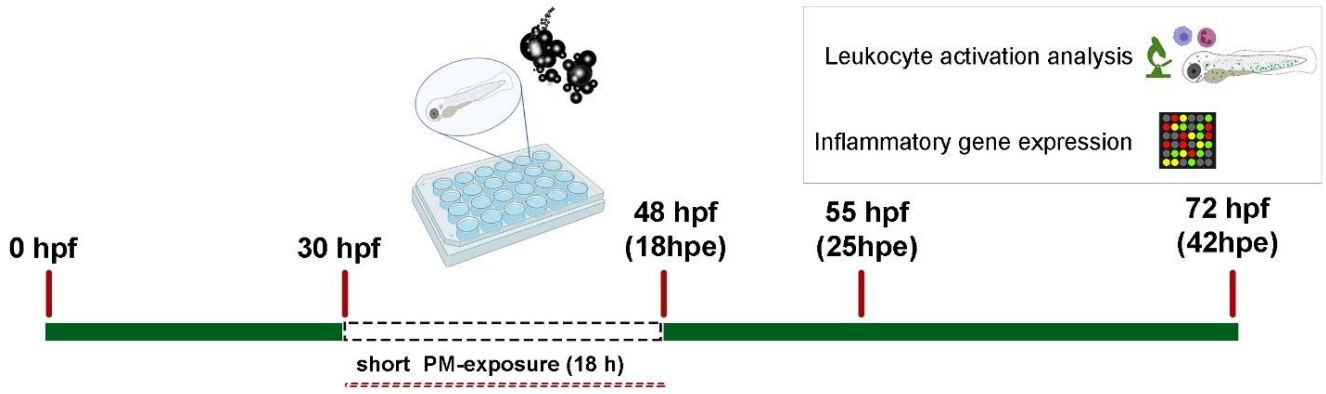

Figure 20. *Schematic representation of model setting. After SES to $PM_{2.5}$, Immune response was analyzed on embryos/larvae at different time point after exposure (hours post-exposure, hpe).*

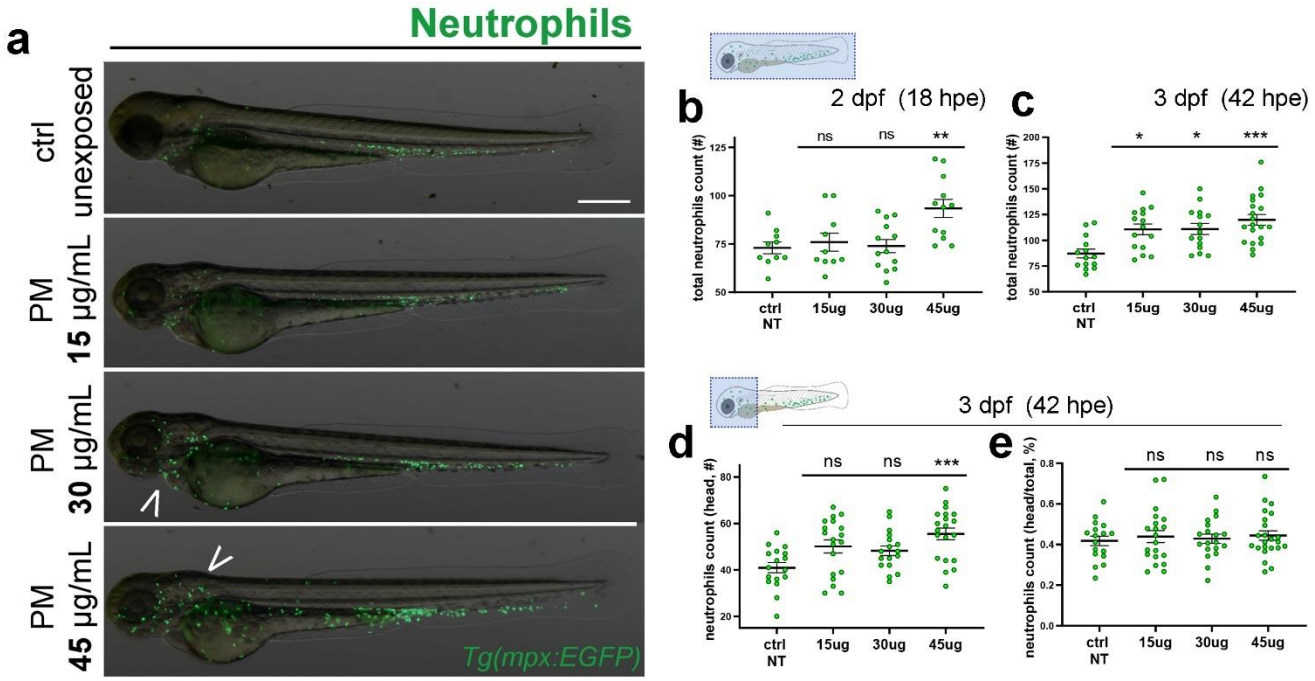

Figure 21. *Effects of $PM_{2.5}$ exposure on neutrophil activation. Tg(mpx:EGFP) embryos were analyzed after SES to $PM_{2.5}$ at 18hpe and 42hpe and compared with unexposed controls.* ***(a)*** *Representative panel of 3 dpf larvae (42 hpe) exposed to different concentrations of $PM_{2.5}$. White arrows indicate neutrophils concentration in the head region of larvae exposed to 30 and 45 µg/mL of $PM_{2.5}$.* ***(b-c)*** *Quantification of total neutrophils (mpx^+ neutrophils in the whole embryo or larva) at 18hpe (b) and 42hpe (c).* ***(d)*** *Quantification of neutrophils in head region (dashed box) and* ***(e)*** *ratio of neutrophils count in head region over total neutrophils count. Each dot represents a single individual and results are presented as mean ± SEM. Statistical significance was assessed by One-way ANOVA followed by Tukey's post hoc test: ***p < 0.001; **p < 0.01; *p < 0.05; ns= not significant. Scale bar=400µm.*

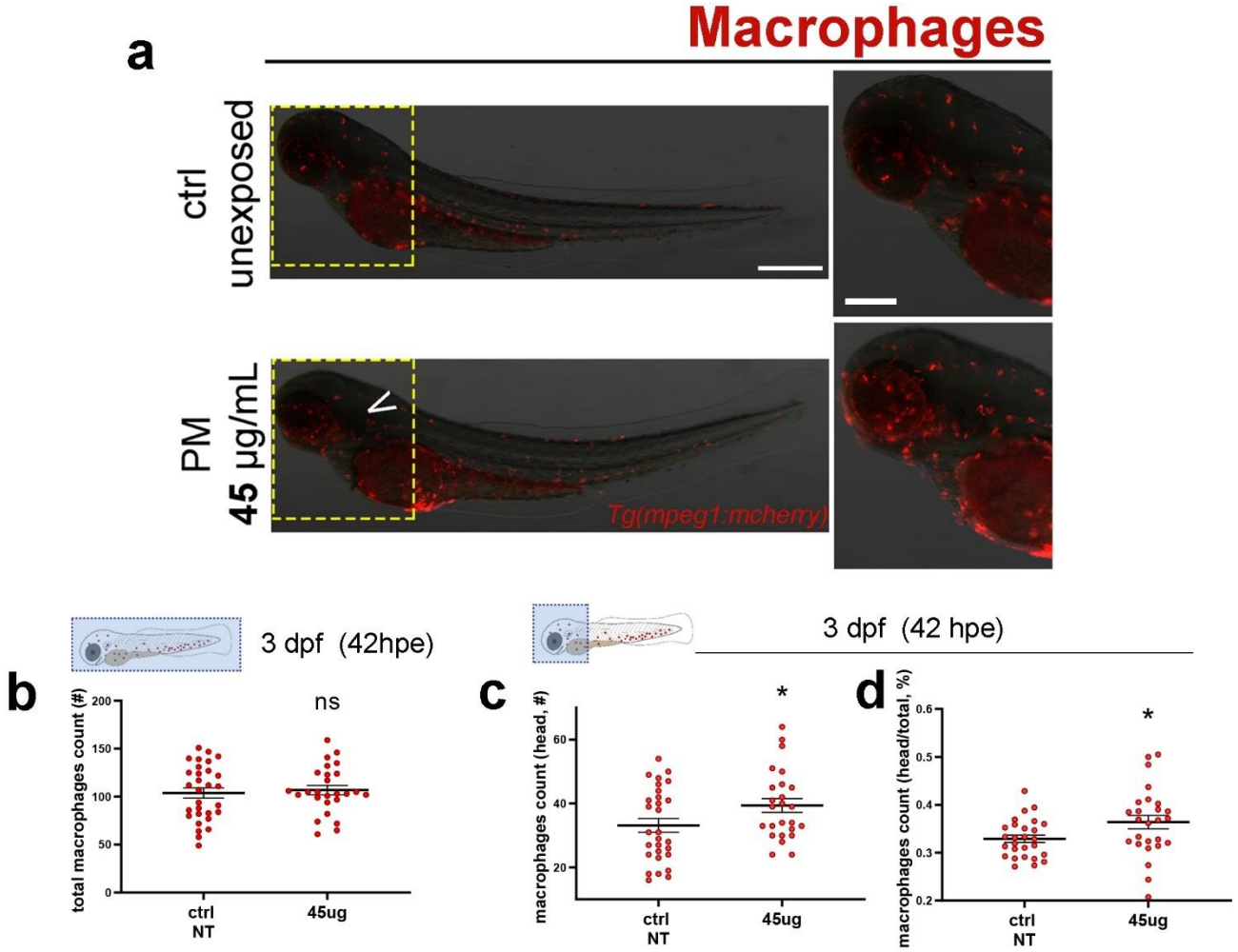

Figure 22. *Effects of $PM_{2.5}$ exposure on macrophage activation. Tg(mpeg1:mcherry) embryos were analyzed after SES to $PM_{2.5}$ at 42hpe and compared with unexposed controls.* ***(a)*** *Representative panel of 3 dpf larvae (42 hpe) exposed to 45 µg/mL of $PM_{2.5}$ or unexposed. White arrow indicates macrophages concentration in the head region of larvae exposed to 45 µg/mL of $PM_{2.5}$. Scale bars=400µm (left) and 200 µm (right)* ***(b)*** *Quantification of total macrophages ($mpeg^+$ macrophages in the whole embryo or larva) at 42hpe.* ***(c-d)*** *Quantification of macrophages in head region (dashed box) and* ***(e)*** *ratio of macrophages count in head region over total macrophages count. Each dot represents a single individual and results are presented as mean ± SEM. Statistical significance was assessed by unpaired t-test with Welch's correction: *p < 0.05; ns= not significant.*

1.3.1.3 $PM_{2.5}$ exposure elicits inflammatory markers overexpression

To further investigate at the molecular level the above-described altered leukocyte activation, the expression levels of pro-inflammatory cytokines and markers of endothelial activation were assessed in parallel experiments on the whole larvae, exposed or not to 45 µg/mL. At 72 hpf (48 hpe). The mRNA expressions of *cxcl8,* the primarily neutrophils chemotactic factor and of the key pro-inflammatory cytokine *il-1β* were increased (*p-value 0.0199* and *0.0456,* respectively) in PM-exposed larvae. Also, $PM_{2.5}$ exposure provoked an increased in the expression of the pro-inflammatory

cytokines *il-6* and *tnf-α* of about 6 and 3.5 times respectively (*p-value 0.0017* and *0.0266,* respectively) in comparison to unexposed controls (***Figure 23a-d***), suggesting the induction of a robust pro-inflammatory state. Interestingly, at 55 hpf (25 hpe) also the expression levels of all analyzed endothelial markers appeared increased in PM-exposed embryos, in particular, *endothelin1* (*edn1*) (*p-value 0.0057*), *endoglin* (*eng*) (*p-value 0.0011*) and *v-cam1a* (*p-value 0.0187*) (***Figure 23f,h,i***). Besides, *selectin* E (*sele*) and *icam1* mRNA expression levels were increased without statistical significance, probably due to high variability (*i.e.,* large SEMs) among the analyzed biological replicates (***Figure 23e,g***).

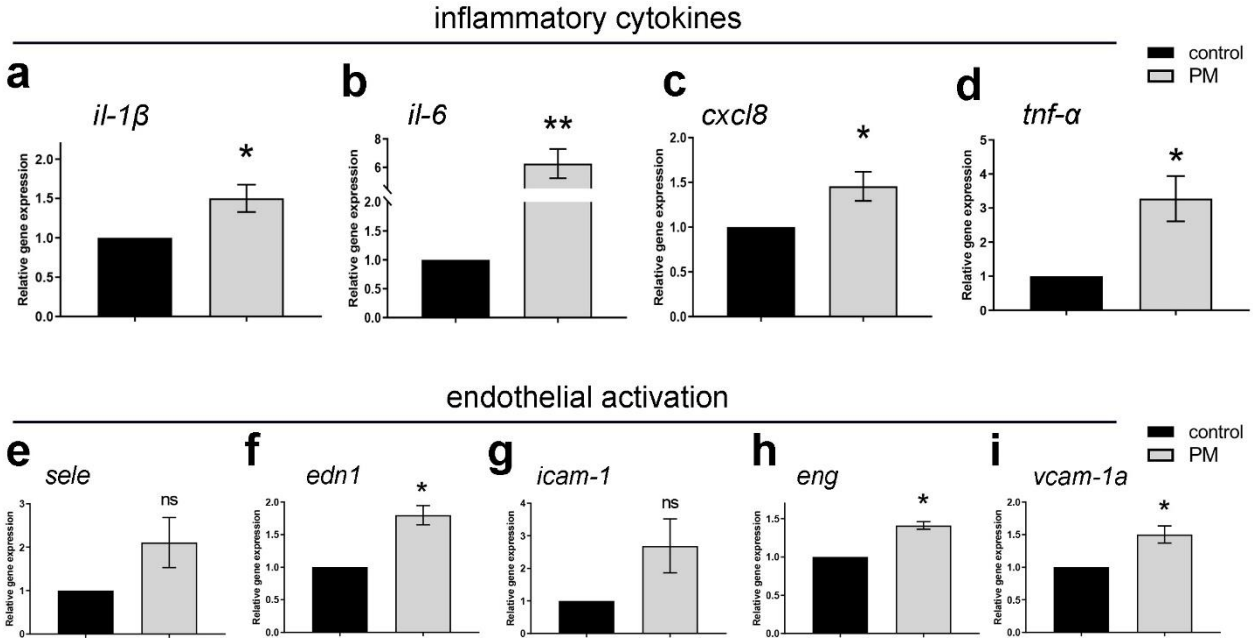

Figure 23*. Immunomodulatory effects of $PM_{2.5}$ exposure on inflammatory markers expression. Embryos were analyzed after SES to 45 µg/mL of $PM_{2.5}$ through RT-qPCR at 25 or 42hpe.* ***(a-d)*** *Relative expression levels of pro-inflammatory cytokines genes measured at 42hpe in larvae exposed or not to PM.* ***(e-i)*** *Relative expression levels of activated endothelial genes measured at 25hpe in larvae exposed or not to PM. Data were normalized on expression levels of control unexposed embryos. For each gene, results are presented as mean ± SEM of at least three independent experiments. Statistical significance was assessed by unpaired t-test: *p < 0.05; ns= not significant*

1.3.2 Effects of $PM_{2.5}$ exposure on the response to a subsequent acute inflammatory stimulus

The effects on innate immunity response of a second inflammatory trigger were assessed on zebrafish larvae exposed to 45 µg/mL of $PM_{2.5}$ for 18 hours (SES). As shown in **Figure 24**, in order to generate models of acute inflammation, two different types of stimuli were induced in 72 hpf larvae (at 48 hpe), a sterile inflammatory trigger, by the amputation of the caudal fin, or local/systemic infectious trigger, by microinjecting bacterial lipopolysaccharide (LPS) into the larva. In the present study, bacterial LPS (derived from *P. aeruginosa*, *Pa*-LPS) is used merely to generate an infectious inflammatory trigger, given its known high pro-inflammatory potential.

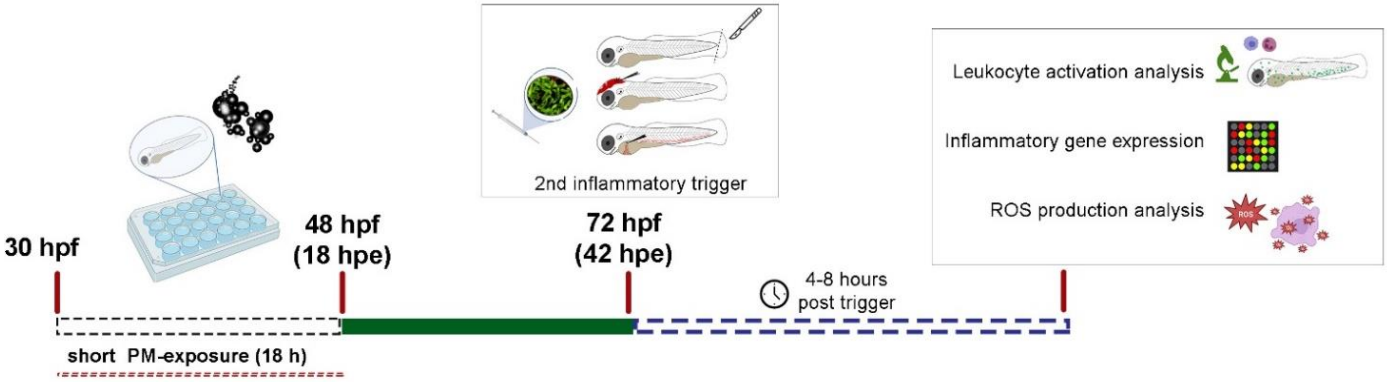

Figure 24. *Schematic representation of model setting. After SES to $PM_{2.5}$, a second inflammatory trigger was provoked to 72 hpf larvae and subsequent innate immune response analyses were performed after 4-8 hours from the second trigger.*

1.3.2.1 $PM_{2.5}$ exposure alters leukocytes migration to infectious stimuli

Leukocytes migratory stimulation was assessed after 6 hours post-injection (hpi) with 2 nL of *Pa*-LPS in the hindbrain ventricle of 3 dpf PM-exposed larvae. Overall, *Pa*-LPS injection induced a migration of both leukocyte populations (**Figure 25a**), as also previously demonstrated by others [70,143]. Neutrophils recruitment toward the injection site was less abundant in larvae pre-exposed to $PM_{2.5}$ compared to not-exposed larvae (i.e., 41.4 vs 29.1, *p-value 0.0221*) (**Figure 25b**). Conversely, macrophage migration was apparently not affected in larvae subjected to the two inflammatory triggers, as the mean number of $mpeg^+$ cells in the ventricle area/larva was similar to controls (i.e., controls=10.9; PM-exposed=11.4) (**Figure 25c**).

To further investigate the response to *Pa*-LPS injection in another anatomical location, intramuscular injection was performed. This infectious trigger induced a strong local immune response in 72 hpf larvae, including leukocyte migration, as shown in the illustrative images of **Figure 26a**. Larvae pre-exposed to $PM_{2.5}$ showed an altered migration of neutrophils toward the injection site at 4 hpi, since

the average number of mpx^{+} cells was lower in comparison with not-exposed larvae (i.e., 29.0 vs 23.2, *p-value* 0.0196) (**Figure 26b**). Interestingly, the same effect in $PM_{2.5}$-exposed larvae was observed on macrophage activation. Indeed at 4 hpi the mean number of mpeg^{+} cells at the site of infection was higher in not-exposed larvae (i.e. 4.6 vs 3.6, *p-value* 0.0444) (**Figure 26c**), highlighting a different sensitivity of the macrophage depending on the location of the generated acute stimulus.

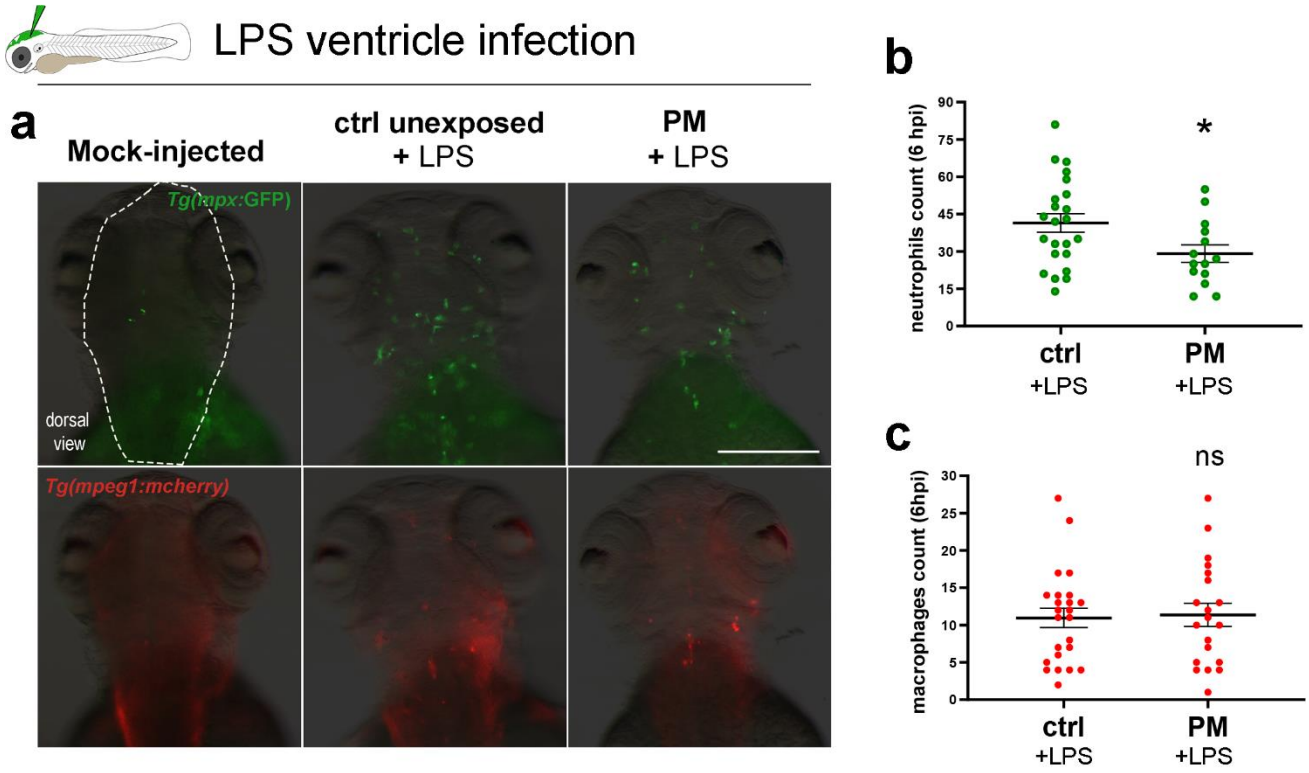

***Figure 25**. Immunomodulatory effects of $PM_{2.5}$ exposure on neutrophil and macrophage recruitment after an acute infectious stimulus. Tg(mpx:EGFP) and Tg(mpeg1:mcherry) embryos exposed or not in SES to 45 µg/mL of $PM_{2.5}$ were analyzed for leukocytes migration at 6 hours post local LPS injection (or mock-injection) into brain ventricle. **(a)** Representative panel of PM-exposed and unexposed 3 dpf larvae at 6 hpi of LPS. **(b)** mpx^{+} neutrophils count and **(c)** mpeg^{+} macrophages count at 6 hpi in head region (dashed box). Each dot represents a single individual and results are presented as mean ± SEM. Statistical significance was assessed by unpaired t-test with Welch's correction: *p < 0.05; ns= not significant. Scale bar=200µm.*

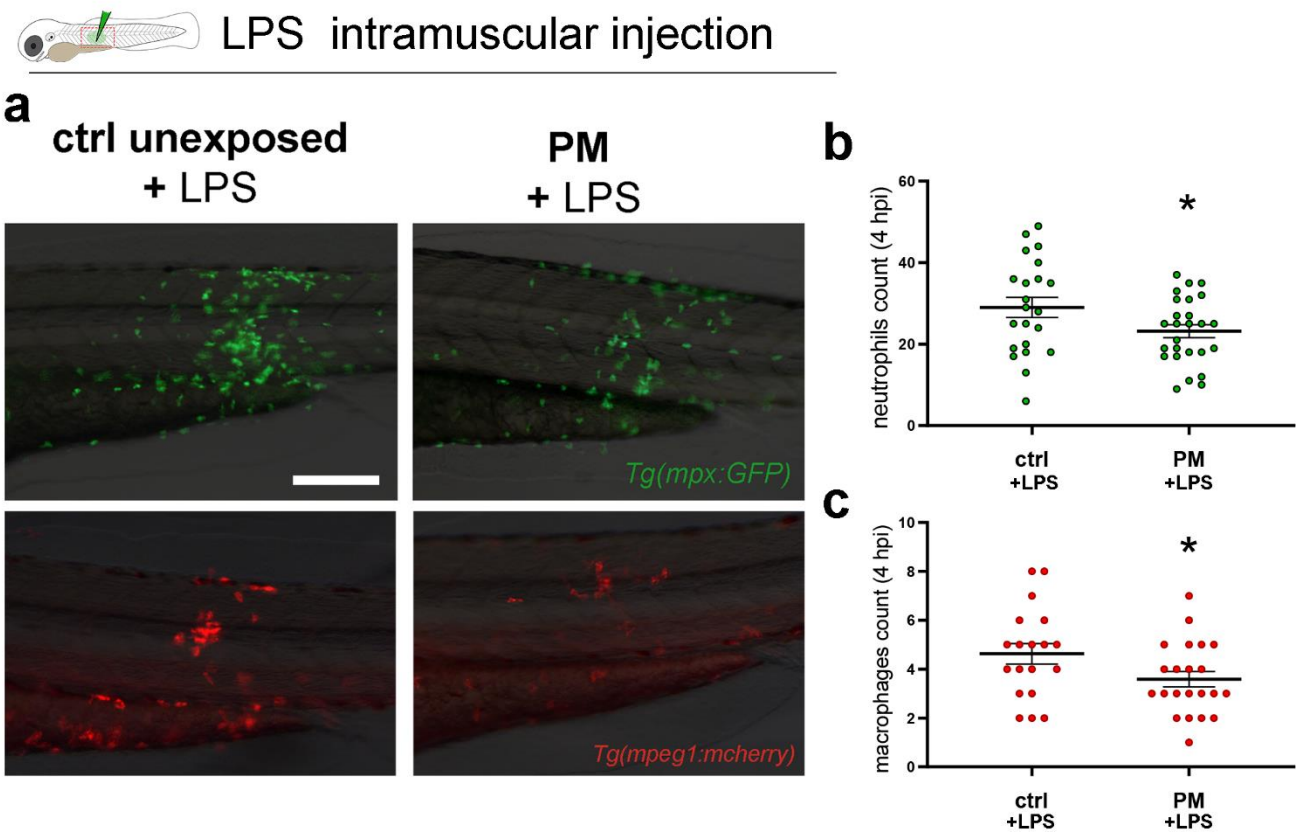

Figure 26. *Immunomodulatory effects of $PM_{2.5}$ exposure on neutrophil and macrophage recruitment after an acute infectious stimulus. Tg(mpx:EGFP) and Tg(mpeg1:mcherry) embryos exposed or not in SES to 45 µg/mL of $PM_{2.5}$ were analyzed for leukocytes migration at 4 hours post local intramuscular injection with LPS.* ***(a)*** *Representative panel of PM-exposed and unexposed 3 dpf larvae at 4 hpi of LPS.* ***(b)*** *mpx^+ neutrophils count and* ***(c)*** *$mpeg^+$ macrophages count at 4 hpi in trunk region (dashed box). Each dot represents a single individual and results are presented as mean ± SEM. Statistical significance was assessed by unpaired t-test with Welch's correction: *p < 0.05. Scale bar=100 µm.*

1.3.2.2 $PM_{2.5}$ dampened the expression of pro-inflammatory genes in response to infectious stimuli

The experimental design described above (section 1.3.2.1) was used also to test the effects on the inflammatory gene expression. 3 dpf exposed and unexposed larvae were systemically injected with *Pa*-LPS suspension into the circulation to quickly induce a strong inflammatory stimulus, as already reported [144,145], and after 8 hours post-injection immune response was assessed. As controls, for both PM-exposed and unexposed larvae, physiological solution was injected. In the graphs is reported the ratio of the expression levels of unexposed over PM-exposed larvae (Nexp/exp), each normalized on the value of the control (physiological solution) of the same category (**Figure 27**). Consistently with the effect on the migration of leukocytes, the relative expression level of the pro-

inflammatory cytokines was significantly lower in PM-exposed larvae. In particular, *il-1β* relative expression resulted more than doubled in unexposed (i.e., ratio= 2.28, *p-value* 0.0352), *il-8* almost doubled (i.e., ratio =1.81, *p-value 0.0217*) and *tnf-α* more than tripled (i.e. ratio=3.2, *p-value 0.0449*) (**Figure 27a,c,d**). Also, ROS production-related marker *cox2a* was lower in larvae upon $PM_{2.5}$ exposure (*p-value 0.0237*) (**Figure 27f**). On the other hand, although not significantly (*p-value* 0.171), the relative level of the anti-inflammatory cytokine *il-10* resulted conversely higher in pre-exposed larvae (**Figure 27e**).

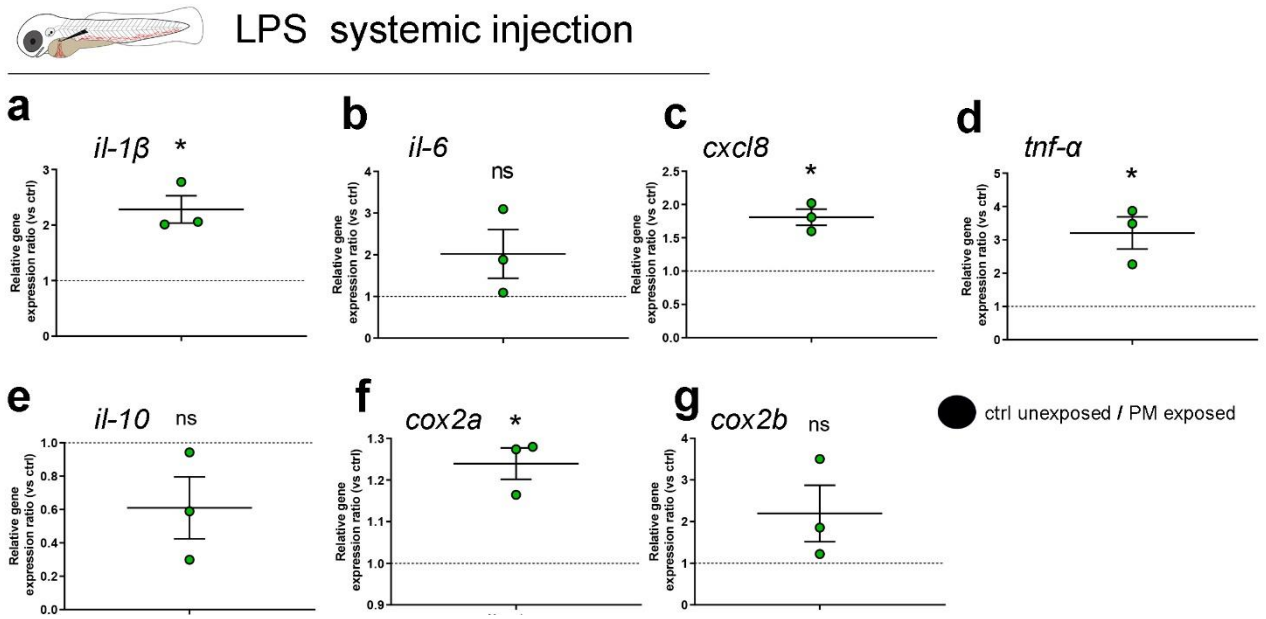

Figure 27. *Immunomodulatory effects of $PM_{2.5}$ exposure on the response to a systemic infectious stimulus. Larvae exposed or not in SES to 45 µg/mL of $PM_{2.5}$ were analyzed for inflammatory markers expression at 4 hours post systemic injection with LPS or physiological solution.* ***(a-g)*** *Relative gene expression of inflammatory markers considering the ratio between levels of ctrl unexposed +LPS over the levels of PM-exposed +LPS larvae (each value normalized on its own control represented by physiological solution-injected larvae). For each gene, results are presented as mean ± SEM of three independent experiments (Dots represent single experiment). Statistical significance was assessed by one sample t-test. *p < 0.05; ns= not significant.*

1.3.2.3 ROS production in response to infectious stimuli is impaired by exposure to $PM_{2.5}$

To investigate whether the effects of $PM_{2.5}$ exposure may impair respiratory burst in response to infectious stimuli, 3 dpf *Pa*-LPS intramuscular-injected *Tg(mpx:GFP)* larvae pre-exposed or not with $PM_{2.5}$ were assessed for intracellular ROS production through Dihydroethidium (DHE) staining, a cell permeable probe that fluoresces (red) when it reacts with superoxide within the cell. At 4 hpi live larvae were stained with DHE, and neutrophils and ROS local quantification was performed (**Figure**

28a). At 4 hpi DHE$^+$ cell count was significantly decreased in larvae pre-exposed to $PM_{2.5}$ (i.e., 6.6 vs 9.3 *p-value 0.0342*), suggesting a dampened ROS-mediated response (**Figure 28b**). Considering the average number of neutrophils actively producing ROS/larva (i.e., mpx$^+$DHE$^+$ cell count) no marked differences between the two categories were observed (**Figure 28c**). However, even though recruited neutrophils at the infection site were less in pre-exposed larvae as expected by previous analyses (see 1.3.2.1, Figure 25), they were able to produce the same amount of ROS with respect to controls. Indeed, the relative amount of mpx$^+$ DHE$^+$ cells normalized on the number of neutrophils locally recruited at the site of infection resulted significantly increased, of about 4.7% (i.e., unexposed controls=13.5% vs PM-exposed=18.2%, *p-value 0.0412*) (**Figure 28d**).

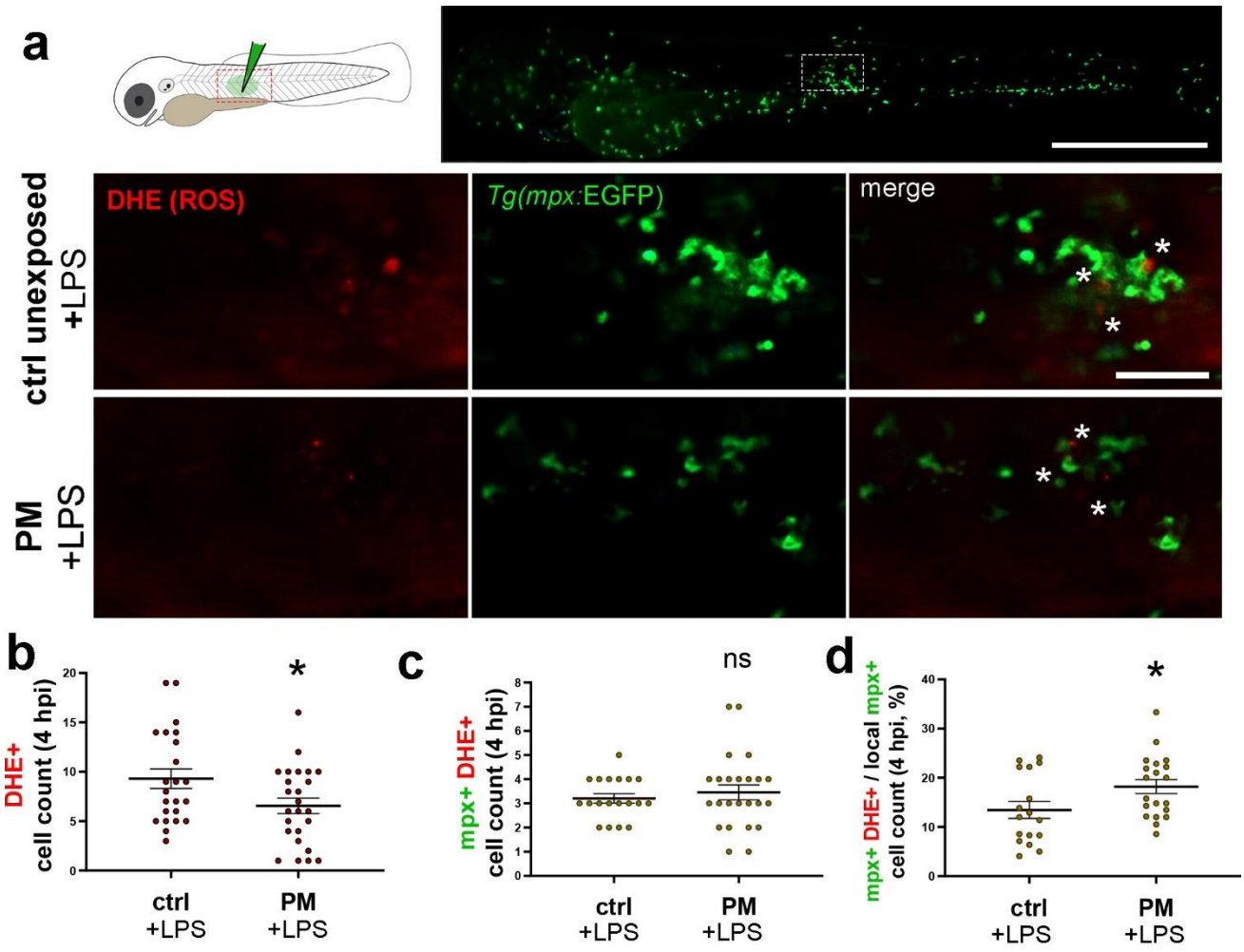

Figure 28. *Immunomodulatory effects of $PM_{2.5}$ exposure on ROS production after an acute infectious stimulus. Tg(mpx:EGFP) embryos exposed or not in SES to 45 µg/mL of $PM_{2.5}$ were analyzed for the production of ROS through DHE staining assay at 4 hours post local intramuscular LPS injection.* ***(a)*** *Representative panel of PM-exposed and unexposed 3 dpf larvae at 4 hpi of LPS. Upper part, schematic representation of injection site and*

lateral view of whole injected-larva; left panel DHE staining, middle panel mpx$^+$ neutrophils, right panel merge, an injection site (dashed box). Scale bars= 500µm (upper panel) and 20 µm (lower panel) ***(b)*** *DHE$^+$ cells quantification in injection region (dashed box);* ***(c)*** *quantification of neutrophils actively producing ROS (mpx$^+$ DHE$^+$ cell count);* ***(d)*** *percent of mpx$^+$DHE$^+$ cells over locally recruited mpx$^+$ cells at the injection region. Results are presented as mean ± SEM (Dots represent data for single individuals). Statistical significance was assessed by unpaired t-test with Welch's correction. *p < 0.05; ns= not significant.*

1.3.2.4 $PM_{2.5}$ exposure alters leukocytic response to sterile wounds

To further analyze the effects of $PM_{2.5}$ exposure on a sterile inflammatory trigger [63], a small portion of the tailfin of 3 dpf larvae pre-exposed or not to $PM_{2.5}$ was amputated and leukocytes recruitment to the caudal region of larva was quantified (**Figure 29a**). At 6 hours post-amputation (hpa), when leukocyte migration reaches the peak at site of injury [51], both neutrophils and macrophages migrated toward the wounded area, but exposure to $PM_{2.5}$ reduced their migration capacity (**Figure 29b-c**).

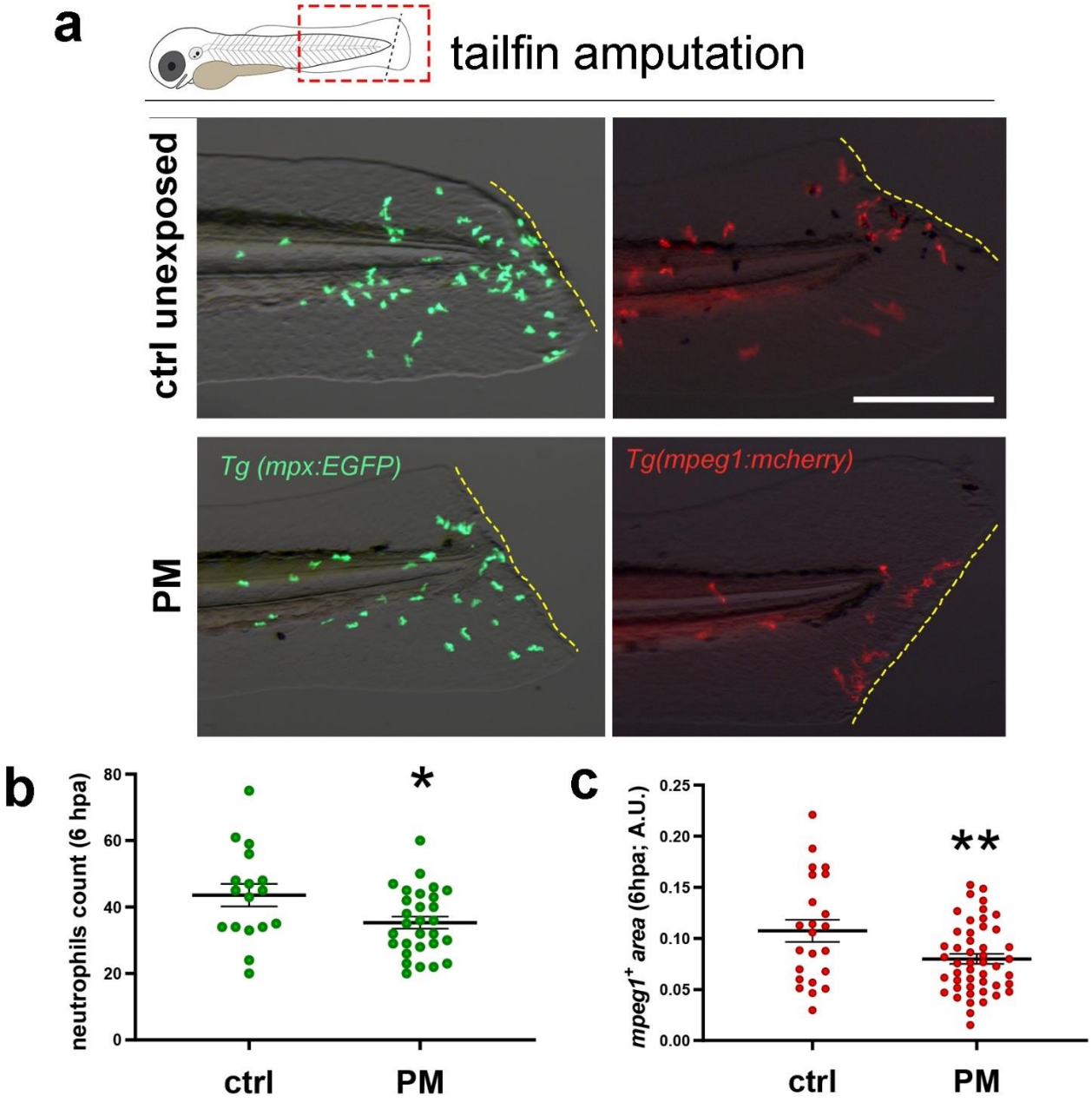

Figure 29. *Immunomodulatory effects of $PM_{2.5}$ exposure on neutrophil and macrophage recruitment after an acute sterile stimulus. Tg(mpx:EGFP) and Tg(mpeg1:mcherry) embryos exposed or not in SES to 45 µg/mL of $PM_{2.5}$ were analyzed for leukocytes migration at 6 hours post amputation (hpa) of the tailfin.* ***(a)*** *Representative panel of PM-exposed and unexposed 3 dpf larvae at 6 hpa.* ***(b)*** *mpx^+ neutrophils count and* ***(c)*** *$mpeg^+$ area at 6 hpa at the site of injury (red dashed box). Each dot represents a single individual and results are presented as mean ± SEM. Statistical significance was assessed by unpaired t-test with Welch's correction: *p < 0.05. Scale bar= 50µm.*

1.4 Discussion

Clinical and epidemiological research extensively demonstrated the association between PM exposure and numerous adverse systemic inflammations and physiological diseases [146,147]. A greater impact has been reported for specific hypersusceptible categories, such as infants [9]. To effectively address this public health danger, strengthening actions are needed, especially for some areas such as the city of Milan, situated in one of the most polluted regions of all Europe (i.e., Po valley), as reported by WHO and EEA [1,148].

Evidence from *in vitro* and *in vivo* studies suggests that short-term exposure to $PM_{2.5}$ and PM_{10} leads to airway inflammation [9,35] mainly due to the induction of high levels of several pro-inflammatory markers, such as the key cytokines IL-1β, IL-6, IL-8, granulocyte/macrophage colony-stimulating factor (GM-CSF), MIP-1α/β, TNF-α, and Cox-2 [9,149,150] and due to increased endothelial activation and oxidative stress [21,32,151]. This scenario promotes a strong recruitment of leukocytes to the airways, with impaired physiological activity (e.g., altered phagocytic ability) [27,39]. The aberrant hyperactivation of immune cells might result in an increased susceptibility to bacterial and viral infections, due to an enhanced infection burden, particularly in infants. For example, high levels of airway inflammation have also been associated with severe bronchiolitis [152,153]. *In vivo* experimental models represent essential tools to shed light on the mechanisms underlying PM toxicity since fundamental information on the biological system can be gathered through the study of peculiar molecular and cellular responses that cause the different physiological outcomes [9]. Mammalian models, despite having an intermediate level of complexity, are generally expensive and time-consuming and have also ethical implications. In the last years, the mouse model has been used to study the effects of PM exposure on the airways, but it resulted not suitable for dissecting the short-term immunomodulatory impact on innate immunity response [9,71], which represents the first fundamental response to exogenous inflammatory stimuli. Zebrafish has emerged as a powerful animal model for environmental and toxicological studies [65–67]. In the last years, studies concerning investigations of the harmful effects of PM on environmental health using zebrafish as an alternative model have been published, as reviewed by Smoot *et al.,* [71]. However, most of these studies are based on the investigation of large-scale effects on multi-organs or developmental toxicity caused by PM exposure [66,73,74].. Zebrafish represents an ideal model for studying innate immunity due to the lack of adaptative response in the first weeks of life [46] and due to the

conservation of the immune cell populations with humans [48]. In this part of the thesis, we generated an *in vivo* zebrafish model with the aim to mimic the immunomodulatory effects of the PM-exposure in humans. For these purposes, the experiments were conducted by using the $PM_{2.5}$ collected in an urban site of the metropolitan area of Milan (Como, 40 km north of Milan) during the winter 2019 and provided by the group of Professor Andrea Cattaneo (University of Insubria, Como) [137]. The chemical composition of the sampled PM had already been characterized and was similar to the PM of urban areas of Milan [154–156], potentially leading to comparable effects on the immune response. To date, only few studies have analyzed the inflammatory effects of PM using zebrafish model [75–77]. Moreover, in the most of them the authors analyzed the effects of urban fine-PM with a different chemical composition in comparison with the present study, due to the different geographical collection area (e.g. the most of studies were conducted in China). Indeed, the PM used in the cited studies, although with similar % content of organic carbon and inorganic ionic components, result in general richer in some metals as lead (10-20 folds), manganese (5-10 folds), cadmium (>100 folds) and chrome (3-5 folds) [66,75,76,157–159]. Moreover, a direct focus on the effects on innate immunity and the functional mechanisms underlying the toxic outcomes of PM is lacking.

The exposure of zebrafish embryos to 45 µg/mL of $PM_{2.5}$ for a relative short time-window (i.e. 18 hours) was individuated as an appropriate exposure setting that did not induce mortality or morphological alterations of the embryos, allowing the study of innate immunity. On the contrary, a concentration-dependent effect was observed as, from the concentration of 75 µg/mL of $PM_{2.5,}$ the mortality rate went to about 75-85% and survival larvae presented marked morphological alteration and diffused necrosis. The toxicity exhibited at concentrations greater than 45 µg/mL could be due to mechanical effects, since $PM_{2.5}$ might be accumulated on the surface of the embryo, therefore inhibiting molecule exchange with the growth medium, such as O_2 uptake. In the few published studies in the field [71], the authors exposed embryos to a concentration of urban-derived $PM_{2.5}$ more than triple and even up to 200 µg/mL without observing high mortality rate. These differences might be explained mainly by a different preparation of PM samples and by different areas of collection (e.g., urban areas of Beijing, China or Washington DC, USA). Moreover, different timing of exposure must be considered: we decided to expose embryos from the stage of 30 hpf, a developmental stage in which they possess fully mature leukocyte populations [50]. In general, we observed that exposure to $PM_{2.5}$ elicited strong pro-inflammatory effects in zebrafish larvae. Some key pro-inflammatory markers, such as *il-1β*, *il-6*, *tnf-α* and *cxcl8* were upregulated, in line with those

described altered in the context of human airway inflammation [9,149,150]. Epidemiological studies on the association of *il*-6 with $PM_{2.5}$ exposure reported inconsistent results [153,160,161], although *il-6* and *cxcl8* overexpression is known to be prognostic markers positively associated with viral-induced respiratory symptoms [9,162]. The described inflammatory environment was confirmed by the analysis of the activation of leukocytes, as already shown following environmental exposure to PM in human subjects [9,163]. The hyperactivation of neutrophils in larvae was observed both in early (25 hours) and late (42 hours) time post-exposure in a concentration-dependent manner. To note, in the late time point analyzed neutrophils activation was even more marked, since it was present also at lower concentrations of $PM_{2.5}$ (i.e., 15 and 30 µg/mL). This outcome may be due to a positive feedback loop effect, dependent on the increased presence of activated neutrophils. Indeed, *cxcl8,* the main chemokine to which neutrophils respond, resulted concurrently upregulated at that time point (42 hpe). This effect has been largely described and feedback amplification is critical to the neutrophil-mediated response to tissue damage by exogenous agents [164]. Interestingly, we did not observe the concomitant activation of the macrophage cell population, suggesting a different responsiveness of the two cell populations to $PM_{2.5}$ exposure. Nevertheless, as for the neutrophil population, we also observed an impaired distribution of macrophages, since their concentration was increased in the head region of larvae at 42 hpe. Notably, in this region, at the stage of 2 dpf, some sensitive structures accessible to exogenous agents, such as branchial arches and rudiment of gills and mouth, are present [136]. The preferential recruitment we observed was likely due to the direct contact between these structures and $PM_{2.5}$ particles, which in turn may have been cleared through local phagocytic activity. Exposure to labeled-PM in future experiments would address this hypothesis. As we used *mpeg* reporter to follow live macrophage activity, we had no information on the predominant pro/anti-inflammatory setting of macrophages [58]. Nonetheless, since the observed overexpression of *tnf-α* at 42hpe*,* we could speculate the pro-inflammatory M1-like setting as the predominant one. Association of PM exposure with endothelial dysfunction (e.g., vascular endothelium activation by increasing VCAM-1 and ICAM-1 level) leads to increased risk of cardiovascular diseases [161,163,165]. In line with this evidence, activated endothelial markers were upregulated in PM-exposed embryos, increasing the value and adherence of this model of inflammation.

Several epidemiological and *in vivo* studies have shown associations between short-term exposure to PM and the alteration of the immune response, leading to an increased risk of contracting and/or exacerbating acute respiratory diseases in children [15,16,166]. For example, RSV infections are

promoted by an inflamed airways environment due to impaired weaker immune defenses, leading to the development of more severe forms of bronchiolitis, especially in infants [25,93,167]. Yet, the mechanisms that alter the immune response to an acute inflammatory stimulus (e.g., bacterial or viral infections), and which underlying short-term $PM_{2.5}$ toxicity is still unclear. Neutrophils and monocytes/macrophages recruitment plays an essential role in the first response to acute inflammatory stimuli [168]. To model this context and dissect the underlying molecular mechanisms, we assessed the effects caused by infectious and sterile second inflammatory triggers on the innate immune response of larvae pre-exposed to 45 µg/mL of $PM_{2.5}$. To our knowledge, this is the first time that immunomodulatory effects of PM exposure have been tested after a second acute inflammatory trigger in the zebrafish model [71]. We took advantage of *Pa*-LPS local/systemic injection models, to induce rapid acute inflammatory stimuli: microinjection of bacterial LPS at high concentration inside the brain ventricle or intramuscularly in larvae at 3 dpf elicited strong leukocytes recruitment [70,169,170]. These models provoke strictly local inflammation sites, thus representing suitable systems to study leukocytes recruitment toward a defined region. The analysis of neutrophil behavior in these models showed a reduced migratory capacity in $PM_{2.5}$-exposed larvae. To note, we did not observe an altered macrophage migration after the brain ventricle inflammatory trigger. $PM_{2.5}$ exposure alone resulted in an augmented concentration of macrophages in head region, thus the altered response to a second inflammatory trigger in the same region could likely be masked and consequently undetectable. Therefore, this effect was probably not due to a different sensitivity of the two leukocyte populations, but was due to the model system used.

The production of ROS is mainly exerted by phagocytes and plays a key role in the elimination of infectious agents through the respiratory burst. Indeed, when ROS production is altered the infections could more easily exacerbate [59,171,172]. It is well known that $PM_{2.5}$ exposure provokes an impairment in ROS production, thus potentially exposing it to oxidative stress and pathogens colonization [173,174]. From our analysis, ROS production following local inflammatory stimulus was decreased in $PM_{2.5}$ pre-exposed larvae. A limitation of the ROS detection assay that we performed (*i.e.* DHE) was the impossibility to determine the effects of PM exposure alone on ROS production. Nevertheless, these data suggest a dampened ROS-mediated response in larvae. However, by analyzing neutrophils actively producing ROS, we did not observe differences between PM-exposed and not-exposed larvae. Therefore, since PM exposure leads to a decrease in neutrophil recruitment at the inflamed site, our results highlighted a potential overload in neutrophils activity in larvae pre-exposed to PM. In turn, the impaired respiratory burst might lead to a lowered responsiveness to

infectious stimuli. In line with this, the gene expression of inflammatory cytokines after an acute systemic inflammatory trigger resulted altered, highlighting an attenuate systemic response to the second stimulus. In addition, we tested this framework in a sterile model of inflammation, by analyzing leukocyte migration toward a wound site, obtaining similar results that emphasized a dampened response of the assessed leukocytic populations.

CHAPTER 2

Effects of PM exposure on bronchiolitis and respiratory microbiota in infants

This chapter is partly based on:

Milani GP, **Cafora M**, Favero C, Luganini A, Carugno M, Lenzi E, Pistocchi A, Pinatel E, Pariota L, Ferrari L, Bollati V.; 2022. *PM2.5, PM10 and bronchiolitis severity: A cohort study*. Pediatric Allergy and Immunology.
doi: 10.1111/pai.13853

2.1 Summary

Acute bronchiolitis is commonly caused by a viral infection of the lower airways and is estimated to be the leading cause of hospitalization of infants and young children worldwide. Respiratory syncytial virus (RSV) infection represents the causative agent of the vast majority of the cases. The severity of the disease is only partially explained by current known risk factors. Since some studies have pointed out as environmental factors, especially air pollution, could modulate the phenotype of this disease, the present chapter of the thesis will investigate the effects of short-term exposure to airborne particulate matter (PM) on the onset and severity of RSV bronchiolitis in infants. The present population study takes advantage of a cohort composed of 110 infants with bronchiolitis and 49 matched healthy controls living in the area of Milan, Italy. The analyses are based on estimates of PM_{10} and $PM_{2.5}$ obtained from ARPA Lombardy and assigned to each subject. The respiratory microbiota is at the interface between the environment and the host and mounting evidence indicates that it has a role in modulating the effects of airway pollutants as well as in the protection against pathogens. Thus, the composition of the upper respiratory tract microbiota of infants was also explored by metataxonomic approaches (16S analysis) on nasal swab samples. The main aims of the present chapter are ***i***) to investigate the relationship between PM exposure and severity of RSV bronchiolitis; ***ii***) to unveil a possible correlation between respiratory microbiota pattern and the probability of being diagnosed with RSV bronchiolitis, as well as the impact of PM exposure on the nasal microbiota alterations identified.

2.2 Materials & Methods

2.2.1 Subject recruitment and schedule

Subjects of this study were recruited between November 2019 and February 2020 at the pediatric emergency department of the Fondazione IRCCS Ca' Granda Ospedale Maggiore Policlinico, Milan, Italy. 110 infants <1 year of age visiting the emergency department for bronchiolitis were enrolled and defined as cases. Bronchiolitis was diagnosed in infants with acute infection of the upper airways in the previous week, followed by acute respiratory distress with persistent cough and diffuse crackles on auscultation, as described in Milani *et al.* [175]. Infants who had pre-existing health conditions that could be associated with a more serious clinical course of bronchiolitis (infants suffering from bronchopulmonary dysplasia or under chronic immunosuppressant treatment) were excluded. 49 infants matched for age and gender and with no symptoms compatible with ongoing inflammatory processes were enrolled during routine visits (e.g., vaccine) and defined as healthy controls (HC). At the enrollment, for each subject, two nasal swabs were collected following WHO guidelines (https://goo.gl/pMzSrT) and stored in sterile plastic vials at -80°C until nucleic acid extraction for downstream analyses. Bronchiolitis severity score on 110 cases was assessed by a trained pediatrician according to standard protocols [176]. This evaluation was based on the following parameters: oxygen saturation (>95% =0, 95–90% =1, <90% =2), thoracic retractions (no retractions =0; present =1; present with nasal flare =2), respiratory frequency (<45/min =0; 45–60/ min =1; >60/ min =2), and capacity to feed (normal =0; reduced =1; strongly reduced =2). From the sum of these parameters, the disease severity was defined as severe (>7), moderate (4-6), or mild (<4) [175,177]. By using a standardized questionnaire, for each infant information including age, gender, weight and length (at birth and enrollment), ethnicity, delivery mode, allergies, attendance to daycare, presence and the number of siblings and pets, and history of antibiotics treatments were collected. Moreover, information about demographics, lifestyle, and habits from both parents was also collected, as well as information on the use of antibiotics during pregnancy/breastfeeding and the outcome of a vaginal swab at the end of the pregnancy for Group B Streptococcus from the mother.

This study was approved by the ethical committee of the Fondazione IRCCS Ca' Granda Ospedale Maggiore Policlinico (Milan, Italy) and an informed consent was obtained by the parents of the infants.

2.2.2 Particulate matter (PM) exposure data collection

Daily airborne PM_{10} and $PM_{2.5}$ concentrations were retrieved from daily mean estimates of municipal aggregate values measured by Regional Environmental Protection Agency (ARPA) Lombardy, which were contained in the Open Data Lombardy Region database (https://www.dati.lombardia.it). Daily pollutant concentrations were estimated based on the ARIA Regional Modeling (www.aria-net.it), a chemical-physical model of air quality that simulates the dispersion and chemical reactions of pollutants in the atmosphere. Meteorological data, emissions, and concentrations at the beginning of a simulation period are integrated with the data measured from the monitoring stations of ARPA Lombardy air quality network. The domain of the simulation with the air quality model ARIA covers the whole Lombard territory, with a grid of 1x1Km^2 cells, providing daily estimates at municipality resolution available from the website. The estimated levels of daily PM_{10} and $PM_{2.5}$ concentrations of the municipality of residence were assigned to each subject for the 29 days preceding the severity score retained for the analysis (from day -1 to day -29). PM levels of the Municipality of Milan were considered as representative of mean concentrations during the day of enrollment (day -0) or during hospitalization. Subsequently, the average exposure levels were calculated for each of the four weeks before enrollment.

2.2.3 RSV RNA detection

To extract viral RNA from the nasal swab sample, Qiagen QIAamp Virlal RNA Mini kit was used according to the manufacturer's guidelines. Purified RNA was eluted in 50 µl and stored at -80°C. The quantification of RSV RNA level was performed by using a commercial RT-qPCR kit (PrimerDesign genesig; PrimerDesign Ltd.). QuantStudio3 real-time PCR system (Applied Biosystem) was used to carry out qPCR and the generation of a standard curve and template negative controls (sterile water) were included in each assay.

2.2.4 Microbiome analysis: sample processing

Total bacterial DNA was extracted from the second nasal swab using QIAamp® UCP Pathogen Mini (QIAGen, Germany) following manufacturers guidelines. The obtained DNA was then stored at -20°C until the samples were shipped to our collaborators (Institute of Biomedical Technologies, National Research Council, Segrate, Italy) to perform quantitative and qualitative assessment, PCR amplification and sequencing analysis (including libraries preparation). Metabarcode sequencing

analyses were performed to investigate the bacterial nasal membership. rRNA gene region V3-V4 was amplified and then sequenced through the Illumina MiSeq platform using a paired-end library of 300 bp insert size.

2.2.5 Microbiome analysis: sequencer output upstream analysis

Raw sequencing reads were, at first, merged in a single fragment covering the whole V3-V4 16S rRNA amplicon (size: ~460bp) by PandaSeq [178] thanks to the fact that the forward and reverse read of the sequencing fragment had about 150 overlapping bases. Then, low-quality bases and reads were removed using the "split_libraries_fastq.py" script in QIIME v.1.9.0 [179]. Operational taxonomic units (OTUs) were created by UCLUST algorithm at 97% identity in QIIME and retaining only those supported by 5 or more reads as bona fide OTUs. Taxonomic assignment of OTUs was performed by RDP classifier [180] against SILVA 132 database (https://www.arb-silva.de/fileadmin/silva_databases/qiime/Silva_132_release.zip) using 0.8 as the confidence threshold. In order to have a meaningful description of the microbial ecosystem, a total of 10 samples with less than 2000 reads each were excluded from the analysis; thus, the final dataset comprised 149 samples, 103 bronchiolitis cases and 46 healthy controls.

2.2.6 Microbiome analysis: downstream analysis

Downstream statistical analyses (including alpha- and beta-diversity evaluations) were also carried out in QIIME 1.9.0 suite. Alpha-diversity analysis was performed using several metrics (i.e.: Shannon's diversity, chao1 diversity index, observed species indices). Beta-diversity analysis was based on unweighted and weighted UniFrac distances [181] and represented by Principal Coordinate Analysis (PCoA), where the first and second principal components (PC1 and PC2) explained the largest possible variance among samples. A Permutational Multivariate Analysis of Variance (PEMANOVA) using Distance Matrices (pseudo-F ratios) was used to define whether there was a significant difference among the experimental groups.

2.2.7 Microbiome analysis: species -level analysis

Species-level identification within the *Haemopilus* genus was performed by aligning with BLAST (v 2.2.26) [182] all the reads belonging to that genus to a custom reference database made up collecting all available reference sequences in NIH-NCBI database (ftp://ftp.ncbi.nlm.nih.gov/genomes/refseq/bacteria/) as of 09/10/2020. All genomes with a

finishing status of “complete genome”, “Scaffold” or “Contigs” were selected. Overall, 45930 sequences from 905 strains belonging to 13 species (i.e.: *H. aegyptius, H. haemoglobinophilus, H. haemolyticus, H. haemophilus, H. influenzae, H. massiliensis, H. paracuniculus, H. parahaemolyticus, H. parainfluenzae, H. paraphrohaemolyticus, H. pittmaniae, H. quentini, H. sputorum*) were retrieved. BLAST-derived matches were filtered in order to retrieve an unequivocal classification for each read. When a read mapped identically on two or more references from different species, the classification was reset to “Unclassified *Haemophilus*”.

2.2.8 Statistical analysis

The summary statistics of the characteristics related to study subjects were reported in terms of in terms of mean and standard deviation (SD) or median and 1st quartile – 3rd quartile, as appropriate, for continuous variables and in terms of frequency and percentage for categorical variables. Differences between case and control groups were assessed through t-test or the Wilcoxon signed sum rank test for continuous variables, as appropriate, or through Pearson’s chi-square test or Fisher’s exact test for categorical data.

Regarding the effect of $PM_{2.5}$ and PM_{10} on bronchiolitis severity, univariate and multivariable ordinal logistic regression models were fitted. The response variable was the severity score, using seven ordinal categories. To evaluate short-term exposure, PM levels were retrieved back to 30 lags day from the day of enrollment and as averages over the following time periods: one week, two weeks, three weeks and one month; the average of PM in first, second, third and fourth week was also calculated.

Multivariable analyses were adjusted for age, gender, ethnicity, and use of antibiotics in the month before enrollment and use of antibiotics during pregnancy. After verifying the presence of an association in an univariate model, potential confounders were included in the multivariable model. Estimated effects are reported as β and 95% CI associated with an increase in PM exposure of 1μg/m^3.

To assess differences between the alpha-diversity indices in cases and controls we applied ANCOVA models adjusted for age, gender, ethnicity, use of antibiotics in the last month, PM mean levels during the third week before the bronchiolitis assessment and apparent temperature. The alpha-diversity indices were log-transformed to achieve a normal distribution. Marginal mean were reported as geometric means and 95% CI.

To evaluate the differences between genera relative abundances in cases and controls, we applied negative binomial regression for over-dispersed count observations. We tested the presence of over-dispersion based upon the Lagrange Multiplier (LM) test. Models were adjusted for age, gender, ethnicity, use of antibiotics in the last month, PM exposure during the third week before the assessment and apparent temperature. Estimated effects are reported as marginal geometric means and 95% CI. To take into account the high number of comparisons, we calculated q-FDR values using the multiple comparison methods based on Benjamini–Hochberg False Discovery Rate (FDR).

To examine the potential modifying effect of PM on the association between case control status and genera relative abundance we added an interaction term between PM and case control status in each model. We evaluated whether the effect of bronchiolitis on genera relative abundances differs depending on PM levels. The values selected for PM were the following: mean - SD (PM_{10}:21.2µg/m^3, $PM_{2.5}$:16.2 µg/m^3), mean (PM_{10}:36.9 µg/m^3, $PM_{2.5}$:28 µg/m^3) and mean + SD (PM_{10}:52.7 µg/m^3, $PM_{2.5}$:39.8 µg/m^3). Statistical analyses were performed with SAS software (version 9.4; SAS Institute Inc., Cary, NC, USA). A two-sided p-value of 0.05 was considered statistically significant.

2.3 Results

2.3.1 Characteristics of the enrolled subjects and PM exposure assessment.

A total of 110 infants with bronchiolitis (mean age 6.3 ± 5.5 months, 60.9 % males), were included as cases for the study. 49 infants matched for age and sex with cases (mean age 6.5 ± 5.7 months, 55.1 % males), during routine primary care visits and with no symptoms compatible with ongoing inflammatory processes, were enrolled as healthy controls (HC). The main characteristics of the overall study population are reported in **Table 3**. The subjects lived mainly in the metropolitan area of Milan (HC=93.9%, cases=98%) and the ethnicity was matched in the two study groups (mostly Caucasians, HC=93.9%, cases=79%). No differences were found between the two study groups for weight and length both at birth and at enrollment. A higher percentage of cases (22.9%) assumed antibiotics after birth with respect to HC (8,2%), but not during the month before the enrollment. Some of the known risk factors for the contraction of RSV infection differed between the two groups and in particular, the mean gestational age, the daycare attendance, and the presence of siblings were higher in cases. No differences were observed between the parents of the two groups (**Suppl**. **Table 1**), excluding the assumption of antibiotics during breastfeeding, which was lower in the mothers of the cases (HC=24,5%, cases=11,1%; *p-value*=0,0309).

Table 3 *- Characteristics of study participants by case-control status (N=159).*

Characteristics	Case (N=110)	HC (N=49)	*p-value*
Age, months mean ± SD	6.3 ± 5.5	6.5 ± 5.7	0.7928 ł
Gender, N (%)			
Males	67 (60.9)	27 (55.1)	0.4916●
Females	43 (39.1)	22 (44.9)	
Birth weigth, g mean ± SD	3204 ± 550	3301 ± 459	0.2857 ł
Birth lenght, cm mean ± SD	49.6 ± 2.2	50.2 ± 2.7	0.1493 ł
Weigth, g mean ± SD	7197 ± 2238	7111 ± 2237	0.8396 ł
Lenght, cm mean ± SD	64.8 ± 10	63.8 ± 8.3	0.6180 ł
Living area, N (%)			
City of Milan	73 (66)	33 (67.4)	0.2690*
Province of Milan, outside city area	35 (32)	13 (26.5)	
Province of Monza Brianza	1 (0.9)	2 (4.1)	
Province of Varese	1 (0.9)	0 (0.0)	
Outside Lombardy region	0 (0.0)	1 (2.0)	

Ethnicity, N (%)			
Cuacasian	87 (79)	46 (93.9)	
African	6 (5.4)	0 (0.0)	
Asian	11 (10.0)	3 (6.1)	0.1042*
Multi-ethnic	6 (5.4)	0 (0.0)	
Delivery mode, N (%)			
Vaginal delivery	68 (61.8)	36 (73.5)	
Vacuum	5 (4.6)	2 (4.1)	
Emergency cesarean section	12 (10.9)	7 (14.3)	0.1455*
Elective cesarean section	25 (22.7)	4 (8.2)	
Systemic antibiotic after birth, N (%)			
Yes	25 (22.9)	4 (8.2)	
No	84 (77.1)	45 (91.8)	0.0274*
Systemic antibiotic in the last month, N(%)			
Yes	6 (5.4)	0 (0.0)	
No	104 (94.6)	49 (100.0)	0.1782*
Allergy, N (%)			
Yes	3 (2.8)	1 (2.1)	
No	105 (97.2)	47 (97.9)	1 *
Daycare attendance, N (%)			
Yes	26 (23.9)	5 (10.2)	
No	83 (76.1)	44 (89.8)	0.0457●
Siblings, N (%)			
Yes	80 (72.7)	20 (40.8)	
No	30 (27.3)	29 (59.2)	0.0001●
Number of siblings, N (%)			
0	31 (28.2)	29 (59.2)	
1	50 (45.4)	14 (28.6)	
2	23 (20.9)	2 (4.1)	
3	6 (5.5)	1 (2.0)	
4	0 (0.0)	2 (4.1)	<0.0001*
5	0 (0.0)	1 (2.0)	
Siblings attending daycare/school, N (%)			
Yes	73 (92.4)	16 (80.0)	0,1130
No	6 (7.6)	4 (20.0)	
Pets at home, N (%)			
Yes	25 (22.7)	7 (14.6)	0.2410●
No	85 (77.3)	41 (85.4)	

Current breastfeeding, N (%)			
Yes	69 (62.7)	33 (67.4)	0.5749●
No	41 (37.3)	16 (32.7)	
Gestational age, weeks median [Q1-Q3]	38 [38-40]	40 [38;40]	0.0096Δ
Bronchiolitis severity score, median [Q1;Q3]	3 [2;4]	0 [0;0]	0.4051●

SD: standard deviation, Q1: first quartile, Q3: third quartile.
Continuous variables are expressed as mean ± SD or as median [Q1;Q3] as appropriate, discrete variables are expressed as counts (%).
ł The p-values were calculated by T-test.
Δ The p-values were calculated by Wilcoxon signed rank sum test.
● The p-values were calculated by chi-square test.
** The p-values were calculated by Fisher exact test*

2.3.2 Bronchiolitis severity assessment

On the total of 110 infants with bronchiolitis enrolled as cases, positivity to RSV was detected in 64 (58%) through RT-qPCR assay. Considering total cases (n=110), the bronchiolitis severity was scored as mild in 75 subjects (68%), moderate in 34 (31%), and severe in only one (0.6%) case. Among the 64 infants positive for RSV (RSV+), the score of bronchiolitis was mild in 39 (61%) and moderate in 25 (39%). Mean severity scores of RSV+ and RSV- categories did not differ significantly (*p-value=* 0,1180) (**Figure 30**).

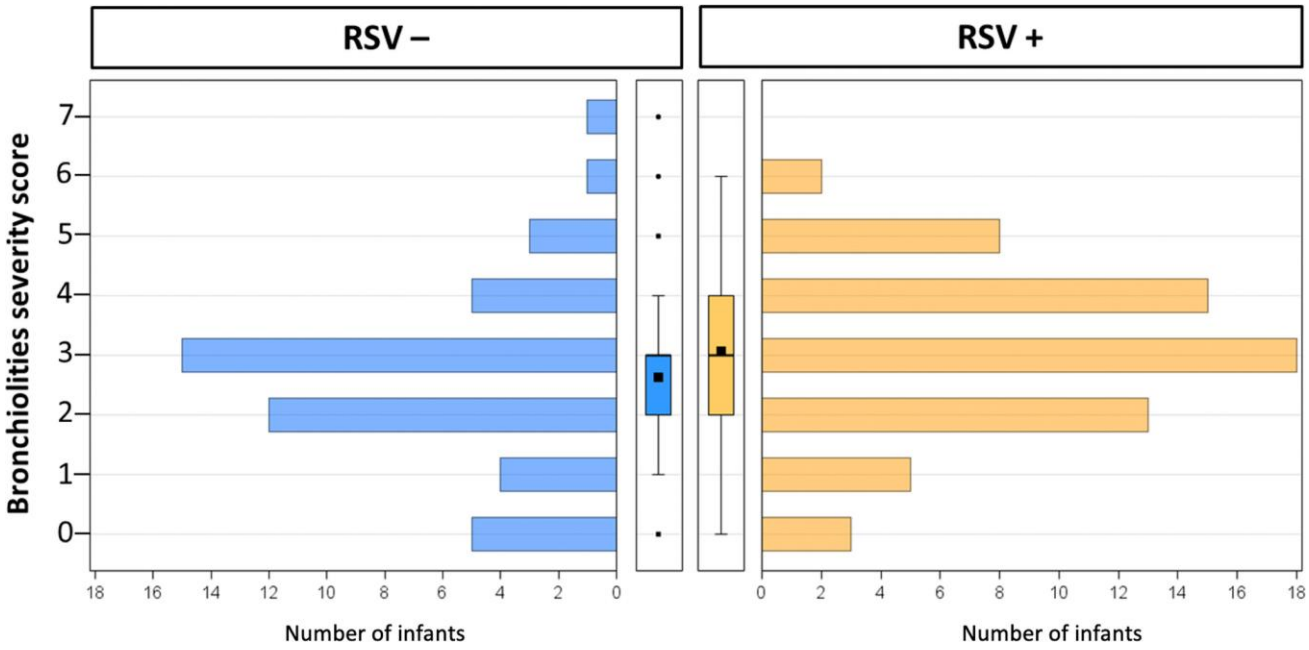

p-value from t-test= 0.1180

	Severity score of bronchiolitis							
	N	**min**	**max**	**median**	**q1**	**q3**	**mean**	**SD**
Cases of bronchiolitis	110	0	7	3	2	4	2.89	1.48
	N	**min**	**max**	**median**	**q1**	**q3**	**mean**	**SD**
RSV -	46	0	7	3	2	3	2.63	1.55
RSV +	64	0	6	3	2	4	3.08	1.41

***Figure* 30.** Bronchiolitis severity score (0 to 7) in infants with (RSV+) or without (RSV+) respiratory syncytial virus infection. Mean, distribution and standard deviation (SD) are shown. q1= 1st quartile; q3= 3rd quartile

2.3.3 Association between short-term PM_{10} and $PM_{2.5}$ exposure and bronchiolitis severity

Daily mean concentrations of PM_{10} and $PM_{2.5}$ were assigned to each case (n=110) and the means calculated for each time lag preceding the bronchiolitis severity peak (Day 0) are given in **Supplementary Table 2**. To verify the possible effect of $PM_{2.5}$ and PM_{10} exposures, a multivariable regression model was applied to bronchiolitis severity scores (N=110) and the results of the analysis are reported in **Table 4**. Mean $PM_{2.5}$ concentrations were positively associated with bronchiolitis severity on day -2 (β 0.0214; 95%CI 0.0011–0.0417; *p* = 0.0386), day -5 (β 0.0313; 95%CI 0.0054–0.0572; *p* = 0.0179), day -14 (β 0.0284; 95%CI 0.0078–0.0490, *p* = 0.0069), day -15 (β 0.0496; 95%CI 0.0242–0.0750; *p* = 0.0001) and day -16 (β 0.0327; 95%CI 0.0080–0.0574; *p* = 0.0093). Mean PM_{10} levels were positively associated with the bronchiolitis severity score on day -2 (β 0.0175; 95%CI 0.0015–0.0326; *p* = 0.0347), day -5 (β 0.0333; 95%CI 0.0067–0.0469; *p* = 0.0036), day -14 (β 0.0268;

95%CI 0.0062–0.0379; p = 0.0026), day -15 (β 0.0477; 95%CI 0.0167–0.0545; p < 0.0001) and day -16 (β 0.0336; 95%CI 0.0049–0.0412; p = 0.0008). Moreover, $PM_{2.5}$ and PM_{10} mean concentration levels of the third week before the enrollment (day -14 -20) were positively associated with the bronchiolitis severity score (β 0.0478, 95%CI 0.0173–0.0679, p = 0.0034; β 0.0426, 95%CI 0.0159–0.0797, p = 0.0010, respectively). Consistent results of association analyses were observed considering only $PM_{2.5}$ and PM_{10} exposure levels and bronchiolitis severity score of RSV^+ infants (**Supplementary Table 3**).

Table 4 *Association between short-term exposure to $PM_{2.5}$ and PM_{10} and bronchiolitis severity score (N=110 cases of bronchiolitis).*

PM_{10}	β	SE	95% CI		P-value
Day 0	0.0099	0.0090	-0.0077	0.0275	0.2684
Day -1	0.0131	0.0078	-0.0022	0.0283	0.0932
Day -2	**0.0175**	**0.0083**	**0.0013**	**0.0338**	**0.0347**
Day -3	0.0051	0.0074	-0.0094	0.0197	0.4876
Day -4	0.0125	0.0086	-0.0044	0.0295	0.1462
Day -5	**0.0333**	**0.0114**	**0.0109**	**0.0557**	**0.0036**
Day -6	0.0088	0.0094	-0.0097	0.0272	0.3504
Day -7	0.0049	0.0096	-0.0139	0.0237	0.6101
Day -8	0.0067	0.0095	-0.0119	0.0252	0.4813
Day -9	0.0061	0.0096	-0.0128	0.0249	0.5287
Day -10	0.0067	0.0087	-0.0103	0.0237	0.4387
Day -11	0.0021	0.0075	-0.0126	0.0168	0.7799
Day -12	0.0136	0.0082	-0.0025	0.0297	0.0985
Day -13	**0.0205**	**0.0095**	**0.0018**	**0.0392**	**0.0321**
Day -14	**0.0268**	**0.0089**	**0.0093**	**0.0443**	**0.0026**
Day -15	**0.0477**	**0.0107**	**0.0268**	**0.0686**	**<0.0001**
Day -16	**0.0336**	**0.0101**	**0.0139**	**0.0534**	**0.0008**
Day -17	**0.0234**	**0.0109**	**0.0021**	**0.0447**	**0.0315**
Day -18	0.0139	0.0088	-0.0034	0.0311	0.1154
Day -19	0.0179	0.0104	-0.0025	0.0383	0.0855
Day -20	0.0193	0.0103	-0.0010	0.0395	0.0621
Day -21	0.0059	0.0097	-0.0130	0.0249	0.5381
Day -22	0.0033	0.0091	-0.0144	0.0211	0.7134
Day -23	-0.0006	0.0092	-0.0186	0.0175	0.9510
Day -24	0.0044	0.0093	-0.0139	0.0227	0.6373
Day -25	0.0056	0.0090	-0.0120	0.0232	0.5344
Day -26	0.0033	0.0086	-0.0135	0.0202	0.6975
Day -27	-0.0041	0.0089	-0.0215	0.0134	0.6479
Day -28	0.0079	0.0080	-0.0077	0.0235	0.3225

$PM_{2.5}$	β	SE	95% CI		P-value
Day 0	0.0067	0.0110	-0.0148	0.0283	0.5399
Day -1	0.0116	0.0092	-0.0065	0.0297	0.2089
Day -2	**0.0214**	**0.0104**	**0.0011**	**0.0417**	**0.0386**
Day -3	0.0070	0.0099	-0.0124	0.0263	0.4802
Day -4	0.0112	0.0100	-0.0083	0.0308	0.2601
Day -5	**0.0313**	**0.0132**	**0.0054**	**0.0572**	**0.0179**
Day -6	0.0040	0.0115	-0.0185	0.0265	0.7279
Day -7	-0.0032	0.0120	-0.0267	0.0204	0.7929
Day -8	0.0035	0.0109	-0.0180	0.0249	0.7506
Day -9	0.0047	0.0122	-0.0192	0.0285	0.7009
Day -10	0.0097	0.0106	-0.0110	0.0304	0.3589
Day -11	0.0029	0.0097	-0.0162	0.0220	0.7652
Day -12	0.0143	0.0100	-0.0053	0.0339	0.1520
Day -13	0.0190	0.0114	-0.0034	0.0414	0.0962
Day -14	**0.0284**	**0.0105**	**0.0078**	**0.0490**	**0.0069**
Day -15	**0.0496**	**0.0130**	**0.0242**	**0.0750**	**0.0001**
Day -16	**0.0327**	**0.0126**	**0.0080**	**0.0574**	**0.0093**
Day -17	0.0250	0.0137	-0.0019	0.0518	0.0681
Day -18	0.0145	0.0110	-0.0071	0.0361	0.1890
Day -19	0.0204	0.0130	-0.0051	0.0459	0.1176
Day -20	0.0238	0.0134	-0.0024	0.0500	0.0754
Day -21	0.0049	0.0125	-0.0196	0.0293	0.6956
Day -22	-0.0030	0.0124	-0.0273	0.0213	0.8091
Day -23	0.0021	0.0122	-0.0219	0.0260	0.8656
Day -24	0.0046	0.0118	-0.0185	0.0278	0.6952
Day -25	0.0092	0.0113	-0.0129	0.0313	0.4146
Day -26	-0.0019	0.0109	-0.0232	0.0195	0.8641
Day -27	-0.0033	0.0111	-0.0251	0.0185	0.7675
Day -28	0.0122	0.0105	-0.0085	0.0329	0.2473

Day -29	0.0056	0.0091	-0.0122	0.0234	0.5381	Day -29	0.0095	0.0114	-0.0129	0.0319	0.4078
-1st week AVG (Day 0-6)	**0.0235**	**0.0117**	**0.0005**	**0.0466**	**0.0449**	-1st week AVG (Day 0-6)	0.0235	0.0143	-0.0046	0.0516	0.1012
-2nd week AVG (Day -7 -13)	0.0151	0.0119	-0.0082	0.0384	0.2040	-2nd week AVG (Day -7 -13)	0.0150	0.0147	-0.0138	0.0438	0.3064
-3rd week AVG (Day -14 -20)	**0.0426**	**0.0129**	**0.0173**	**0.0679**	**0.0010**	**-3rd week AVG (Day -14 -20)**	**0.0478**	**0.0163**	**0.0159**	**0.0797**	**0.0034**
-4th week AVG (Day -21 -27)	0.0032	0.0110	-0.0184	0.0248	0.7688	-4th week AVG (Day -21 -27)	0.0030	0.0143	-0.0251	0.0311	0.8327
-2 week AVG (Day 0 -13)	**0.0284**	**0.0143**	**0.0003**	**0.0565**	**0.0473**	-2 week AVG (Day 0 -13)	0.0289	0.0177	-0.0058	0.0635	0.1025
-3 week AVG (Day 0 -20)	**0.0425**	**0.0154**	**0.0122**	**0.0728**	**0.0059**	-3 week AVG (Day 0 -20)	0.0051	0.0094	-0.0133	0.0234	0.5890
-4 week AVG (Day -21 -27)	**0.0318**	**0.0151**	**0.0023**	**0.0614**	**0.0348**	-4 week AVG (Day -21 -27)	0.0336	0.0191	-0.0038	0.0709	0.0782

β (95% CIs) at different time lags (from day of bronchiolitis assessment to the previous 30 days) and for different 7-day moving average are calculated for a 1 $\mu g/m^3$ increase in PM_{10} and $PM_{2.5}$. Multivariable continuous ordinal regression models adjusted for age, sex, ethnicity, assumption of systemic antibiotics during pregnancy and assumption of systemic antibiotic in the last month were used to estimate β-regression coefficients. Significant associations are in bold.

2.3.4 Compositional overview and diversity evaluation of bacterial nasal microbiota (bNM) in the entire study population

Amplicon-based 16S sequencing analysis was performed to characterize the bNM of both cases with bronchiolitis and HC in order to explore the composition, evaluate diversity, and to further investigate possible impacts of PM exposure on the analyzed bacterial community. The bNM analysis was conducted on a final number of 149 nasal swabs collected from 103 cases and 46 HC. Considering the entire study population, 6 phyla made up 99,5% of the total relative abundance of the bNM, which was dominated by the Proteobacteria (mean relative abundance= 62,3%), Firmicutes (20,5%) and Actinobacteria (11,4%) phyla, as showed in **Figure 31**. Examining the nasal bacterial community in more detail, of the 367 genera identified, 20 made up about 90% of the total relative abundance. Among them, the top 5 represented taxa were identified as *Moraxella* (39,8%), *Haemophilus* (13,9%), *Streptococcus* (11,2%), and *Corynebacterium_1* (8,9%) (**Figure 32)**.

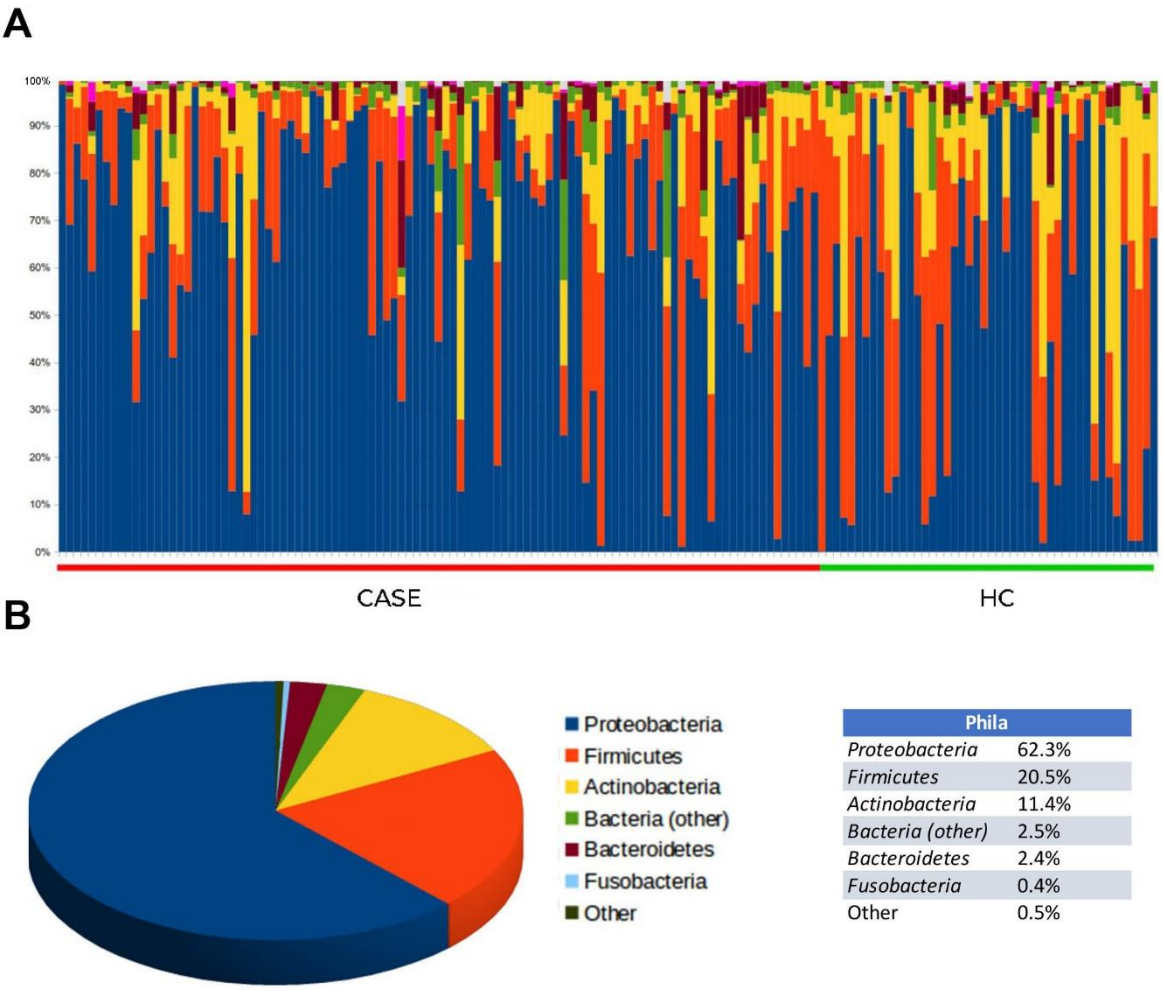

Phila	
Proteobacteria	62.3%
Firmicutes	20.5%
Actinobacteria	11.4%
Bacteria (other)	2.5%
Bacteroidetes	2.4%
Fusobacteria	0.4%
Other	0.5%

***Figure 31**. Descriptive bNM phylum-profile composition. (**A**) Mean relative abundances of the entire study population (cases, N= 103; HC, N= 46). (**B**) Average top 6 phila relative abundance in the entire study population.*

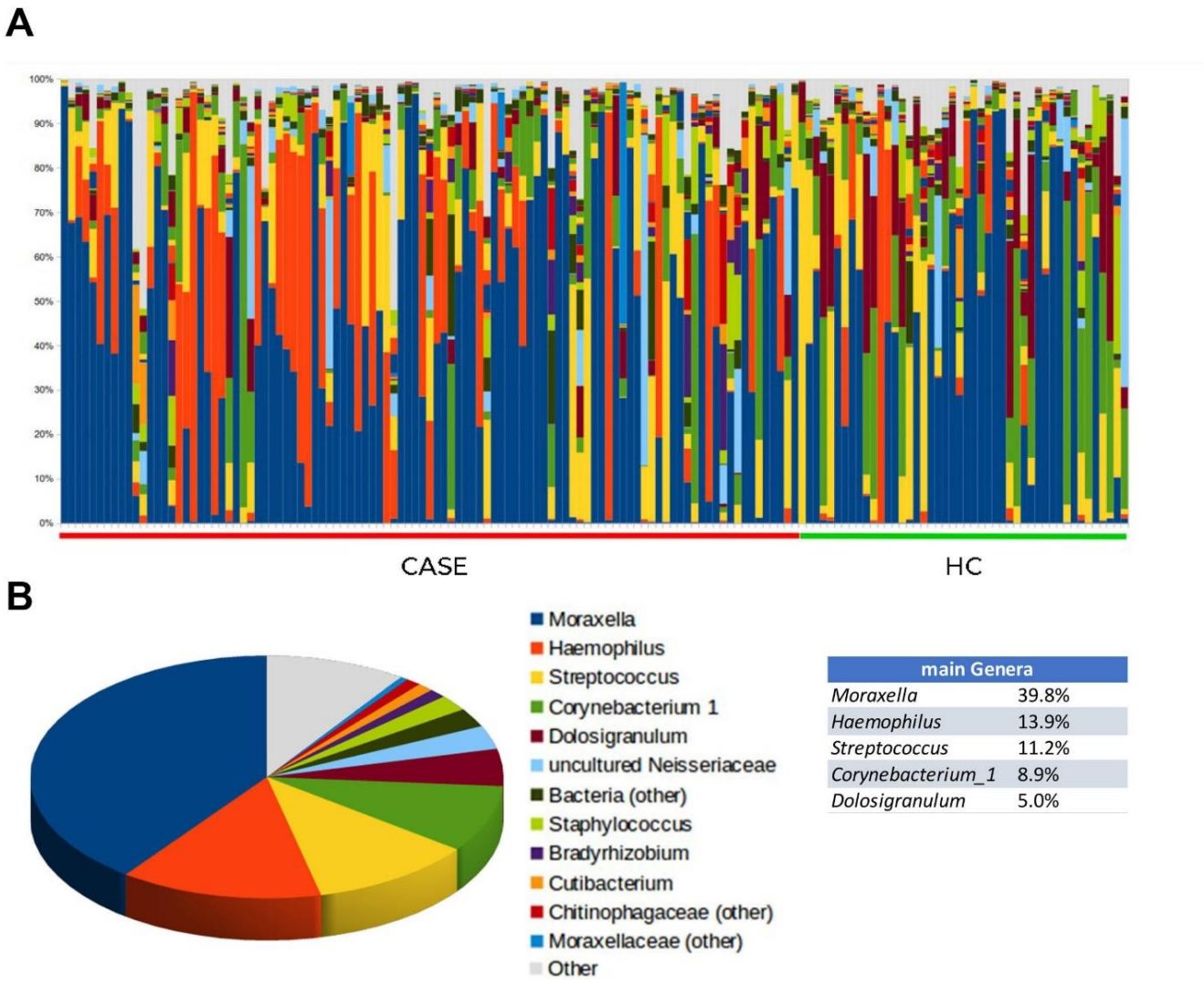

***Figure 32**. Descriptive bNM genus-profile composition. (**A**) Mean relative abundances of the entire study population (cases, N= 103; HC, N= 46). (**B**) Average top 6 genera relative abundance in the entire study population.*

Alpha and beta-diversity analyses were performed to describe bNM diversity features in the case and HC groups. To investigate the diversity within the collected samples, alpha-diversity analysis was performed by using the Shannon, Chao1, and observed_species indices, providing information about the evenness and richness features of the examined bacterial communities. The comparison of the three indices pointed out no differences between cases and HC groups (*p-value* ≥ 0,05). For each tested index, geometric means and *p-value* derived from the statistical analysis adjusted for the $PM_{2.5}$ and PM_{10} mean levels of the third week before assessment (-3rd week AVG) are shown

in **Tables 5** and **6**, respectively. Beta-diversity analyses were performed by applying both the Unweighted and Weighted_Normalized UniFrac metrics to compare the composition of the bNM communities between cases and HC groups. A Principal coordinate analysis (PCoA) plot was generated, pointing out that the principal components (PC) 1 and 2 explained 6,0% and 3,8% of the variance between the nasal bacterial communities of cases and HC when both taxa presence and abundance as well as phylogenetic diversity were considered, as illustrated in **Figure 33**. Analysis of similarity (PERMANOVA) showed a separation between cases and HC samples (Unweighted Normalized UniFrac distance, *p-value*=0,001; Weighted Normalized UniFrac distance, *p-value*=0,004), suggesting differences in bNM diversity.

Table 5 *- α-diversity indices in case and control group (considering PM_{10} mean levels).*

	CASE (N=103)			HC (N=46)			*p-value*
	Geometric mean	**95% CI**		**Geometric mean**	**95% CI**		
Shannon	5,3241	4,6593	5,989	5,241	4,4703	6,0116	0,6860
Chao1	2102,82	1759,75	2445,89	2058,22	1660,57	2455,87	0,6743
Observed species	395,92	339,69	452,15	396,93	331,75	462,11	0,9538

Means and relative 95% CI were estimated by linear regression models adjusted for age, gender, ethnicity, use of antibiotics in the last month, PM_{10} mean levels during the third week before the bronchiolitis assessment and apparent temperature.

Table 6 - α-diversity indices in case and control group (considering $PM_{2.5}$ mean levels).

	CASE (N=103)			HC (N=46)			*p-value*
	Geometric mean	**95% CI**		**Geometric mean**	**95% CI**		
Shannon	5,3256	4,6618	5,9893	5,2415	4,4712	6,0119	0,6825
Chao1	2105,92	1763,49	2448,35	2059,78	1662,33	2457,24	0,6633
Observed species	396,5	340,34	452,66	397,19	332,01	462,38	0,9682

Means and relative 95% CI were estimated by linear regression models adjusted for age, gender, ethnicity, use of antibiotics in the last month, $PM_{2.5}$ mean levels during the third week before the bronchiolitis assessment and apparent temperature.

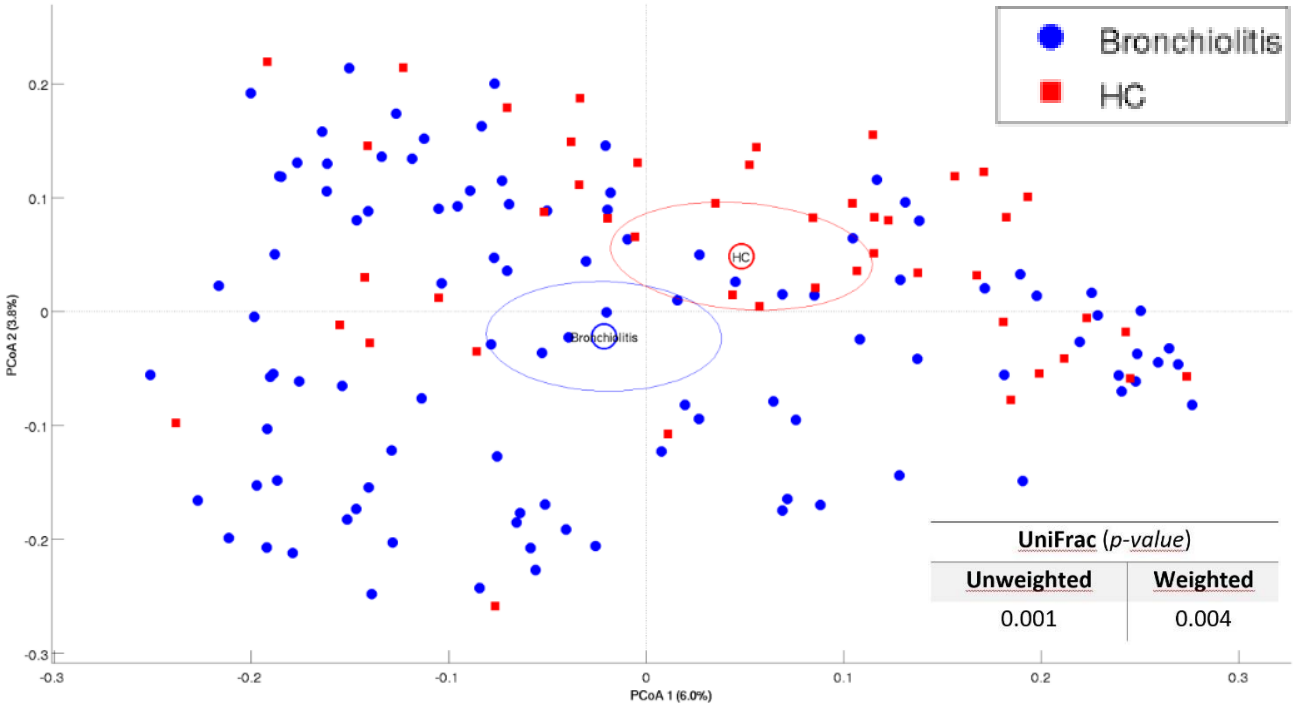

Figure 33. β-diversity analysis**.** PCoA plot of the similarities between the case and HC groups based on Unweighted and Weighted normalized UniFrac distance. Samples referred to cases and HC are colored in blue and orange, respectively.

2.3.5 bNM composition and PM exposure effects in cases and controls

Since a positive association was observed between the mean PM levels of the third week before enrollment (-3rd week AVG, see section 2.3.3) and bronchiolitis severity, further analyses on PM effects were conducted considering this specific exposure interval. The -3rd week AVG PM exposure levels of the study population are reported in **Table 7**. Including these levels in the model of analysis, of the total genera identified (N=367), the top 6 in which relative abundance was ≥ 1% in at least one experimental group are reported in **Tables 8** (adjusted for PM_{10} exposure) and **9** (adjusted for $PM_{2.5}$ exposure). Among them, only *Haemophilus* and *Dolosigranulum* were differentially represented between cases and HC groups: in both the implemented models the mean relative abundance of *Dolosigranulum* was higher in HC (FDR from PM_{10} adjusted model= 0,0078; FDR from $PM_{2.5}$ adjusted model= 0,0070). On the contrary, the mean relative abundance of *Haemophilus* was higher in cases (FDR from PM_{10} adjusted model= 0,0099; FDR from $PM_{2.5}$ adjusted model= 0,0267).

***Table 7**. Mean PM exposure levels in the entire study population (N case= 103, N HC=46)*

	Mean (µg/m³)	SD
PM_{10} mean levels during the third week before the assessment	36,95	15,73
$PM_{2.5}$ mean levels during the third week before the assessment	28,01	11,77

***Table 8.** Genera relative abundances adjusted for PM_{10} exposure in case (N=103) and HC (N=46) groups.*

	CASE (N=103)			HC (N=46)				
GENUS	**geometric mean**	**95% ci**		**geometric mean**	**95% ci**		**p-value**	**FDR p-value**
Dolosigranulum	**0,70**	**0,18**	**2,8**	**2,89**	**0,67**	**12,54**	**0,0000**	**0,0078**
Haemophilus	**12,33**	**4,20**	**36,18**	**3,23**	**0,90**	**11,51**	**0,0001**	**0,0099**
Corynebacterium_1	2,60	1,01	6,67	5,55	1,93	15,99	0,0022	0,2652
Neisseria	0,51	0,24	1,10	1,38	0,45	4,25	0,0130	0,7975
Staphylococcus	2,55	0,94	6,88	3,58	1,13	11,36	0,3189	1,0000
Moraxella	39,86	17,93	88,57	36,06	14,36	90,59	0,7034	1,0000
Streptococcus	5,24	2,42	11,34	4,91	1,96	12,32	0,7683	1,0000

Means and relative 95% CI were estimated by negative binomial regression models adjusted for age, gender, ethnicity, use of antibiotics in the last month, PM_{10} mean levels during the third week before the assessment and apparent temperature. In bold the genera with significant differences between cases and HC (according to FDR p-value).

***Table 9.** Genera relative abundances adjusted for $PM_{2.5}$ exposure in case (N=103) and control (N=46) groups.*

	CASE (N=103)			HC (N=46)				
GENUS	**geometric mean**	**95% ci**		**geometric mean**	**95% ci**		**p-value**	**FDR p-value**
Dolosigranulum	**0,72**	**0,18**	**2,84**	**2,92**	**0,67**	**12,64**	**0,0000**	**0,0070**
_Haemophilus	**11,67**	**3,99**	**34,13**	**2,80**	**0,78**	**10,11**	**0,0001**	**0,0267**
Corynebacterium_1	2,59	1,01	6,64	5,55	1,93	15,95	0,0021	0,2601
Neisseria	0,53	0,25	1,14	1,43	0,47	4,38	0,0127	0,7793
Staphylococcus	2,63	0,98	7,08	3,52	1,12	11,08	0,2503	1,0000
Moraxella	39,78	17,85	88,67	36,13	14,37	90,83	0,6934	1,0000
Streptococcus	5,22	2,40	11,32	4,87	1,93	12,25	0,7823	1,0000

Means and relative 95% CI were estimated by negative binomial regression models adjusted for age, gender, ethnicity, use of antibiotics in the last month, $PM_{2.5}$ mean levels during the third week before the assessment and apparent temperature. In bold the genera with significant differences between cases and HC (according to FDR p-value).

Further investigation was performed to assess whether -3rd week AVG PM_{10} and $PM_{2.5}$ exposure could modify the relation between cases or HC and the relative abundance of *Haemophilus* and *Dolosigranulum* genera. A significant interaction was observed only for *Haemophilus* and -3rd week AVG PM_{10} exposure level (p-value of interaction= 0,0489), suggesting a modifier effect of PM_{10} exposure, while no interactions emerged for *Dolosigranulum* (**Table 10**). Therefore, further analyses were focused on the *Haemophilus* genus. The modifier effect of PM_{10} and $PM_{2.5}$ on *Haemophilus* relative abundance was also assessed by studying different levels of exposure (i.e. -3rd week AVG PM levels ± SD, **Figure 34**). Significant differences between case and HC groups on *Haemophilus* relative abundance were observed at the three selected PM levels, -3rd week AVG PM levels (PM_{10} p-value< 0,0001, $PM_{2.5}$ p-value= 0,0002), -3rd week AVG PM levels + SD (PM_{10} p-value< 0,0001, $PM_{2.5}$ p-value= 0,0004), and -3rd week AVG PM levels - SD (PM_{10} p-value> 0,05, $PM_{2.5}$ p-value= 0,0218). Interestingly, differences in *Haemophilus* relative abundance between case and HC increased with increasing PM exposure levels, for both PM_{10} and $PM_{2.5}$, except for $PM_{2.5}$ mean vs mean - SD.

***Table 10**. Interaction of case and HC between genera and-3rd week AVG PM exposure.*

Genus	Parameter	*p-value* of interaction
Haemophilus	-3rd week AVG PM_{10} *case_HC	0,0489
Dolosigranulum	-3rd week AVG PM_{10} *case_HC	0,871
Haemophilus	-3rd week AVG $PM_{2.5}$ *case_HC	0,3927
Dolosigranulum	-3rd week AVG $PM_{2.5}$ *case_HC	0,8597

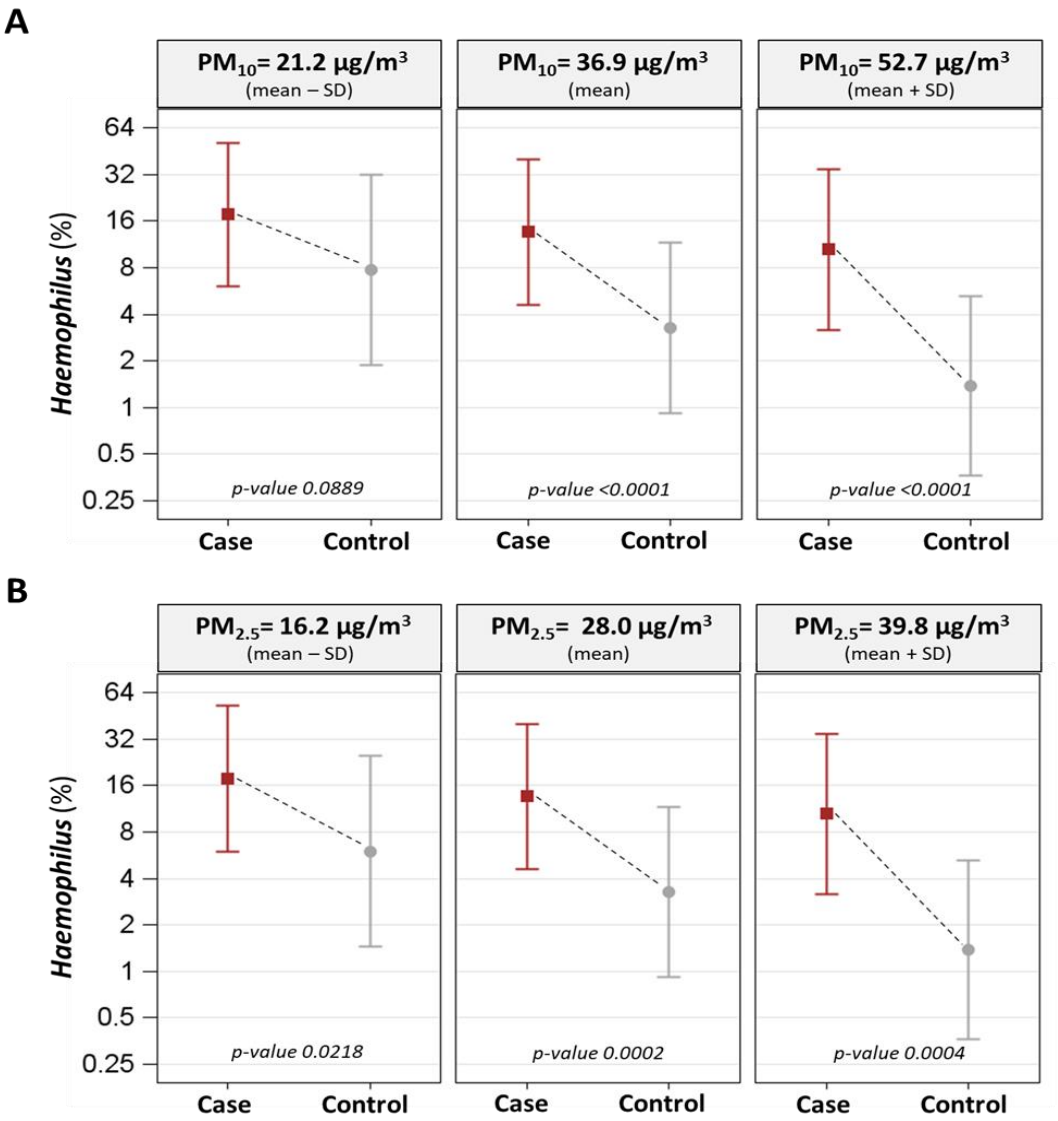

Figure 34*. Interaction effect of case_HC status and PM on Haemophilus relative abundance. Difference between case and HC group on Haemophilus relative abundance at 3 selected levels of PM (mean - SD, mean, and mean + SD values). Data derived from negative binomial regression models adjusted for age, gender, ethnicity, apparent temperature and use of antibiotics in the last month. Adjusted geometric means and relative 95% CI are reported. (A) Modifier effect of PM_{10}, (B) modifier effect of $PM_{2.5}$*

2.3.6 Species-level analysis on *Haemophilus* genus

Species-level composition was investigated for *Haemophilus genus* by employing paired reads derived from 16S analysis. Since analysis of the full *Haemophilus* species NCBI database pointed out 69% of unclassified reads, therefore, in order to predict possible species composition, only high-quality reads derived from a subgroup of 139 cases and HC were mapped against *ad hoc Haemophilus* species database obtained from modified NCBI database. As a result, a lower % of unclassified reads was obtained (38,8% of the total analyzed reads), mainly due to the overlap of

the two species *influenzae* and *aegyptius*, frequently reported as being part of the same species with the latter classified as a biogroup of the former. The most represented predicted species were *influenzae,* identified in most cases and HC (82,52% and 73,91% respectively), followed by *haemolyticus* (in 48,54% of cases and 41,3% of HC) and *parainfluenzae* (in 34,95% of cases and 52,17% of HC), as shown in **Table 11**. In terms of relative abundance, *Haemophilus influenzae* was predicted as the most represented species in both cases (57,3 %) and HC (47,4%), in fact representing almost the entire composition of the taxa. (**Figure 35**). These results suggested that *influenzae* is the species that colonized the upper respiratory tract of infants.

***Table 11**. Subjects with relative abundance of Haemophilus species >0 in cases and HC groups.*

		subjects with relative abundance > 0 (N)	subjects with relative abundance > 0 (%)
genus			
Haemophilus	case	96	90,57
	HC	43	89,58
species			
h__influenzae	**case**	**85**	**82,52**
	HC	**34**	**73,91**
h__haemolyticus	case	50	48,54
	HC	19	41,3
h__parainfluenzae	case	36	34,95
	HC	24	52,17
h__aegyptius	case	25	24,27
	HC	2	4,35
h__sputorum	case	10	9,71
	HC	9	19,57
h__pittmaniae	case	6	5,83
	HC	3	6,52
h__massiliensis	case	3	2,91
	HC	0	0
h__quentini	case	2	1,94
	HC	0	0

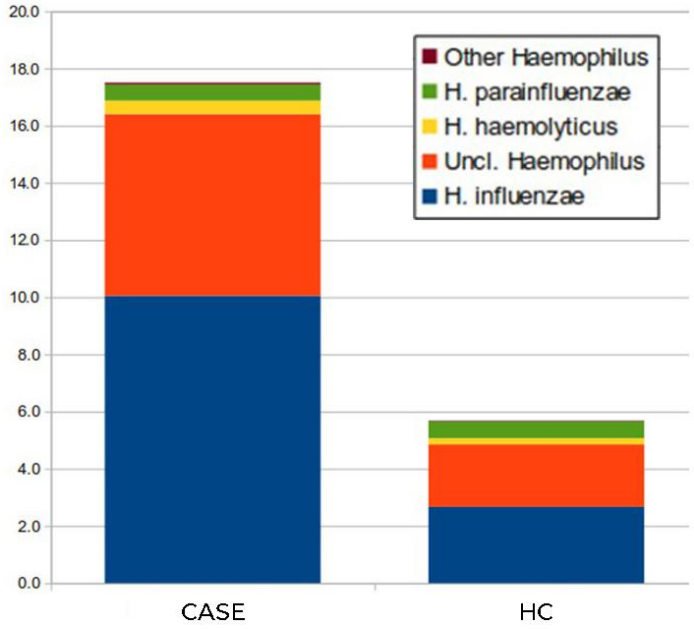

main species (%)		
	case	HC
influenzae	**57,3 %**	**47,4 %**
unclassified	35,9 %	38,3 %
haemolyticus	3 %	3,6 %
parainfluenzae	3 %	9,5 %
other	0,8 %	1,2 %

Figure 35. Bar plot of mean relative abundance of *Haemophilus* species in bNM of cases and HC. Average top 3 and unclassified species ("Uncl. Haemophilus") relative abundance in cases and HC samples are reported.

2.4 Discussion

Acute bronchiolitis is a common clinical condition characterized by inflammation and obstruction of the bronchioles affecting mainly infants. This syndrome is considered the main cause of hospitalization of infants worldwide [80]. In the vast majority of cases, it is caused by a viral infection of the lower airways, and respiratory syncytial virus (RSV) is the most prevalent viral agent for bronchiolitis in infants [80–82]. Although some risk factors have been recognized (e.g. pre-existing pulmonary diseases and young age) [90,91], most cases of illness occur without any prior predisposing risk factors in infants [80]. Some evidence suggests that environmental factors such as air pollution (e.g. particulate matter (PM)) are related to the worsening of respiratory diseases in young children [13,183]. In the present population study involving infants younger than one year of age we have demonstrated for the first time an association between the severity of bronchiolitis and $PM_{2.5}$ and PM_{10} exposure levels. The results of previous retrospective studies investigating a link between PM exposure and the risk of hospitalization or clinical encounters in infants with bronchiolitis were inconsistent. On one hand, in two studies conducted in USA and Canada, on a large cohort of infants (~10.000 and 20.000 subjects involved), the authors found no association between exposure levels of $PM_{2.5}$/PM_{10} and bronchiolitis hospitalization or patient clinical encounters for bronchiolitis, respectively [94,95]. On the other hand, studies carried out in Italy, France, and Israel found that higher exposure to PM_{10} increased the risk of hospitalization of infants with bronchiolitis [16,25,96]. A similar association also emerged in a study conducted in Hong Kong over the period 2008-2018 on ~30.000 children younger than 2 years of age, in which acute bronchiolitis-related hospitalization was associated with a high concentration of PM_{10} [98]. Lastly, the findings of a study involving approximately 12.000 polish infants who had been hospitalized for RSV bronchiolitis indicated that short-term $PM_{2.5}$ and PM_{10} exposure, together with other air pollutants, might explain more than 20% of total hospitalizations [99]. A full understanding of the role of air pollution in the onset and exacerbation of bronchiolitis is still lacking. By examining individual data of 110 infants visiting the pediatric emergency department of Polyclinic hospital of Milan, the potential role of PM in bronchiolitis development was confirmed, as a positive association was observed between short-term $PM_{2.5}$ and PM_{10} exposure levels and increased disease severity. It has been suggested that exposure to air pollutants, especially PM, might play a key role in the viral spread and transmission [184,185], and in particular, it could influence the inflammatory cascade leading to RSV infection with, as consequence, the development of bronchiolitis in infants

[25,93]. Since it is known that the peak of bronchiolitis symptoms occurs approximately within two weeks after the viral infection [16,186], the positive association here described between bronchiolitis severity and the exposure levels of $PM_{2.5}$ and PM_{10} of the third week before enrollment supports the hypothesis that elevated levels of PM can worsen the pathogenesis of the disease. Moreover, these data were also strengthened considering that the same positive association was observed by analyzing the data of the subpopulation of infants with RSV^+ bronchiolitis.

There is increasing evidence indicating that $PM_{2.5}$ and PM_{10} exposure can trigger airway inflammation [9,35] by inducing the expression of pro-inflammatory cytokines such as IL-1β, IL-6, and IL-8 [9,149,150]. In turn, severe bronchiolitis is correlated with elevated levels of airway inflammation [152,153]. Consistently, these evidence could provide a rationale for the link observed in this study between the severity of bronchiolitis in infants living in Milan and $PM_{2.5}$ and PM_{10} exposure levels of the third week preceding the severity peak. Moreover, the data on *in vivo* model shown in chapter 1 of the thesis, which elucidated the effects of a PM similar to the $PM_{2.5}$ in the urban area of Milan [154–156] and collected in the same winter of the present study, demonstrated a pro-inflammatory impact of $PM_{2.5}$, together with the capacity of impairing the immune response to an infectious inflammatory stimulus. Overall, these results support the hypothesis that PM influences the pathogenesis of bronchiolitis in infants (**Figure 36**).

To better elucidate the mechanism underlying the effects of PM that we have described, we studied the upper airway bacterial community of the entire study population, by comparing the composition of the bacterial nasal microbiota (bNM) of 106 infants with bronchiolitis (cases) and 48 healthy controls (HC). The colonization of the respiratory microbiota by certain bacteria can confer a protective or deleterious effect on viral infections [187], possibly modulating the immune system [188,189]. In particular, some species (e.g., *Moraxella catarrhalis*) have been shown to reduce host antiviral defense functions of bronchial epithelial cells [190–192], and this effect has been suggested also for RSV infections [193,194], thus potentially affecting the severity of the disease [90,195]. In general, the Phila-structure we observed is consistent with other studies, since *Proteobacteria* is commonly a dominant taxa in nasal and lung microbiota of infants < 2 years of age [196,197], as well as for the composition of the microbiota genera, which revealed *Corynebacterium*, *Moraxella*, *Haemophilus,* and *Staphylococcus* to represent the majority of genera [198]. However, as pointed out by β-diversity analyses, we observed a respiratory dysbiosis at genus-level in bNM of infants with bronchiolitis in comparison to matched HC. Indeed, besides bNM structure consistency, the reduction in terms of bNM diversity of cases was mainly attributable to the increase in common

respiratory pathobionts, such as of *Haemophilus genus,* and to the concomitant decrease of beneficial commensal bacteria of *Dolosigranulum* and *Corynebacterium* genera. These latter are reported to control the rate of proliferation of common respiratory pathobionts, especially in younger individuals [106,199]. Since it has been previously described that exposure to air pollution alters respiratory tract microbial composition [102], we further investigated whether PM_{10} and/or $PM_{2.5}$ exposure influenced the bNM composition of infants. The bacterial nasal community is considered the first structure hit by PM inhaled particles because of its anatomical location, therefore, the modifying effects of short-term PM exposure can be easily studied. The models adjusted for -3rd week AVG PM exposure pointed out *Haemophilus* and *Dolosigranulum* as differential genera in infants with bronchiolitis. Interestingly, a modifier effect of -3rd week AVG PM_{10} exposure on being case or HC was observed only on *Haemophilus* relative abundance, while no interactions emerged for *Dolosigranulum.* Since $PM_{2.5}$ levels are sometimes affected by estimation errors, we further performed analyses on specific levels of -3rd week AVG PM exposure for both PM_{10} and $PM_{2.5}$. From these analyses, we were able to describe a modifier effect on *Haemophilus* not only for PM_{10} but also for $PM_{2.5}$, with a greater impact as exposure levels increased. These results suggested that *Haemophilus* was the only *genus* affected by PM as a dampened impact of PM emerged in cases with bronchiolitis. Therefore, PM exposure could modify the relationship of the relative abundance of *Haemophilus* between cases and HC, with greater difference as the PM level increases.

Species-level analyses on *Haemophilus genus* were also performed by using 16S data on *ad hoc* database to predict the putative composition of the bNM. The most represented predicted species were *influenzae,* identified in the most of subjects, both cases and HC, and with higher relative abundance. These results suggested that *influenzae* was the species that colonized the upper respiratory tract of infants since it was the closest to the trend showed by *Haemophilus genus,* and in parallel, the other identified species were scarcely represented. Consistently with our findings, other studies have shown that the upper respiratory tract microbiota of infants < 1 year old and with RSV infection resulted characterized by an overrepresentation of the genus *Haemophilus*, which also emerged associated with nasopharyngeal viral load and increased level of pro-inflammatory cytokines (e.g. CXCL8) [193]. In this context, *Haemophilus influenzae* was usually described as the most represented predicted species [90,200]. This and our evidence suggest that interactions between respiratory viruses, especially RSV, and specific components of the upper tract

as *Haemophylus influenzae* could modulate the host immune response, thus potentially driving clinical disease severity.

We further investigated the features of *Haemophilus influenzae* to evaluate its immunomodulatory potential, and to better elucidate its potential involvement in airway inflammation and promotion of viral infection. In particular, in the last part of the present thesis, we performed functional analyses *in vivo* to assess the effects of its secreted extracellular vesicles on the host immune response.

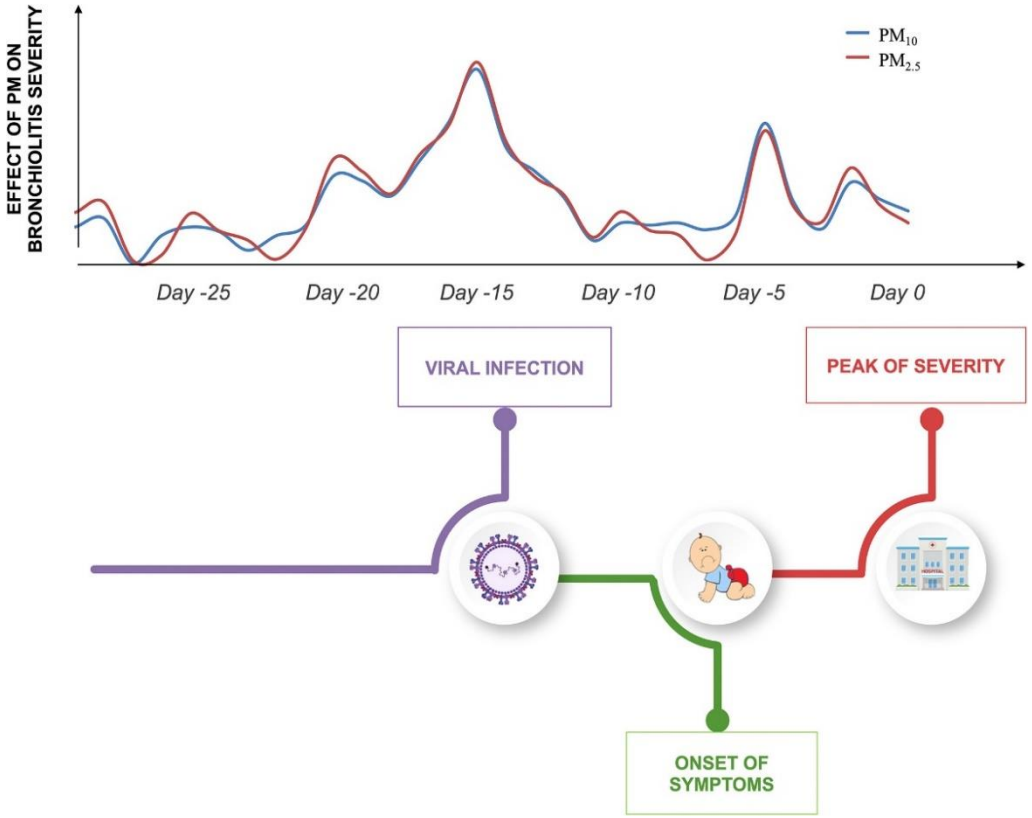

***Figure 36**. Hypothesis linking PM exposure and bronchiolitis severity.*

2.5 Appendix

Supplementary Table 1 *- Characteristics of the parents of study participants (N=159).*

Characteristics (Mother)	Case (N=110)	HC (N=49)	*p-value*
Age, years mean ± SD	35 ± 4.6	34.8 ± 5.6	0.8500 ǂ
Education, N (%)			
Elementary school	0 (0.0)	5 (4.6)	
Junior high school	2 (4.1)	14 (12.8)	
High school	12 (24.5)	29 (26.6)	0.1176●
University	35 (71.4)	61 (56.0)	
Smoking, N (%)			
Yes	7 (14.6)	10 (9.2)	
No	41 (85.4)	99 (90.8)	0.3150●
Maternal smoking during pregnancy, N (%)			
Yes	4 (8.5)	7 (6.4)	
No	43 (91.5)	102 (93.6)	0.7351*
Chronic diseases, N (%)			
Yes	11 (22.5)	31 (28.7)	
No	38 (77.6)	77 (71.3)	0.4120●
Allergy, N (%)			
Yes	17 (34.7)	43 (39.4)	
No	32 (65.3)	66 (60.6)	0.5989●
Systemic antibiotics during pregnancy, N (%)			
Yes	13 (26.5)	27 (25.0)	
No	36 (73.5)	81 (75.0)	0.8384●

Systemic antibiotics during breastfeeding, N (%)			
Yes	12 (24.5)	12 (11.1)	0.0309●
No	37 (75.5)	96 (88.9)	
Vaginal swab for Group B Streptococcus, N (%)			
Positive	5 (10.6)	14 (13.6)	0.6139●
Negative	42 (89.4)	89 (86.4)	

Characteristics (Father)	**Case (N=110)**	**HC (N=49)**	***p-value***
Age, *years mean ± SD*	37.1 ± 6.3	38.7 ± 6.5	0.1612 ł
Education*, N (%)*			
Elementary school	1 (1.0)	0 (0.0)	0.1800*
Junior high school	17 (16.5)	8 (16.7)	
High school	36 (35.0)	10 (20.8)	
University	49 (47.6)	29 (60.4)	
Above University	0 (0.0)	1 (2.1)	
Smoking*, N (%)*			
Yes	41 (38.7)	13 (27.1)	0.1625●
No	65 (61.3)	35 (72.9)	
Chronic diseases*, N (%)*			
Yes	13 (12.3)	7 (14.9)	0.6562●
No	93 (87.7)	40 (85.1)	
Allergies, *N (%)*			
Yes	30 (28.3)	17 (35.4)	0.3745●
No	76 (71.7)	31 (64.6)	

SD: standard deviation.

Continuous variables are expressed as mean ± SD or as median [Q1;Q3] as appropriate, discrete variables are expressed as counts (%).

ł The p-values were calculated by T-test.

Δ The p-values were calculated by Wilcoxon signed rank sum test.

● The p-values were calculated by chi-square test.

** The p-values were calculated by Fisher exact test*

Supplementary Table 2. *Levels of PM_{10} and $PM_{2.5}$ exposure for each time lag (N=110 cases of bronchiolitis).*

	PM_{10} ($\mu g/m^3$)				**$PM_{2.5}$** ($\mu g/m^3$)			
	Min	**Max**	**Mean**	**SD**	**Min**	**Max**	**Mean**	**SD**
Day 0	9.7	96.3	41.8	19.8	7.8	70.1	31.7	15.4
Day -1	9.7	130.6	42.0	21.8	6.9	105.9	31.6	17.2
Day -2	8.8	130.6	42.4	21.5	4.4	105.9	32.0	16.1
Day -3	12.7	135.0	44.3	23.2	9.9	105.9	33.3	16.6
Day -4	9.7	130.6	42.5	22.5	6.2	105.9	32.5	17.7
Day -5	4.9	89.3	38.9	18.5	5.0	70.0	29.6	14.5
Day -6	8.1	130.6	42.3	23.1	6.5	105.9	32.3	17.9
Day -7	6.9	130.6	42.1	23.2	5.5	105.9	31.8	17.5
Day -8	7.3	130.6	41.5	20.3	5.7	105.9	31.3	16.0
Day -9	9.7	123.9	40.9	20.8	6.7	96.3	30.8	16.0
Day -10	8.9	130.6	41.9	22.0	7.1	105.9	32.0	17.0
Day -11	5.5	130.6	40.8	22.0	4.8	105.9	31.0	16.5
Day -12	8.9	130.6	39.5	21.3	7.8	105.9	30.2	16.1
Day -13	7.2	89.3	37.2	19.7	5.7	70.0	28.3	15.2
Day -14	9.7	130.6	37.4	22.0	6.3	105.9	28.4	17.2
Day -15	11.0	96.3	37.7	18.5	6.8	70.1	28.4	14.1
Day -16	9.7	96.3	38.1	19.4	7.5	70.1	28.8	14.4
Day -17	9.7	90.4	36.8	18.6	8.1	67.4	28.0	13.9
Day -18	9.2	135.0	37.7	22.2	7.8	92.6	28.7	16.7
Day -19	7.2	130.6	37.8	22.6	6.4	105.9	28.7	17.0
Day -20	9.7	96.3	35.7	19.0	5.8	70.1	27.1	14.4
Day -21	8.2	130.6	35.9	19.9	6.4	105.9	27.3	15.5
Day -22	9.7	92.7	36.1	19.2	7.1	69.1	27.6	14.4
Day -23	3.1	96.3	37.0	21.5	1.1	70.1	27.9	15.7
Day -24	5.6	90.4	36.2	20.2	4.5	70.0	27.6	15.3
Day -25	11.3	130.6	35.2	20.1	6.7	105.9	26.9	15.4
Day -26	7.3	135.0	36.5	21.0	4.5	92.6	27.9	15.9
Day -27	7.8	87.6	36.4	19.6	5.8	64.3	27.4	14.9
Day -28	6.9	130.6	35.5	22.3	4.4	105.9	27.0	16.7
Day -29	9.7	130.6	35.7	19.1	8.2	105.9	27.3	14.7
-1st week AVG (Day 0-6)	15.0	77.0	42.3	15.9	11.0	59.0	32.1	11.9
-2nd week AVG (Day -7 -13)	16.0	80.0	40.7	16.3	12.0	61.0	30.9	12.2
-3rd week AVG (Day -14 -20)	16.0	79.0	37.5	15.9	14.0	60.0	28.4	11.9
-4th week AVG (Day -21 -27)	13.0	79.0	36.3	16.8	10.0	60.0	27.7	12.6
-2 week AVG (Day 0 -13)	15.0	73.0	41.5	14.0	12.0	55.0	31.4	10.3
-3 week AVG (Day 0 -20)	18.0	68.0	40.0	13.3	-14.0	82.0	19.1	17.3
-4 week AVG (Day 0 -27)	18.0	68.0	38.9	13.1	13.0	51.0	29.6	9.6

Supplementary Table 3. Association between exposure to $PM_{2.5}$ and PM_{10} and bronchiolitis severity score (N= 64 cases of RSV^+ bronchiolitis).

PM_{10}	β	SE	95% CI		P-value
Day 0	0.0077	0.0108	-0.0134	0.0289	0.4730
Day -1	**0.0187**	**0.0093**	**0.0005**	**0.0369**	**0.0442**
Day -2	**0.0310**	**0.0123**	**0.0069**	**0.0551**	**0.0118**
Day -3	0.0036	0.0098	-0.0155	0.0228	0.7085
Day -4	0.0116	0.0114	-0.0107	0.0339	0.3068
Day -5	0.0218	0.0143	-0.0063	0.0499	0.1277
Day -6	0.0018	0.0135	-0.0246	0.0283	0.8915
Day -7	0.0000	0.0138	-0.0271	0.0270	0.9976
Day -8	0.0123	0.0131	-0.0135	0.0381	0.3494
Day -9	0.0029	0.0139	-0.0243	0.0301	0.8341
Day -10	0.0058	0.0111	-0.0161	0.0276	0.6049
Day -11	0.0008	0.0109	-0.0206	0.0223	0.9404
Day -12	0.0153	0.0110	-0.0062	0.0369	0.1639
Day -13	0.0158	0.0130	-0.0097	0.0412	0.2238
Day -14	**0.0285**	**0.0115**	**0.0059**	**0.0511**	**0.0135**
Day -15	**0.0611**	**0.0150**	**0.0318**	**0.0904**	**<0.0001**
Day -16	**0.0437**	**0.0136**	**0.0170**	**0.0704**	**0.0014**
Day -17	**0.0336**	**0.0151**	**0.0040**	**0.0631**	**0.0261**
Day -18	0.0089	0.0102	-0.0111	0.0289	0.3816
Day -19	0.0175	0.0127	-0.0074	0.0424	0.1691
Day -20	**0.0276**	**0.0137**	**0.0009**	**0.0544**	**0.0430**

$PM_{2.5}$	β	SE	95% CI		P-value
Day 0	0.0069	0.0140	-0.0205	0.0344	0.6192
Day -1	0.0218	0.0118	-0.0013	0.0448	0.0639
Day -2	**0.0416**	**0.0165**	**0.0092**	**0.0739**	**0.0118**
Day -3	0.0106	0.0145	-0.0178	0.0390	0.4644
Day -4	0.0127	0.0143	-0.0153	0.0408	0.3741
Day -5	0.0249	0.0188	-0.0120	0.0618	0.1858
Day -6	0.0033	0.0179	-0.0318	0.0383	0.8539
Day -7	-0.0012	0.0185	-0.0374	0.0351	0.9496
Day -8	0.0152	0.0172	-0.0186	0.0490	0.3775
Day -9	0.0051	0.0192	-0.0325	0.0428	0.7892
Day -10	0.0079	0.0140	-0.0196	0.0353	0.5738
Day -11	0.0025	0.0146	-0.0261	0.0311	0.8657
Day -12	0.0167	0.0141	-0.0109	0.0443	0.2353
Day -13	0.0179	0.0166	-0.0146	0.0505	0.2809
Day -14	**0.0337**	**0.0143**	**0.0056**	**0.0618**	**0.0186**
Day -15	**0.0820**	**0.0200**	**0.0429**	**0.1212**	**<0.0001**
Day -16	**0.0617**	**0.0183**	**0.0258**	**0.0976**	**0.0008**
Day -17	**0.0493**	**0.0199**	**0.0102**	**0.0884**	**0.0134**
Day -18	0.0125	0.0138	-0.0144	0.0395	0.3625
Day -19	0.0216	0.0171	-0.0120	0.0551	0.2083
Day -20	**0.0373**	**0.0182**	**0.0017**	**0.0729**	**0.0402**

Day -21	0.0078	0.0139	-0.0194	0.0351	0.5735	Day -21	0.0166	0.0183	-0.0193	0.0525	0.3647
Day -22	-0.0026	0.0132	-0.0285	0.0232	0.8429	Day -22	-0.0068	0.0184	-0.0429	0.0293	0.7118
Day -23	0.0041	0.0133	-0.0221	0.0302	0.7609	Day -23	0.0142	0.0186	-0.0223	0.0506	0.4464
Day -24	0.0104	0.0130	-0.0151	0.0358	0.4252	Day -24	0.0197	0.0175	-0.0146	0.0539	0.2607
Day -25	0.0063	0.0136	-0.0203	0.0330	0.6416	Day -25	0.0176	0.0192	-0.0200	0.0552	0.3593
Day -26	0.0019	0.0109	-0.0195	0.0234	0.8606	Day -26	0.0017	0.0149	-0.0274	0.0309	0.9072
Day -27	-0.0045	0.0118	-0.0277	0.0186	0.7001	Day -27	-0.0067	0.0153	-0.0366	0.0232	0.6601
Day -28	0.0146	0.0106	-0.0062	0.0354	0.1695	Day -28	0.0215	0.0138	-0.0056	0.0485	0.1194
Day -29	0.0009	0.0134	-0.0254	0.0272	0.9487	Day -29	0.0054	0.0182	-0.0303	0.0410	0.7684
-1st week AVG (Day 0-6)	0.0225	0.0152	-0.0073	0.0522	0.1391	-1st week AVG (Day 0-6)	0.0313	0.0208	-0.0094	0.0720	0.1314
-2nd week AVG (Day -7 -13)	0.0165	0.0165	-0.0159	0.0490	0.3179	-2nd week AVG (Day -7 -13)	0.0227	0.0221	-0.0206	0.0661	0.3047
-3rd week AVG (Day -14 -20)	**0.0466**	**0.0166**	**0.0141**	**0.0792**	**0.0050**	**-3rd week AVG (Day -14 -20)**	**0.0659**	**0.0224**	**0.0220**	**0.1099**	**0.0033**
-4th week AVG (Day -21 -27)	0.0034	0.0158	-0.0276	0.0343	0.8305	-4th week AVG (Day -21 -27)	0.0118	0.0218	-0.0309	0.0545	0.5877
-2 week AVG (Day 0 -13)	0.0291	0.0191	-0.0083	0.0666	0.1272	-2 week AVG (Day 0 -13)	0.0417	0.0266	-0.0104	0.0938	0.1169
-3 week AVG (Day 0 -20)	**0.0454**	**0.0204**	**0.0054**	**0.0854**	**0.0260**	-3 week AVG (Day 0 -20)	0.0078	0.0117	-0.0152	0.0307	0.5059
-4 week AVG (Day 0 -27)	0.0401	0.0211	-0.0012	0.0814	0.0573	**-4 week AVG (Day 0 -27)**	**0.0622**	**0.0300**	**0.0034**	**0.1210**	**0.0380**

β (95% CIs) at different time lags (from day of bronchiolitis assessment to the previous 30 days) and for different 7-day moving average are estimated for a 1 µg/m^3 increase in PM_{10} and $PM_{2.5}$. Multivariable continuous ordinal regression models adjusted for age, sex, ethnicity, assumption of systemic antibiotics during pregnancy and assumption of systemic antibiotic in the last month were used to estimate β-regression coefficients. Significant associations are in bold.

CHAPTER 3:

in vivo investigation of the immunomodulatory potential of bacterial EVs (bEVs) on zebrafish model

This chapter is partly based on:

1) **Cafora M**, Hoxha M, Cantone L, Bollati V, Pistocchi A, Ferrari L; 2020. *Assessment of innate immune response activation following the injection of extracellular vesicles isolated from human cell cultures in zebrafish embryos.* Methods in Enzymology.
doi: 10.1016/bs.mie.2020.06.004

2) Greco MF, Rizzuto AS, Zarà M, **Cafora M**, Favero C, Solazzo G, Giusti I, Adorni MP, Zimetti F, Dolo V, Banfi C, Ferri N, Sirtori CR, Corsini A, Barbieri SS, Pistocchi A, Bollati V, Macchi C, Ruscica M.; 2022. *PCSK9 Confers Inflammatory Properties to Extracellular Vesicles Released by Vascular Smooth Muscle Cells*. Int J Mol Sci.
doi: 10.3390/ijms232113065

3) Urzì O, **Cafora M**, Rabienezhad Ganji N, Tinnirello V, Gasparro R, Raccosta S , Manno M, Corsale AM, Conigliaro A, Pistocchi A, Raimondo S, Alessandro R; 2023. *Lemon-derived nanovesicles achieve antioxidant effects activating the AhR/Nrf2 signaling pathway: in vitro and in vivo evidence.*
Paper under revision

3.1 Summary

Extracellular vesicles (EVs) are emerging as essential intercellular messengers and there is evidence that bacterial-derived EVs (bEVs) could play a crucial role in interregnum communication, being able to modulate the host immune system. In the present chapter, the immunomodulatory potential of the EVs will be investigated in an *in vivo* model. We took advantage of the zebrafish embryo model, which recently emerged as a suitable model to study EVs biology and their effect on the innate immune response. We set-up a method to study the immunomodulatory effects of EVs derived from different biological sources, which was published on a methodological journal [201]. Furthermore, in this framework we studied EVs derived from human smooth muscle cells and plant-derived EVs. The former exhibited pro-inflammatory potential and the latter exhibited anti-inflammatory and antioxidant properties, thus demonstrating the reliability of the zebrafish model, capable of detecting the immunomodulatory properties of EVs regardless of the kingdom of derivation. The first study was published on an international journal [140] and the second is now under revision (listed with #3 in the previous page).

Haemophilus influenzae (*Hi*) was individuated as the main species of interest from the metataxonomic analysis described in the chapter 2, since its mean relative abundance was higher in infants with bronchiolitis compared with controls and this difference was observed after the exposure to different levels of both PM_{10} and $PM_{2.5}$. Given this evidence, the main aim of this chapter is to investigate how *Hi* may affect the immune response in the host, with a potential relapse in the pathogenesis of the acute bronchiolitis. At this purpose, the immunomodulatory potential of *Hi* deriving bEVs isolated from *in vitro* exponential phase culture was investigated by using the zebrafish functional model.

3.2 Materials & Methods

3.2.1 Isolation and characterization of bacterial derived EVs

Not typeable strain of *Haemophilus influenzae* (strain L-378, ATCC 49766) was cultured on BD Chocolate Agar (GC II Agar with IsoVitaleX) at 37°C in microaerophilia o/n and then inoculated in Brain heart infusion (BHI) broth supplemented with Vitox (1:50) and HTM (1:250 [= NAD 15ug/ml +EME 15ug/ml]) until exponential phase is reached (OD_{600} ~= 1.8), after ~6-7 hours post *inoculum* **Figure 37**. bEVs of exponential phase culture were isolated following MISEV 2018 guidelines [202]. In brief, *Hi* bacterial culture was serially centrifuged at 1000 xg, 2000 xg and 3000 xg for 15' at 4°C each step. 20 mL of exponential phase culture were centrifuged at 5000 xg for 15' at 4°C and supernatant was filtered at 0,2 µm pore size. Aliquot of filtered supernatant was plated on Chocolate agar to assess for bacterial presence. Then, to completely remove bacterial cells debris, supernatant was filtered with 0,45 µm pore size filter. 32 mL of filtered supernatant were transferred in four ultracentrifuge tubes and centrifuged at 110.000 xg for 4 hours at 4°C. For each tube, pellet was resuspended in 1 mL of the obtained supernatant in the tubes, the rest of supernatant was carefully discarder. 8 mL of the filtered supernatant (not ultracentrifuged) of the same experiment were added to the tubes. The samples were ultracentrifuged at 110.000 xg for 4 hours at 4°C. The supernatant was thoroughly discarder and pellet was resuspended in 300 µL of triple filtered PBS (with 0,1 µm pore size filter). As control, 16 mL of BHI supplemented with HTM and Vitox without bacterial inoculum was processed with the same procedure. For *in vivo* experiments, an aliquot of bEVs was added with 0,04 M sucrose and stored in a cooling box at -80°C until use.

In parallel, immediately after isolation procedure, an aliquot of bEVs was characterized by flow cytometry analysis. Immunophenotypization assay was performed to quantify the EVs of Gram-negative origin, using a flow cytometer (MACSQuant, Miltenyi Biotec) according to a standardized protocol [203]. Before the analysis, a step of gating calibration was carried out using Fluoresbrite Carboxylate Size Range Kit I (0.2, 0.5, 0.75, and 1 µm) to properly set the instrumentation. 60 µL aliquots of each sample (i.e. derived from bacterial culture and from processed growth medium as control) were stained in the dark with 5(6)-carboxyfluorescein diacetate N-succinimidyl ester (CFSE) 0.2 µM at 37°C for 20'. CFSE is a cell permeant non-fluorescent pro-dye, which produces fluorescent reaction when reacts with intracellular esterases, that convert the molecule to a fluorescent ester.

CFSE^{+} is used to assess EV integrity and can be detected through the FITC detection channel. Then, CFSE stained samples were incubated with specific anti-LPS unconjugated primary antibody (LPS; gram-negative; Invitrogen Thermo Fisher Scientific, Waltham, USA) combined with a secondary IgG-antimouse (IgG (H + L), Superclonal™ Recombinant Secondary Antibody, Alexa Fluor 647-Invitrogen) for 20min at 4°C before detection procedure. To eliminate aggregates, Ab was previously centrifuged at 17,000 xg for 30' at 4°C. Autofluorescence of the antibodies was also detected by acquiring a PBS-stained control. To determine the concentration of double stained EVs (CFSE and LPS (APC) positive events/µL), quantitative multiparameter analysis on flow cytometry data was carried out by using FlowJo Software (Tree Star, Inc.) (**Figure 38)**. For each experiment, *Hi*-bEVs suspensions were diluted in triple filtered PBS to a concentration of 100 and 200 LPS^{+}/CFSE^{+} events/µL (bEVs 100 and bEVs 200, respectively).

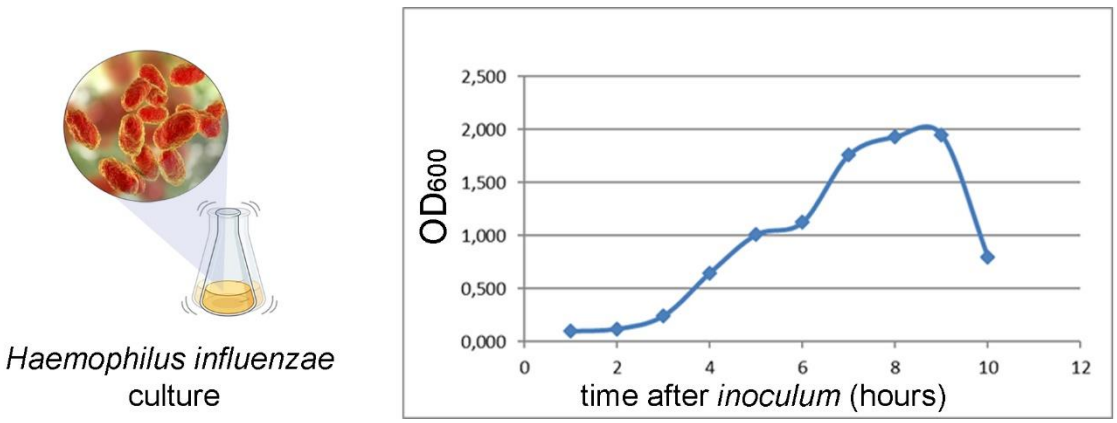

Figure 37. *Representative growth curve of Haemophilus influenzae liquid culture under optimal conditions. OD_{600}= optical density measured at a wavelength of 600 nm.*

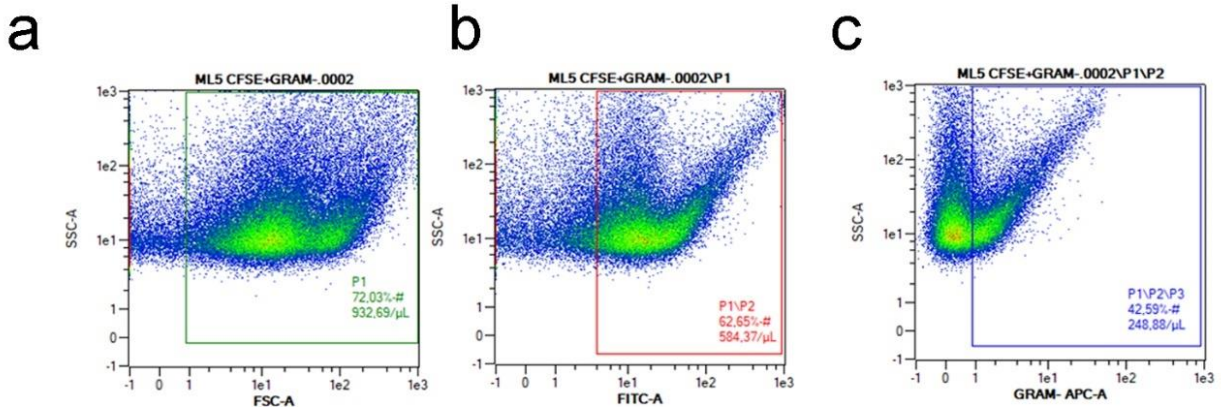

Figure 38*. Representative outcome of flow cytometry analysis for the quantification of Hi-EVs suspension. (a) side scatter (SSC) plot; (b) dot plot with gating for CFSE^{+} fluorescence (FITC); (c) dot plot for experimental sample (SSC+ CFSE + ANTI-*LPS *antibody* (APC)).

3.2.2 Microinjection of zebrafish with EVs

For gene expression experiments, to directly administrate EVs suspensions into the circulation, 2 dpf larvae were microinjected systemically into the duct of Cuvier with 2 nL of the indicated concentration of *Hi* bEVs, as described in [201]. At least 20 larvae were injected for each condition and incubated in E3 at 28,5°C. After 20 hpi, total RNA was extracted from 3 dpf larvae for quantitative PCR analysis. For leukocyte recruitment experiments, *Tg(mpx:EGFP)* and *Tg(mpeg1:mcherry)* were used to follow the behaviour of neutrophils and macrophages, respectively. 3 dpf larvae were locally injected with 1 nL of EVs suspension in the hindbrain ventricle. At least 9 larvae were injected for each condition and incubated in PTU at 28,5°C. At 6hpi, injected larvae were fixed in PFA 4% in PBS for 2 hours at RT and washed three times in PBS before leukocytes analysis. As control, larvae were systemically/locally injected with processed growth medium or bacterial broth prepared as described above (section 3.2.1). Each experiment was conducted at least in biological duplicate.

3.2.3 Acute sterile inflammatory stimulus model (tailfin amputation)

To generate zebrafish local acute inflammation, 3 dpf *Tg(mpx:EGFP)* and *Tg(mpeg1:mcherry)* larvae were amputated of a portion of the tailfin with the use of a sterile scalpel blade, without damaging circulatory loop, as described in [51,141]. Properly amputated larvae were selected for the assay and exposed to bEVs or processed bacterial broth (control) diluted 1:10 in a total volume of 500 µL of PTU at 28,5°. After 6 hours post-amputation (hpa), larvae were fixed in 4% PFA in PBS for 2 hours at RT and leukocyte recruitment in the caudal area of the tailfin was assessed through fluorescence microscopy.

3.2.4 Leukocyte migration analysis: image acquisition and quantification of leukocytes

To study leukocytes activation and migration, *Tg(mpx:EGFP)* and *Tg(mpeg1:mcherry)* zebrafish transgenic reporter lines were used. Single slice bright-field and fluorescent images of lateral side (for tailfin amputation model) or dorsal side (for brain ventricle model) of larvae were sequentially acquired using an epi-fluorescence stereomicroscope (M205FA, Leica, Wetzlar, Germany) equipped with a fluorescent lamp and a digital camera and mounting mcherry-filter (excitation 587 nm) and GFP-filter (excitation of 488 nm). Images were processed using Adobe software when necessary to merge different focal planes. Neutrophils were quantified through mpx^+ cell count and macrophages through $mpeg1^+$ cell count. For local injection experiments, leukocyte recruitment was measured in

the defined region of interest (i.e. brain ventricle, caudal fin region; dashed boxes) and was assessed at 6 hpi in brain ventricle model, and after 6 hours from injury in tailfin amputation model. For both experimental settings, cell count was performed by computation using of Fiji (ImageJ software, developer: Wayne Rasband) as already described [70,142]: i) manually selecting of the region of interest for the analysis with "polygon selection" tool (e.g. brain ventricle of the larva); ii) using of "subtract background" command, to avoid interference by the autofluorescence of the yolk sac; iii) running of the "Find maxima" function to detect single fluorescent cells. Mean and SEM of cell count of at least two independent experiments are reported on graphs.

Zebrafish husbandry: See Materials and methods of Chapter 1 section 1.2.1.

Determination of the expression level of inflammation mediator genes: See Materials and methods of Chapter 1, section 1.2.8.

Statistical analysis: See Materials and methods of Chapter 1 section 1.2.9.

3.3 RESULTS

3.3.1 Immumodulatory effects of bEVs derived from *Haemophylus influenzae* (*Hi*)

The immunomodulatory potential of EVs derived from *in vitro* exponential phase culture of a not typeable strain of *Hi* was tested by using the zebrafish functional model. The general experimental method used for the following experiments is reported in **Figure 39.**

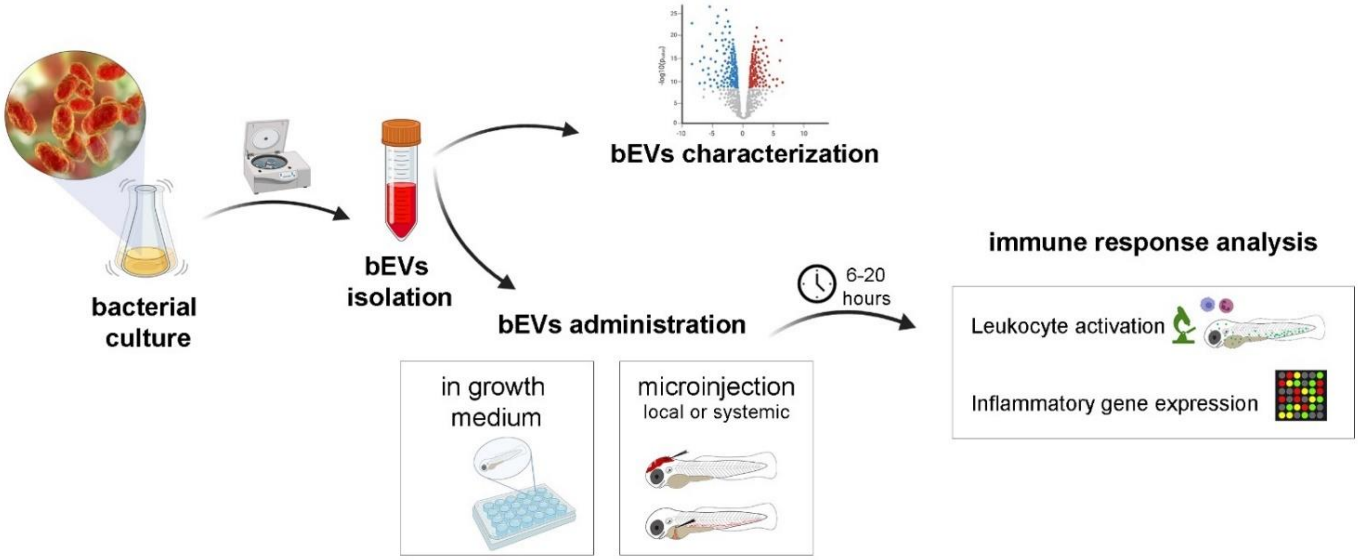

Figure 39. *Schematic representation of the experimental method used for the study of the bacterial EVs derived from Hi.*

3.3.1.1 Effects of *Hi*-bEVs injection on innate immune response

The immunomodulatory potential of bEVs derived from exponential phase culture of *Hi* was tested by administration through microinjection in zebrafish larvae. Effects on leukocyte populations was investigated to dissect mechanisms of interaction by taking advantage of *Tg*(*mpx*:*EGFP)* and *Tg*(*mpeg1*:mcherry) zebrafish transgenic reporter lines, with labeled neutrophils and macrophages, respectively. 1 nL of different doses of *Hi*-bEVs suspensions was locally microinjected in the hindbrain ventricle of 3 dpf larvae and leukocytes recruitment was quantified after 6 hpi in the defined area of head (dashed box, **Figure 40a**). As control, 1 nL of processed *Hi* growth medium was injected. The mean number of mpeg^{+} macrophages at the site of bEVs injection was higher in larvae treated with the higher dose of bEVs (bEVs 200) in comparison with controls (i.e. 8.6 vs 14.9, *p-value 0.0030*). While the lower dose (bEVs 100) induced no substantial effects on the migratory capacity

of macrophages, underlining a dose-dependent pro-inflammatory effect (**Figure 40b**). Neutrophils are normally the first responders at a site of bacterial infection and moreover some studies have reported an important role upon Gram-negative bEVs challenge [125,126]. Interestingly, with respect to macrophages, a more pronounced effect was observed on mpx^+ neutrophils after local bEVs inoculation. Indeed, both high and low doses were able to elicit a significant increase in neutrophil recruitment to the brain ventricle area (i.e., control= 6.2; vs bEVs100=12.6, *p-value 0.0011* ; bEVs200=22.6, *p-value<0.0001*). To note, higher dose elicited a significant increase in migration with respect to the lower one (**Figure 40c**). The described result indicates that *Hi*-bEVs can act as chemotactic stimulus, particularly toward neutrophil population, provoking an alteration in leukocyte trafficking. To dissect at molecular level the impact of *Hi*-bEVs on innate immunity, in parallel experiments, the bEVs were systemically injected in 48 hpf embryos and the expression of pro-inflammatory cytokines was assessed at 20 hpi. Consistently with the effect on leukocyte behavior, a pro-inflammatory effect on larvae was observed upon bEVs treatment. In particular, the levels of *il-1β* and *tnf-α* were increased in bEVs200-injected larvae of approximately 8- and 4-fold in comparison to control, respectively (*1β*, *p-value* 0.0153*; tnf-α, p-value* 0.0191*)* (**Figure 41**), suggesting *Hi*-bEVs to favor an inflammatory milieu in larvae. Moreover, both the tested doses were able to increase the levels of *il-6* and *cxcl8* mRNA (*il-6* bEVs100, *p-value* 0.0485*; il-6* bEVs200, *p-value 0.0229; cxcl8* bEVs100 *p-value* 0.0276*; cxcl8* bEVs200 *p-value* 0.0137). The latter is a chemokine linked to neutrophils activity, which were observed hyperactivated in the above-described model. To remark, dose dependence was observed in gene expression modulation (**Figure 41**).

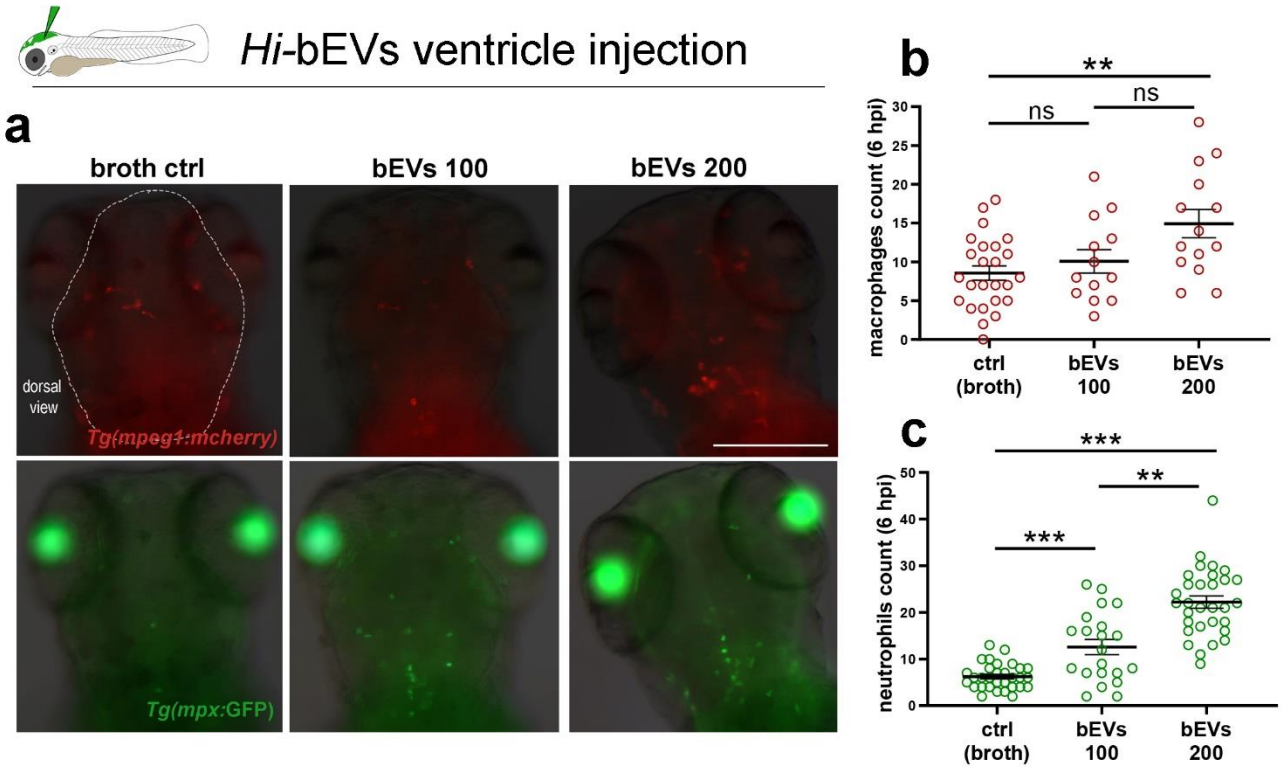

Figure 40. *Immunomodulatory effects of Hi-EVs on neutrophil and macrophage recruitment. Tg(mpx:EGFP) and Tg(mpeg1:mcherry) 3 dpf larvae were analyzed for leukocytes migration at 6 hours post local injection of different doses of bEVs suspension or broth (ctrl) into the brain ventricle.* ***(a)*** *Representative panel of 3 dpf larvae at 6 hpi.* ***(b)*** *mpeg^{+} macrophages count and* ***(c)*** *mpx^{+} neutrophils count at 6 hpi in head region (dashed box). Each dot represents a single individual and results are presented as mean ± SEM. Statistical significance was assessed by One-way ANOVA followed by Tukey's post hoc test: ***p < 0.001; **p < 0.01; *p < 0.05; ns= not significant. Scale bar=200µm.*

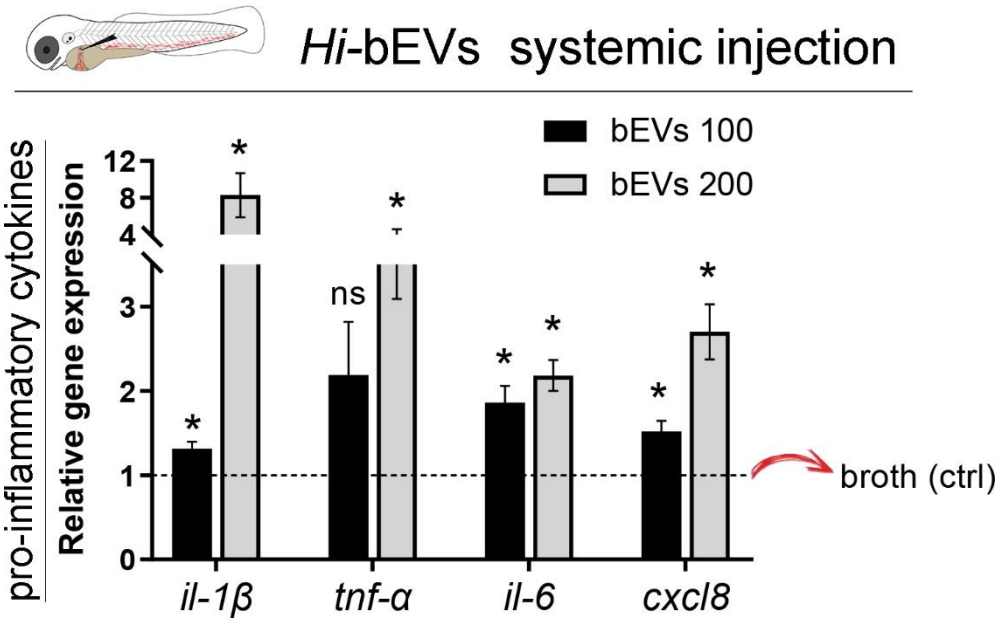

Figure 41. *Immunomodulatory effects of Hi-EVs on inflammatory markers expression. Larvae were analyzed for the expression of pro-inflammatory cytokines through RT-qPCR at 8 hours post systemic injection of different doses of bEVs suspension or broth (ctrl). Relative gene expression levels of bEVs-treated larvae are normalized on expression levels of control larvae (broth-injected, dashed line=1). For each gene, results are presented as mean ± SEM of at least three independent experiments. Statistical significance was assessed by One sample t-test. *p < 0.05; ns= not significant*

3.3.1.2 Effect of *Hi*-bEVs exposure on an acute inflammatory trigger

The immunomodulatory effects of *Hi*-derived EVs were also assessed in a model of acute inflammatory trigger using the zebrafish tailfin transection model. Previous studies have shown that leukocytes are recruited toward wound site in zebrafish larvae, representing a model of inflammatory response [204,205]. A piece of the caudal fin was sterilely amputated and larvae were subsequently exposed to the higher selected dose of *Hi*-bEVs (bEVs 200) suspension, directly added in growth medium. Leukocytes recruitment to the region of the tailfin was quantified at 6 hours post-amputation (hpa), when leukocyte migration reaches the peak at the site of injury [51] (**Figure 41a**). At this time point, exposure to *Hi*-bEVs did not elicit a significant impairment in leukocytes migratory capacity at the wound-site, as the average numbers of mpx^+ neutrophils and $mpeg^+$ macrophages were like controls exposed to *Hi* broth (**Figure 41b-c**). Probably a higher dose of bEV might be necessary to elicit a response using this type of inflammation model.

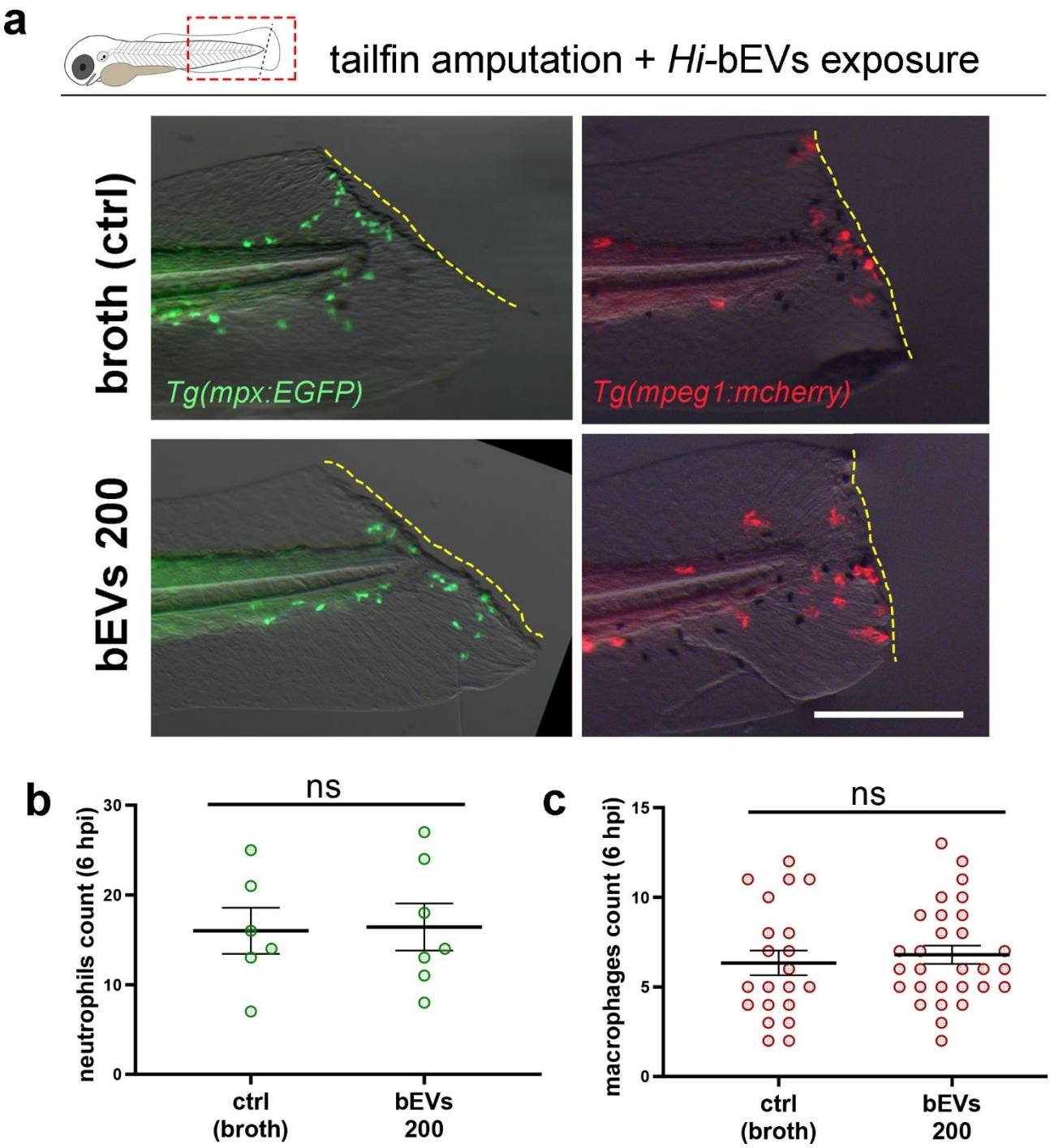

Figure 42. *Immunomodulatory effects of Hi-EVs on neutrophil and macrophage recruitment after an acute sterile stimulus. Tg(mpx:EGFP) and Tg(mpeg1:mcherry) embryos were exposed to bEVs200 or to broth (ctrl) and analyzed for leukocytes migration at 6 hours post amputation (hpa) of the tailfin.* ***(a)*** *Representative panel of bEVs-exposed and broth-exposed 3 dpf larvae at 6 hpa.* ***(b)*** *mpx^+ neutrophils count and* ***(c)*** *$mpeg^+$ macrophages count at 6 hpa at the site of injury (red dashed box). Each dot represents a single individual and results are presented as mean ± SEM. Statistical significance was assessed by unpaired t-test with Welch's correction: ns=not significant. Scale bar=50µm.*

3.4 DISCUSSION

EVs are microscopic membranous structures secreted by most type of both eukaryotic and prokaryotic cells. They have been emerged as essential intercellular messengers, capable of modulating the host's immune system [110–112]. Recent research has provided evidence that bacterial-derived EVs (bEVs) have a fundamental role in the interactions with mammalian host cells and are able to modulate host immune response [125]. Nevertheless, providing evidence of their physiological relevance remains challenging due to the lack of suitable model organisms [134]. Thus, *in vivo* models are needed to study the effects of EVs of different type and derivation on innate immunity. In the last years, zebrafish has emerged as an adequate model to study EVs biology and their impact on innate immune response [134,135], due to the lack of adaptative response in the first weeks of life and to the essential conservation of the molecular pathways driving immune response as well immune cells with human [46,48]. Moreover, the optical transparency of the embryo allows for direct visualization of both immune cells and EVs [135]. We have set-up a zebrafish model to investigate on the immunomodulatory effects of EVs derived from different biological sources [201]. The aim of this chapter was to dissect the potential role of EVs derived from *Haemophilus influenzae* (*Hi*) in the context discussed above in the chapter 2. Firstly, we have set-up the model by analyzing the effects of EVs derived from human cell culture. EVs were isolated from *in vitro* culture following the MISEV guidelines, thus through largely standardized protocols [202]. We demonstrated that, when delivered *in vivo,* EVs derived from cancer cell lines (e.g., Caco-2 cell line) can modulate immune system response. Caco-2 EVs were able to decrease the level of pro-inflammatory markers when systemically injected in zebrafish embryos. Caco-2 are partially differentiated cells that represent an early step of tumorigenesis in which immunosuppressant potential is crucial for tumor survival [206]. In another study, zebrafish model was used to assess the immunomodulatory effects of EVs derived from human vascular smooth muscle cells (hVSMC) overexpressing the enzyme PCSK9, involved in atherosclerosis [207]. Overexpression of PCSK9 has been shown to induce the generation of EVs with an increased pro-inflammatory potential in terms of expression of *il-1β* and *cxcl8* and an higher activation of macrophages [140]. Moreover, we showed that plant-derived EVs, secreted by *Citrus limon L.* [208], elicited anti-inflammatory and antioxidant effects when delivered in the growth medium of zebrafish larvae before an acute inflammatory stimulus (paper under revision). Therefore, we demonstrated the reliability of the

zebrafish model, capable of detecting the immunomodulatory properties of EVs derived from different kingdoms. As far as we know, this is one of the first works in which zebrafish is used to study the effects of exogenous EVs on conserved biological mechanisms [134]. Recent works have shown a direct interaction between exogenous EVs and zebrafish immune cells, confirming the prospect of using the zebrafish embryo as a powerful tool. Indeed, when injected, labeled exogenous EVs are taken up by macrophages and endothelial cells, promoting downstream effects [135].

EVs secreted from Gram-negative bacteria (bEVs) naturally modulate host immune signaling [125], however their effects on innate immunity still not completely understood and may vary depending on bacterial genre and milieu. In literature, Gram-negative derived bEVs are often described to promote pro-inflammatory effects, due to the presence of LPS, but in some cases they can promote immune escape effects toward host immunity, by dampening leukocytic response [125]. *Hi* is an opportunistic pathogen of human airways [209]. In the previous chapter 2, *Hi* has been identified as the main species of interest from the metataxonomic analysis since its mean relative abundance was higher in infants with bronchiolitis compared with controls. Therefore, in this chapter the immunomodulatory potential of *Hi* deriving bEVs isolated from *in vitro* exponential phase culture was investigated. We observed a strong pro-inflammatory potential of *Hi*-bEVs when injected in zebrafish embryos, with an increase of about 3,5 and 8-fold of the two main pro-inflammatory cytokines *tnf*-α and *il-1*β respectively, after intravascular delivery. Also, following the injection of *Hi*-bEVs in the hindbrain ventricle of larvae, a method commonly used to study leukocytes migration as it is a closed and vascularized cavity, the migration of leukocytes was increased, as already described for other bacterial species [125]. Neutrophils are normally the first responders at a site of infection and some *in vitro* studies reported an important role upon Gram-negative bEVs challenge [125,126]. Consistently, in our model a more pronounced effect was observed on neutrophils than in macrophages after local bEVs inoculation. The results indicated that the *Hi*-bEVs can act as strong chemotactic stimulus, highlighting an alteration in leukocyte trafficking, particularly of neutrophil population. Interestingly, the specificity of these effects was demonstrated with the dose-dependence response. Only in the tailfin amputation model, we did not observe any effect following bEVs administration, probably due to a too low dose of bEV added to the medium.

In conclusion, we had successfully demonstrated the potency of zebrafish as a model for the study of the immunomodulatory potential of different types of human and non-human derived EVs. With this model we demonstrate that *Hi*-bEVs promote an inflammatory response that, in the human

respiratory tract, might represent a favorable situation for further infections such as RSV infection. For future analyses, we plan to compare the effects of bEVs derived from bacterial culture in different growth phases (e.g. stationary phase and biofilm) [210] to better recapitulate airway scenario. Moreover, EV cargo analysis could improve the informative power of the model, implementing the possibility to correlate immune system response to specific molecules. Lastly, to better elucidate the impact of PM on the nature of bEVs secreted by *Hi*, bEVs isolated from *in vitro Hi* culture exposed to PM would have to be tested.

CONCLUSIONS

Overall, in the present work we have described the evidence supporting the role of PM exposure in the modulation of acute viral bronchiolitis in infants. To address aim 1, we set up a new reliable model of zebrafish in order to study the immunomodulatory effects of the short-term exposure to PM. With this model we demonstrated a pro-inflammatory effect of PM exposure and its ability to affect the host's innate immune response against an infectious inflammatory trigger. Concerning the zebrafish model of PM exposure, it is a promising system to dissect the mechanisms underlying the toxic effects of different types of PM, as well as a rapid and sensitive tool for toxicity screening. In regard to aim 2, we found a direct association between both $PM_{2.5}$ and PM_{10} exposure levels and the severity of bronchiolitis. In particular, the PM levels in the third week preceding the peak of severity were associated with the severity of the disease. According to the results obtained, we strengthened the hypothesis that PM could modulate airway inflammation and consequently promote viral infection. Therefore, we can speculate that the use of preventive measures to limit the spread of respiratory viruses (e.g. reducing the duration of exposure to environments that may carry contagious agents) or to alleviate inflammation of the airways (e.g. proactively utilizing inhaled anti-inflammatory compounds) in the days following high levels of $PM_{2.5}$ or PM_{10} exposure could be an effective strategy, especially for infants at risk of severe bronchiolitis. Future prospective studies should investigate and confirm whether preventive strategies might reduce the burden of this disease.

To address aim 3, we characterized upper respiratory tract bacterial dysbiosis in infants with bronchiolitis, showing the overrepresentation of the genus *Haemophilus* and predicting *influenzae* as the most represented species. We showed that these taxa were modulated by PM during bronchiolitis, suggesting that their abundance within bacterial nasal community could affect the severity of bronchiolitis in the period following high levels of PM exposure. Therefore, we speculate that the interactions between specific bacteria of the upper respiratory tract, as *Haemophylus influenzae* (*Hi*), and respiratory viruses, especially RSV, might modulate the host immune response, thus potentially driving disease severity. Concerning aim 4, we further elucidated a potential mechanism underlying the described effect by setting up a new zebrafish model to study the effects of bacterial extracellular vesicles (bEVs), through which we demonstrated the pro-inflammatory

potential of *Hi*-derived EVs. This study has some limitations, since we did not evaluate synergistic or antagonistic effects of PM in modulating the inflammatory pathways when in presence of *Hi*-bEVs, as well as the impact of PM on the nature of the secreted bEVs. Furthermore, analyses on bEVs derived from *Hi* cultures exposed to PM could provide stronger support to our hypothesis. However, in the present study the aim was to evaluate the immunomodulatory potential of EVs, and our evidence supports the hypothesis that the bacterial EVs release may be involved in the microbiota-host immune response interaction, by modulating airways inflammation thus promoting further pathogen (viral) infections, such as RSV.

REFERENCES

1. (WHO), W. health organization *WHO global air quality guidelines 2021*; 2021;
2. Bernstein, J.A.; Alexis, N.; Barnes, C.; Bernstein, I.L.; Bernstein, J.A.; Nel, A.; Peden, D.; Diaz-Sanchez, D.; Tarlo, S.M.; Williams, P.B. Health effects of air pollution. *J. Allergy Clin. Immunol.* **2004**, doi:10.1016/j.jaci.2004.08.030.
3. EEA *PM2.5 annual mean in 2018*; 2020;
4. AA, C. Diagnosis and control of particulate matter: total suspended particles PM10 breathable fraction. *Luna Azul* **2012**, 195–213.
5. Yang, L.; Li, C.; Tang, X. The Impact of PM2.5 on the Host Defense of Respiratory System. *Front. Cell Dev. Biol.* 2020.
6. Organization, W.H. *Ambient (outdoor) air quality and health*; 2016;
7. Faustini, A.; Alessandrini, E.R.; Pey, J.; Perez, N.; Samoli, E.; Querol, X.; Cadum, E.; Perrino, C.; Ostro, B.; Ranzi, A.; et al. Short-term effects of particulate matter on mortality during forest fires in Southern Europe: Results of the MED-PARTICLES project. *Occup. Environ. Med.* **2015**, doi:10.1136/oemed-2014-102459.
8. Mallone, S.; Stafoggia, M.; Faustini, A.; Paolo Gobbi, G.; Marconi, A.; Forastiere, F. Saharan dust and associations between particulate matter and daily mortality in Rome, Italy. *Environ. Health Perspect.* **2011**, doi:10.1289/ehp.1003026.
9. Arias-Pérez, R.D.; Taborda, N.A.; Gómez, D.M.; Narvaez, J.F.; Porras, J.; Hernandez, J.C. Inflammatory effects of particulate matter air pollution. *Environ. Sci. Pollut. Res.* 2020.
10. Chen, S.Y.; Chan, C.C.; Su, T.C. Particulate and gaseous pollutants on inflammation, thrombosis, and autonomic imbalance in subjects at risk for cardiovascular disease. *Environ. Pollut.* **2017**, doi:10.1016/j.envpol.2017.01.037.
11. Holland, N.A.; Fraiser, C.R.; Sloan, R.C.; Devlin, R.B.; Brown, D.A.; Wingard, C.J. Ultrafine Particulate Matter Increases Cardiac Ischemia/Reperfusion Injury via Mitochondrial Permeability Transition Pore. *Cardiovasc. Toxicol.* **2017**, doi:10.1007/s12012-017-9402-6.
12. Beelen, R.; Raaschou-Nielsen, O.; Stafoggia, M.; Andersen, Z.J.; Weinmayr, G.; Hoffmann, B.; Wolf, K.; Samoli, E.; Fischer, P.; Nieuwenhuijsen, M.; et al. Effects of long-term exposure to air pollution on natural-cause mortality: An analysis of 22 European cohorts within the multicentre ESCAPE project. *Lancet* **2014**, doi:10.1016/S0140-6736(13)62158-3.
13. Rush, B.; McDermid, R.C.; Celi, L.A.; Walley, K.R.; Russell, J.A.; Boyd, J.H. Association between chronic exposure to air pollution and mortality in the acute respiratory distress syndrome. *Environ. Pollut.* **2017**, doi:10.1016/j.envpol.2017.02.014.
14. Burnett, R.; Chen, H.; Szyszkowicz, M.; Fann, N.; Hubbell, B.; Pope, C.A.; Apte, J.S.; Brauer, M.; Cohen, A.; Weichenthal, S.; et al. Global estimates of mortality associated with longterm exposure to outdoor fine particulate matter. *Proc. Natl. Acad. Sci. U. S. A.* **2018**, doi:10.1073/pnas.1803222115.
15. Nhung, N.T.T.; Amini, H.; Schindler, C.; Kutlar Joss, M.; Dien, T.M.; Probst-Hensch, N.; Perez, L.; Künzli, N. Short-term association between ambient air pollution and pneumonia in children: A systematic review and meta-analysis of time-series and case-crossover studies. *Environ. Pollut.* 2017.
16. Carugno, M.; Dentali, F.; Mathieu, G.; Fontanella, A.; Mariani, J.; Bordini, L.; Milani, G.P.; Consonni, D.; Bonzini, M.; Bollati, V.; et al. PM10 exposure is associated with increased hospitalizations for respiratory syncytial virus bronchiolitis among infants in Lombardy, Italy. *Environ. Res.* **2018**, doi:10.1016/j.envres.2018.06.016.
17. Xing, Y.F.; Xu, Y.H.; Shi, M.H.; Lian, Y.X. The impact of PM2.5 on the human respiratory system. *J. Thorac. Dis.* 2016.
18. Duan, Z.; DU, F. yan; Yuan, Y. dong; Zhang, Y. ping; Yang, H. shen; Pan, W. sen [Effects of PM2.5 exposure on Klebsiella pneumoniae clearance in the lungs of rats]. *Zhonghua Jie He He Hu Xi Za Zhi* **2013**.
19. He, F.; Liao, B.; Pu, J.; Li, C.; Zheng, M.; Huang, L.; Zhou, Y.; Zhao, D.; Li, B.; Ran, P. Exposure to Ambient Particulate Matter Induced COPD in a Rat Model and a Description of the Underlying

Mechanism. *Sci. Rep.* **2017**, doi:10.1038/srep45666.
20. Lee, A.; Kinney, P.; Chillrud, S.; Jack, D. A systematic review of innate immunomodulatory effects of household air pollution secondary to the burning of biomass fuels. *Ann. Glob. Heal.* 2015.
21. Sayan, M.; Mossman, B.T. The NLRP3 inflammasome in pathogenic particle and fibre-associated lung inflammation and diseases. *Part. Fibre Toxicol.* **2016**, doi:10.1186/s12989-016-0162-4.
22. Uh, S.T.; Koo, S.M.; Kim, Y.; Kim, K.; Park, S.; Jang, A.S.; Kim, D.; Kim, Y.H.; Park, C.S. The activation of NLRP3-inflammsome by stimulation of diesel exhaust particles in lung tissues from emphysema model and RAW 264.7 cell line. *Korean J. Intern. Med.* **2017**, doi:10.3904/kjim.2016.033.
23. Horne, B.D.; Joy, E.A.; Hofmann, M.G.; Gesteland, P.H.; Cannon, J.B.; Lefler, J.S.; Blagev, D.P.; Kent Korgenski, E.; Torosyan, N.; Hansen, G.I.; et al. Short-term elevation of fine particulate matter air pollution and acute lower respiratory infection. *Am. J. Respir. Crit. Care Med.* **2018**, doi:10.1164/rccm.201709-1883OC.
24. Darrow, L.A.; Klein, M.; Dana Flanders, W.; Mulholland, J.A.; Tolbert, P.E.; Strickland, M.J. Air pollution and acute respiratory infections among children 0-4 years of age: An 18-year time-series study. *Am. J. Epidemiol.* **2014**, doi:10.1093/aje/kwu234.
25. Ségala, C.; Poizeau, D.; Mesbah, M.; Willems, S.; Maidenberg, M. Winter air pollution and infant bronchiolitis in Paris. *Environ. Res.* **2008**, doi:10.1016/j.envres.2007.05.003.
26. Øvrevik, J.; Låg, M.; Holme, J.A.; Schwarze, P.E.; Refsnes, M. Cytokine and chemokine expression patterns in lung epithelial cells exposed to components characteristic of particulate air pollution. *Toxicology* **2009**, doi:10.1016/j.tox.2009.01.028.
27. Farina, F.; Sancini, G.; Battaglia, C.; Tinaglia, V.; Mantecca, P.; Camatini, M.; Palestini, P. Milano Summer Particulate Matter (PM10) Triggers Lung Inflammation and Extra Pulmonary Adverse Events in Mice. *PLoS One* **2013**, doi:10.1371/journal.pone.0056636.
28. Trend, S.; Chang, B.J.; O'Dea, M.; Stick, S.M.; Kicic, A. Use of a primary epithelial cell screening tool to investigate phage therapy in cystic fibrosis. *Front. Pharmacol.* **2018**, doi:10.3389/fphar.2018.01330.
29. Zeng, X.; Liu, D.; Wu, W.; Huo, X. PM2.5 exposure inducing ATP alteration links with NLRP3 inflammasome activation. *Environ. Sci. Pollut. Res.* 2022.
30. Duan, S.; Wang, N.; Huang, L.; Zhao, Y.; Shao, H.; Jin, Y.; Zhang, R.; Li, C.; Wu, W.; Wang, J.; et al. NLRP3 inflammasome activation is associated with PM2.5-induced cardiac functional and pathological injury in mice. *Environ. Toxicol.* **2019**, doi:10.1002/tox.22825.
31. Yang, B.; Chen, D.; Zhao, H.; Xiao, C. The effects for PM2.5 exposure on non-small-cell lung cancer induced motility and proliferation. *Springerplus* **2016**, doi:10.1186/s40064-016-3734-8.
32. Wang, H.; Song, L.; Ju, W.; Wang, X.; Dong, L.; Zhang, Y.; Ya, P.; Yang, C.; Li, F. The acute airway inflammation induced by PM 2.5 exposure and the treatment of essential oils in Balb/c mice. *Sci. Rep.* **2017**, doi:10.1038/srep44256.
33. Münzel, T.; Gori, T.; Al-Kindi, S.; Deanfield, J.; Lelieveld, J.; Daiber, A.; Rajagopalan, S. Effects of gaseous and solid constituents of air pollution on endothelial function. *Eur. Heart J.* 2018.
34. Lakey, P.S.J.; Berkemeier, T.; Tong, H.; Arangio, A.M.; Lucas, K.; Pöschl, U.; Shiraiwa, M. Chemical exposure-response relationship between air pollutants and reactive oxygen species in the human respiratory tract. *Sci. Rep.* **2016**, doi:10.1038/srep32916.
35. Choi, J.; Sim, J.K.; Oh, J.Y.; Lee, Y.S.; Hur, G.Y.; Lee, S.Y.; Shim, J.J.; Moon, J. yong; Min, K.H. Relationship between Particulate Matter (PM10) and Airway Inflammation Measured with Exhaled Nitric Oxide Test in Seoul, Korea. *Can. Respir. J.* **2020**, doi:10.1155/2020/1823405.
36. Migliaccio, C.T.; Kobos, E.; King, Q.O.; Porter, V.; Jessop, F.; Ward, T. Adverse effects of wood smoke PM2.5 exposure on macrophage functions. *Inhal. Toxicol.* **2013**, doi:10.3109/08958378.2012.756086.
37. Park, E.J.; Roh, J.; Kim, Y.; Park, K.; Kim, D.S.; Yu, S. Do PM 2.5 collected in a residential area induced Th1-type inflammatory responses with oxidative stress in mice. *Environ. Res.* **2011**, doi:10.1016/j.envres.2010.11.001.
38. Sigaud, S.; Goldsmith, C.A.W.; Zhou, H.; Yang, Z.; Fedulov, A.; Imrich, A.; Kobzik, L. Air pollution particles diminish bacterial clearance in the primed lungs of mice. *Toxicol. Appl. Pharmacol.* **2007**,

doi:10.1016/j.taap.2007.04.014.
39. Bengalli, R.; Molteni, E.; Longhin, E.; Refsnes, M.; Camatini, M.; Gualtieri, M. Release of IL-1 β triggered by milan Summer PM10: Molecular pathways involved in the cytokine release. *Biomed Res. Int.* **2013**, doi:10.1155/2013/158093.
40. Miyata, R.; van Eeden, S.F. The innate and adaptive immune response induced by alveolar macrophages exposed to ambient particulate matter. *Toxicol. Appl. Pharmacol.* **2011**, doi:10.1016/j.taap.2011.09.007.
41. Dolci, M.; Favero, C.; Bollati, V.; Campo, L.; Cattaneo, A.; Bonzini, M.; Villani, S.; Ticozzi, R.; Ferrante, P.; Delbue, S. Particulate matter exposure increases JC polyomavirus replication in the human host. *Environ. Pollut.* **2018**, doi:10.1016/j.envpol.2018.05.044.
42. Chen, X.; Liu, J.; Zhou, J.; Wang, J.; Chen, C.; Song, Y.; Pan, J. Urban particulate matter (PM) suppresses airway antibacterial defence. *Respir. Res.* **2018**, doi:10.1186/s12931-017-0700-0.
43. Mebratu, Y.A.; Smith, K.R.; Agga, G.E.; Tesfaigzi, Y. Inflammation and emphysema in cigarette smoke-exposed mice when instilled with poly (I:C) Or infected with influenza A or respiratory syncytial viruses. *Respir. Res.* **2016**, doi:10.1186/s12931-016-0392-x.
44. Vandini, S.; Bottau, P.; Faldella, G.; Lanari, M. Immunological, viral, environmental, and individual factors modulating lung immune response to respiratory syncytial virus. *Biomed Res. Int.* **2015**, doi:10.1155/2015/875723.
45. Harrod, K.S.; Jaramillo, R.J.; Rosenberger, C.L.; Wang, S.Z.; Berger, J.A.; McDonald, J.D.; Reed, M.D. Increased susceptibility to rsv infection by exposure to inhaled diesel engine emissions. *Am. J. Respir. Cell Mol. Biol.* **2003**, doi:10.1165/rcmb.2002-0100OC.
46. Novoa, B.; Figueras, A. Zebrafish: Model for the study of inflammation and the innate immune response to infectious diseases. *Adv. Exp. Med. Biol.* **2012**, *946*, 253–275, doi:10.1007/978-1-4614-0106-3_15.
47. Trede, N.S.; Langenau, D.M.; Traver, D.; Look, A.T.; Zon, L.I. The use of zebrafish to understand immunity. *Immunity* 2004.
48. Forn-Cuní, G.; Varela, M.; Pereiro, P.; Novoa, B.; Figueras, A. Conserved gene regulation during acute inflammation between zebrafish and mammals. *Sci. Rep.* **2017**, doi:10.1038/srep41905.
49. Meeker, N.D.; Trede, N.S. Immunology and zebrafish: Spawning new models of human disease. *Dev. Comp. Immunol.* 2008.
50. Rosowski, E.E. Determining macrophage versus neutrophil contributions to innate immunity using larval zebrafish. *DMM Dis. Model. Mech.* 2020.
51. Chatzopoulou, A.; Heijmans, J.P.M.; Burgerhout, E.; Oskam, N.; Spaink, H.P.; Meijer, A.H.; Schaaf, M.J.M. Glucocorticoid-induced attenuation of the inflammatory response in zebrafish. *Endocrinology* **2016**, doi:10.1210/en.2015-2050.
52. Meijer, A.H.; Spaink, H.P. Host-pathogen interactions made transparent with the zebrafish model. *Curr. Drug Targets* **2011**, doi:10.2174/138945011795677809.
53. Henry, K.M.; Loynes, C.A.; Whyte, M.K.B.; Renshaw, S.A. Zebrafish as a model for the study of neutrophil biology. *J. Leukoc. Biol.* **2013**, doi:10.1189/jlb.1112594.
54. Torraca, V.; Masud, S.; Spaink, H.P.; Meijer, A.H. Macrophage-pathogen interactions in infectious diseases: New therapeutic insights from the zebrafish host model. *DMM Dis. Model. Mech.* 2014.
55. Le Guyader, D.; Redd, M.J.; Colucci-Guyon, E.; Murayama, E.; Kissa, K.; Briolat, V.; Mordelet, E.; Zapata, A.; Shinomiya, H.; Herbomel, P. Origins and unconventional behavior of neutrophils in developing zebrafish. *Blood* **2008**, doi:10.1182/blood-2007-06-095398.
56. Lieschke, G.J.; Oates, A.C.; Paw, B.H.; Thompson, M.A.; Hall, N.E.; Ward, A.C.; Ho, R.K.; Zon, L.I.; Layton, J.E. Zebrafish SPI-1 (PU.1) marks a site of myeloid development independent of primitive erythropoiesis: Implications for axial patterning. *Dev. Biol.* **2002**, doi:10.1006/dbio.2002.0657.
57. Herbomel, P.; Thisse, B.; Thisse, C. Ontogeny and behaviour of early macrophages in the zebrafish embryo. *Development* **1999**, doi:10.1242/dev.126.17.3735.
58. Nguyen-Chi, M.; Laplace-Builhe, B.; Travnickova, J.; Luz-Crawford, P.; Tejedor, G.; Phan, Q.T.; Duroux-Richard, I.; Levraud, J.P.; Kissa, K.; Lutfalla, G.; et al. Identification of polarized macrophage subsets in zebrafish. *Elife* **2015**, doi:10.7554/eLife.07288.

59. Phan, Q.T.; Sipka, T.; Gonzalez, C.; Levraud, J.P.; Lutfalla, G.; Nguyen-Chi, M. Neutrophils use superoxide to control bacterial infection at a distance. *PLoS Pathog.* **2018**, doi:10.1371/journal.ppat.1007157.
60. Rosowski, E.E.; Deng, Q.; Keller, N.P.; Huttenlocher, A. Rac2 Functions in Both Neutrophils and Macrophages To Mediate Motility and Host Defense in Larval Zebrafish. *J. Immunol.* **2016**, doi:10.4049/jimmunol.1600928.
61. Palić, D.; Andreasen, C.B.; Ostojić, J.; Tell, R.M.; Roth, J.A. Zebrafish (Danio rerio) whole kidney assays to measure neutrophil extracellular trap release and degranulation of primary granules. *J. Immunol. Methods* **2007**, doi:10.1016/j.jim.2006.11.003.
62. Ellett, F.; Pase, L.; Hayman, J.W.; Andrianopoulos, A.; Lieschke, G.J. mpeg1 promoter transgenes direct macrophage-lineage expression in zebrafish. *Blood* **2011**, doi:10.1182/blood-2010-10-314120.
63. Renshaw, S.A.; Loynes, C.A.; Trushell, D.M.I.; Elworthy, S.; Ingham, P.W.; Whyte, M.K.B. Atransgenic zebrafish model of neutrophilic inflammation. *Blood* **2006**, doi:10.1182/blood-2006-05-024075.
64. Lau, D.; Mollnau, H.; Eiserich, J.P.; Freeman, B.A.; Daiber, A.; Gehling, U.M.; Brümmer, J.; Rudolph, V.; Münzel, T.; Heitzer, T.; et al. Myeloperoxidase mediates neutrophil activation by association with CD11b/CD18 integrins. *Proc. Natl. Acad. Sci. U. S. A.* **2005**, doi:10.1073/pnas.0405193102.
65. Floris, P.; Garbujo, S.; Rolla, G.; Giustra, M.; Salvioni, L.; Catelani, T.; Colombo, M.; Mantecca, P.; Fiandra, L. The role of polymeric coatings for a safe-by-design development of biomedical gold nanoparticles assessed in zebrafish embryo. *Nanomaterials* **2021**, doi:10.3390/nano11041004.
66. Duan, J.; Hu, H.; Zhang, Y.; Feng, L.; Shi, Y.; Miller, M.R.; Sun, Z. Multi-organ toxicity induced by fine particulate matter PM2.5 in zebrafish (Danio rerio) model. *Chemosphere* **2017**, doi:10.1016/j.chemosphere.2017.04.013.
67. McGrath, P.; Li, C.Q. Zebrafish: a predictive model for assessing drug-induced toxicity. *Drug Discov. Today* 2008.
68. Sangabathuni, S.; Murthy, R.V.; Chaudhary, P.M.; Subramani, B.; Toraskar, S.; Kikkeri, R. Mapping the Glyco-Gold Nanoparticles of Different Shapes Toxicity, Biodistribution and Sequestration in Adult Zebrafish. *Sci. Rep.* **2017**, doi:10.1038/s41598-017-03350-3.
69. Chakraborty, C.; Sharma, A.R.; Sharma, G.; Lee, S.S. Zebrafish: A complete animal model to enumerate the nanoparticle toxicity. *J. Nanobiotechnology* **2016**, doi:10.1186/s12951-016-0217-6.
70. Cafora, M.; Poerio, N.; Forti, F.; Loberto, N.; Pin, D.; Bassi, R.; Aureli, M.; Briani, F.; Pistocchi, A.; Fraziano, M. Evaluation of phages and liposomes as combination therapy to counteract Pseudomonas aeruginosa infection in wild-type and CFTR-null models. *Front. Microbiol.* **2022**, *13*, 13:979610, doi:10.3389/fmicb.2022.979610.
71. Smoot, J.; Padilla, S.; Farraj, A.K. The utility of alternative models in particulate matter air pollution toxicology. *Curr. Res. Toxicol.* **2022**, *3*, 100077, doi:10.1016/j.crtox.2022.100077.
72. Geisler, R.; Köhler, A.; Dickmeis, T.; Strähle, U. Archiving of zebrafish lines can reduce animal experiments in biomedical research. *EMBO Rep.* **2017**, doi:10.15252/embr.201643561.
73. Roper, C.; Delgado, L.S.; Barrett, D.; Massey Simonich, S.L.; Tanguay, R.L. PM 2.5 Filter Extraction Methods: Implications for Chemical and Toxicological Analyses. *Environ. Sci. Technol.* **2019**, doi:10.1021/acs.est.8b04308.
74. Zhang, Y.; Jia, Z.; Rajendran, R.S.; Zhu, C.; Wang, X.; Liu, K.; Cen, J. Exposure of particulate matter (PM10) induces neurodevelopmental toxicity in zebrafish embryos. *Neurotoxicology* **2021**, *87*, 208–218, doi:10.1016/j.neuro.2021.10.004.
75. Cen, J.; Jia, Z. li; Zhu, C. yue; Wang, X. fang; Zhang, F.; Chen, W. yun; Liu, K. chun; Li, S. yu; Zhang, Y. Particulate matter (PM10) induces cardiovascular developmental toxicity in zebrafish embryos and larvae via the ERS, Nrf2 and Wnt pathways. *Chemosphere* **2020**, doi:10.1016/j.chemosphere.2020.126288.
76. Zhang, Y.; Li, S.; Li, J.; Han, L.; He, Q.; Wang, R.; Wang, X.; Liu, K. Developmental toxicity induced by PM2.5 through endoplasmic reticulum stress and autophagy pathway in zebrafish embryos. *Chemosphere* **2018**, doi:10.1016/j.chemosphere.2018.01.092.
77. Kühnert, A.; Vogs, C.; Altenburger, R.; Küster, E. The internal concentration of organic substances in fish embryos-A toxicokinetic approach. *Environ. Toxicol. Chem.* **2013**, doi:10.1002/etc.2239.

78. Smyth, R.L.; Openshaw, P.J. Bronchiolitis. *Lancet* 2006.
79. Ali, S.; Plint, A.C.; Klassen, T.P. Bronchiolitis. In *Kendig and Chernick's Disorders of the Respiratory Tract in Children*; 2012 ISBN 9781437719840.
80. Florin, T.A.; Plint, A.C.; Zorc, J.J. Viral bronchiolitis. *Lancet* 2017.
81. Stockman, L.J.; Curns, A.T.; Anderson, L.J.; Fischer-Langley, G. Respiratory syncytial virus-associated hospitalizations among infants and young children in the United States, 1997-2006. *Pediatr. Infect. Dis. J.* **2012**, doi:10.1097/INF.0b013e31822e68e6.
82. Nair, H.; Nokes, D.J.; Gessner, B.D.; Dherani, M.; Madhi, S.A.; Singleton, R.J.; O'Brien, K.L.; Roca, A.; Wright, P.F.; Bruce, N.; et al. Global burden of acute lower respiratory infections due to respiratory syncytial virus in young children: a systematic review and meta-analysis. *Lancet* **2010**, doi:10.1016/S0140-6736(10)60206-1.
83. Mansbach, J.M.; Piedra, P.A.; Teach, S.J.; Sullivan, A.F.; Forgey, T.; Clark, S.; Espinola, J.A.; Camargo, C.A. Prospective multicenter study of viral etiology and hospital length of stay in children with severe bronchiolitis. *Arch. Pediatr. Adolesc. Med.* **2012**, doi:10.1001/archpediatrics.2011.1669.
84. Miller, E.K.; Gebretsadik, T.; Carroll, K.N.; Dupont, W.D.; Mohamed, Y.A.; Morin, L.L.; Heil, L.; Minton, P.A.; Woodward, K.; Liu, Z.; et al. Viral etiologies of infant bronchiolitis, croup and upper respiratory illness during 4 consecutive years. *Pediatr. Infect. Dis. J.* **2013**, doi:10.1097/INF.0b013e31829b7e43.
85. Haynes, A.K.; Prill, M.M.; Iwane, M.K.; Gerber, S.I.; Centers for Disease Control and Prevention (CDC) Respiratory syncytial virus--United States, July 2012-June 2014. *MMWR. Morb. Mortal. Wkly. Rep.* **2014**.
86. Rossi, G.A.; Colin, A.A. Infantile respiratory syncytial virus and human rhinovirus infections: Respective role in inception and persistence of wheezing. *Eur. Respir. J.* **2015**, doi:10.1183/09031936.00062714.
87. Malhotra, R.; Ward, M.; Bright, H.; Priest, R.; Foster, M.R.; Hurle, M.; Blair, E.; Bird, M. Isolation and characterisation of potential respiratory syncytial virus receptor(s) on epithelial cells. *Microbes Infect.* **2003**, doi:10.1016/S1286-4579(02)00079-5.
88. Rallabhandi, P.; Phillips, R.L.; Boukhvalova, M.S.; Pletneva, L.M.; Shirey, K.A.; Gioannini, T.L.; Weiss, J.P.; Chow, J.C.; Hawkins, L.D.; Vogel, S.N.; et al. Respiratory syncytial virus fusion protein-induced toll-like receptor 4 (TLR4) signaling is inhibited by the TLR4 antagonists rhodobacter sphaeroides lipopolysaccharide and eritoran (E5564) and requires direct interaction with MD-2. *MBio* **2012**, doi:10.1128/mBio.00218-12.
89. Aherne, W.; Bird, T.; Court, S.D.; Gardner, P.S.; McQuillin, J. Pathological changes in virus infections of the lower respiratory tract in children. *J. Clin. Pathol.* **1970**, doi:10.1136/jcp.23.1.7.
90. De Steenhuijsen Piters, W.A.A.; Heinonen, S.; Hasrat, R.; Bunsow, E.; Smith, B.; Suarez-Arrabal, M.C.; Chaussabel, D.; Cohen, D.M.; Sanders, E.A.M.; Ramilo, O.; et al. Nasopharyngeal microbiota, host transcriptome, and disease severity in children with respiratory syncytial virus infection. *Am. J. Respir. Crit. Care Med.* **2016**, doi:10.1164/rccm.201602-0220OC.
91. Boyce, T.G.; Mellen, B.G.; Mitchel, E.F.; Wright, P.F.; Griffin, M.R. Rates of hospitalization for respiratory syncytial virus infection among children in Medicaid. *J. Pediatr.* **2000**, doi:10.1067/mpd.2000.110531.
92. Jo, Y.S.; Lim, M.N.; Han, Y.J.; Kim, W.J. Epidemiological study of PM2.5and risk of COPD-related hospital visits in association with particle constituents in Chuncheon, Korea. *Int. J. COPD* **2018**, doi:10.2147/COPD.S149469.
93. Vandini, S.; Corvaglia, L.; Alessandroni, R.; Aquilano, G.; Marsico, C.; Spinelli, M.; Lanari, M.; Faldella, G. Respiratory syncytial virus infection in infants and correlation with meteorological factors and air pollutants. *Ital. J. Pediatr.* **2013**, doi:10.1186/1824-7288-39-1.
94. Karr, C.; Lumley, T.; Shepherd, K.; Davis, R.; Larson, T.; Ritz, B.; Kaufman, J. A case-crossover study of wintertime ambient air pollution and infant bronchiolitis. *Environ. Health Perspect.* **2006**, doi:10.1289/ehp.8313.
95. Karr, C.J.; Demers, P.A.; Koehoorn, M.W.; Lencar, C.C.; Tamburic, L.; Brauer, M. Influence of ambient air pollutant sources on clinical encounters for infant bronchiolitis. *Am. J. Respir. Crit. Care Med.* **2009**, doi:10.1164/rccm.200901-0117OC.

96. Nenna, R.; Evangelisti, M.; Frassanito, A.; Scagnolari, C.; Pierangeli, A.; Antonelli, G.; Nicolai, A.; Arima, S.; Moretti, C.; Papoff, P.; et al. Respiratory syncytial virus bronchiolitis, weather conditions and air pollution in an Italian urban area: An observational study. *Environ. Res.* **2017**, doi:10.1016/j.envres.2017.06.014.
97. Yitshak-Sade, M.; Yudovitch, D.; Novack, V.; Tal, A.; Kloog, I.; Goldbart, A. Air pollution and hospitalization for bronchiolitis among young children. *Ann. Am. Thorac. Soc.* **2017**, doi:10.1513/AnnalsATS.201703-191OC.
98. Leung, S.Y.; Lau, S.Y.F.; Kwok, K.L.; Mohammad, K.N.; Chan, P.K.S.; Chong, K.C. Short-term association among meteorological variation, outdoor air pollution and acute bronchiolitis in children in a subtropical setting. *Thorax* **2021**, doi:10.1136/thoraxjnl-2020-215488.
99. Wrotek, A.; Badyda, A.; Czechowski, P.O.; Owczarek, T.; Dąbrowiecki, P.; Jackowska, T. Air pollutants' concentrations are associated with increased number of rsv hospitalizations in polish children. *J. Clin. Med.* **2021**, doi:10.3390/jcm10153224.
100. Man, W.H.; De Steenhuijsen Piters, W.A.A.; Bogaert, D. The microbiota of the respiratory tract: Gatekeeper to respiratory health. *Nat. Rev. Microbiol.* 2017.
101. Kumpitsch, C.; Koskinen, K.; Schöpf, V.; Moissl-Eichinger, C. The microbiome of the upper respiratory tract in health and disease. *BMC Biol.* 2019.
102. Mariani, J.; Favero, C.; Spinazzè, A.; Cavallo, D.M.; Carugno, M.; Motta, V.; Bonzini, M.; Cattaneo, A.; Pesatori, A.C.; Bollati, V. Short-term particulate matter exposure influences nasal microbiota in a population of healthy subjects. *Environ. Res.* **2018**, doi:10.1016/j.envres.2017.12.016.
103. Rawls, M.; Ellis, A.K. The microbiome of the nose. *Ann. Allergy, Asthma Immunol.* 2019.
104. Wos-Oxley, M.L.; Chaves-Moreno, D.; Jáuregui, R.; Oxley, A.P.A.; Kaspar, U.; Plumeier, I.; Kahl, S.; Rudack, C.; Becker, K.; Pieper, D.H. Exploring the bacterial assemblages along the human nasal passage. *Environ. Microbiol.* **2016**, doi:10.1111/1462-2920.13378.
105. Hibbing, M.E.; Fuqua, C.; Parsek, M.R.; Peterson, S.B. Bacterial competition: Surviving and thriving in the microbial jungle. *Nat. Rev. Microbiol.* 2010.
106. Khan, R.; Petersen, F.C.; Shekhar, S. Commensal bacteria: An emerging player in defense against respiratory pathogens. *Front. Immunol.* 2019.
107. Hoggard, M.; Waldvogel-Thurlow, S.; Zoing, M.; Chang, K.; Radcliff, F.J.; Mackenzie, B.W.; Biswas, K.; Douglas, R.G.; Taylor, M.W. Inflammatory endotypes and microbial associations in chronic rhinosinusitis. *Front. Immunol.* **2018**, doi:10.3389/fimmu.2018.02065.
108. Petersen, C.; Round, J.L. Defining dysbiosis and its influence on host immunity and disease. *Cell. Microbiol.* 2014.
109. Mariani, J.; Iodice, S.; Cantone, L.; Solazzo, G.; Marraccini, P.; Conforti, E.; Bulsara, P.A.; Lombardi, M.S.; Howlin, R.P.; Bollati, V.; et al. Particulate matter exposure and allergic rhinitis: The role of plasmatic extracellular vesicles and bacterial nasal microbiome. *Int. J. Environ. Res. Public Health* **2021**, doi:10.3390/ijerph182010689.
110. Van Niel, G.; D'Angelo, G.; Raposo, G. Shedding light on the cell biology of extracellular vesicles. *Nat. Rev. Mol. Cell Biol.* 2018.
111. Zha, Q. Bin; Yao, Y.F.; Ren, Z.J.; Li, X.J.; Tang, J.H. Extracellular vesicles: An overview of biogenesis, function, and role in breast cancer. *Tumor Biol.* 2017.
112. Greening, D.W.; Gopal, S.K.; Xu, R.; Simpson, R.J.; Chen, W. Exosomes and their roles in immune regulation and cancer. *Semin. Cell Dev. Biol.* 2015.
113. Han, F.; Wang, W.; Shi, M.; Zhou, H.; Yao, Y.; Li, C.; Shang, A. Outer membrane vesicles from bacteria: Role and potential value in the pathogenesis of chronic respiratory diseases. *Front. Cell. Infect. Microbiol.* **2022**, *12*, doi:10.3389/fcimb.2022.1093327.
114. Baumgarten, T.; Heipieper, H.J. Outer Membrane Vesicle Secretion: From Envelope Stress to Biofilm Formation. In *Stress and Environmental Regulation of Gene Expression and Adaptation in Bacteria*; 2016 ISBN 9781119004813.
115. MacDonald, I.A.; Kuehna, M.J. Stress-induced outer membrane vesicle production by Pseudomonas aeruginosa. *J. Bacteriol.* **2013**, doi:10.1128/JB.02267-12.
116. Toyofuku, M.; Nomura, N.; Eberl, L. Types and origins of bacterial membrane vesicles. *Nat. Rev.*

Microbiol. 2019.
117. Orench-Rivera, N.; Kuehn, M.J. Environmentally controlled bacterial vesicle-mediated export. *Cell. Microbiol.* 2016.
118. Roier, S.; Zingl, F.G.; Cakar, F.; Schild, S. Bacterial outer membrane vesicle biogenesis: A new mechanism and its implications. *Microb. Cell* 2016.
119. Kulp, A.J.; Sun, B.; Ai, T.; Manning, A.J.; Orench-Rivera, N.; Schmid, A.K.; Kuehn, M.J. Genome-wide assessment of outer membrane vesicle production in Escherichia coli. *PLoS One* **2015**, doi:10.1371/journal.pone.0139200.
120. Elhenawy, W.; Bording-Jorgensen, M.; Valguarnera, E.; Haurat, M.F.; Wine, E.; Feldman, M.F. LPS remodeling triggers formation of outer membrane vesicles in salmonella. *MBio* **2016**, doi:10.1128/mBio.00940-16.
121. Turnbull, L.; Toyofuku, M.; Hynen, A.L.; Kurosawa, M.; Pessi, G.; Petty, N.K.; Osvath, S.R.; Cárcamo-Oyarce, G.; Gloag, E.S.; Shimoni, R.; et al. Explosive cell lysis as a mechanism for the biogenesis of bacterial membrane vesicles and biofilms. *Nat. Commun.* **2016**, doi:10.1038/ncomms11220.
122. Sjöström, A.E.; Sandblad, L.; Uhlin, B.E.; Wai, S.N. Membrane vesicle-mediated release of bacterial RNA. *Sci. Rep.* **2015**, doi:10.1038/srep15329.
123. Bitto, N.J.; Chapman, R.; Pidot, S.; Costin, A.; Lo, C.; Choi, J.; D'Cruze, T.; Reynolds, E.C.; Dashper, S.G.; Turnbull, L.; et al. Bacterial membrane vesicles transport their DNA cargo into host cells. *Sci. Rep.* **2017**, doi:10.1038/s41598-017-07288-4.
124. Jan, A.T. Outer Membrane Vesicles (OMVs) of gram-negative bacteria: A perspective update. *Front. Microbiol.* **2017**, doi:10.3389/fmicb.2017.01053.
125. Tiku, V.; Tan, M.W. Host immunity and cellular responses to bacterial outer membrane vesicles. *Trends Immunol.* 2021.
126. Lapinet, J.A.; Scapini, P.; Calzetti, F.; Pérez, O.; Cassatella, M.A. Gene expression and production of tumor necrosis factor alpha, interleukin-1β (IL-1β), IL-8, macrophage inflammatory protein 1α (MIP-1α), MIP-1β, and gamma interferon-inducible protein 10 by human neutrophils stimulated with group B meningococcal outer me. *Infect. Immun.* **2000**, doi:10.1128/IAI.68.12.6917-6923.2000.
127. Lee, J.; Yoon, Y.J.; Kim, J.H.; Dinh, N.T.H.; Go, G.; Tae, S.; Park, K.S.; Park, H.T.; Lee, C.; Roh, T.Y.; et al. Outer membrane vesicles derived from Escherichia coli regulate neutrophil migration by induction of endothelial IL-8. *Front. Microbiol.* **2018**, doi:10.3389/fmicb.2018.02268.
128. Jung, A.L.; Stoiber, C.; Herkt, C.E.; Schulz, C.; Bertrams, W.; Schmeck, B. Legionella pneumophila-Derived Outer Membrane Vesicles Promote Bacterial Replication in Macrophages. *PLoS Pathog.* **2016**, doi:10.1371/journal.ppat.1005592.
129. Söderblom, T.; Oxhamre, C.; Wai, S.N.; Uhlén, P.; Aperia, A.; Uhlin, B.E.; Richter-Dahlfors, A. Effects of the Escherichia coli toxin cytolysin A on mucosal immunostimulation via epithelial CA2+ signalling and Toll-like receptor 4. *Cell. Microbiol.* **2005**, doi:10.1111/j.1462-5822.2005.00510.x.
130. Cecil, J.D.; O'Brien-Simpson, N.M.; Lenzo, J.C.; Holden, J.A.; Singleton, W.; Perez-Gonzalez, A.; Mansell, A.; Reynolds, E.C. Outer membrane vesicles prime and activate macrophage inflammasomes and cytokine secretion in vitro and in vivo. *Front. Immunol.* **2017**, doi:10.3389/fimmu.2017.01017.
131. Deo, P.; Chow, S.H.; Han, M.L.; Speir, M.; Huang, C.; Schittenhelm, R.B.; Dhital, S.; Emery, J.; Li, J.; Kile, B.T.; et al. Mitochondrial dysfunction caused by outer membrane vesicles from Gram-negative bacteria activates intrinsic apoptosis and inflammation. *Nat. Microbiol.* **2020**, doi:10.1038/s41564-020-0773-2.
132. Davis, J.M.; Carvalho, H.M.; Rasmussen, S.B.; O'Brien, A.D. Cytotoxic necrotizing factor type 1 delivered by outer membrane vesicles of uropathogenic Escherichia coli attenuates polymorphonuclear leukocyte antimicrobial activity and chemotaxis. *Infect. Immun.* **2006**, doi:10.1128/IAI.00637-06.
133. Waller, T.; Kesper, L.; Hirschfeld, J.; Dommisch, H.; Kölpin, J.; Oldenburg, J.; Uebele, J.; Hoerauf, A.; Deschner, J.; Jepsen, S.; et al. Porphyromonas gingivalis outer membrane vesicles induce selective tumor necrosis factor tolerance in a Toll-like receptor 4- and mTOR-dependent manner. *Infect. Immun.* **2016**, doi:10.1128/IAI.01390-15.

134. Verweij, F.J.; Hyenne, V.; Van Niel, G.; Goetz, J.G. Extracellular Vesicles: Catching the Light in Zebrafish. *Trends Cell Biol.* 2019.
135. Hyenne, V.; Ghoroghi, S.; Collot, M.; Bons, J.; Follain, G.; Harlepp, S.; Mary, B.; Bauer, J.; Mercier, L.; Busnelli, I.; et al. Studying the Fate of Tumor Extracellular Vesicles at High Spatiotemporal Resolution Using the Zebrafish Embryo. *Dev. Cell* **2019**, doi:10.1016/j.devcel.2019.01.014.
136. Kimmel, C.; Ballard, W.; Kimmel, S.; Ullmann, B.; Schilling, T. Stages of embryonic development of the zebrafish. *Dev. Dyn.* **1995**, *203*, 253–310, doi:10.1002/aja.1002030302.
137. Rovelli, S.; Cattaneo, A.; Binda, G.; Borghi, F.; Spinazzè, A.; Campagnolo, D.; Keller, M.; Fanti, G.; Ferrari, L.; Biggeri, A.; et al. How to obtain large amounts of location- and time-specific PM2.5 with homogeneous mass and composition? A possible approach, from particulate collection to chemical characterization. *Atmos. Pollut. Res.* **2021**, doi:10.1016/j.apr.2021.101193.
138. Cafora, M.; Forti, F.; Briani, F.; Ghisotti, D.; Pistocchi, A. Phage therapy application to counteract pseudomonas aeruginosa infection in cystic fibrosis zebrafish embryos. *J. Vis. Exp.* **2020**, doi:10.3791/61275.
139. Kwon, D.H.; Kim, G.Y.; Cha, H.J.; Kim, S.; Kim, H.S.; Hwang, H.J.; Choi, Y.H. Nargenicin a1 attenuates lipopolysaccharide-induced inflammatory and oxidative response by blocking the nf-Kb signaling pathway. *EXCLI J.* **2021**, doi:10.17179/excli2021-3506.
140. Greco, M.F.; Rizzuto, A.S.; Zarà, M.; Cafora, M.; Favero, C.; Solazzo, G.; Giusti, I.; Adorni, M.P.; Zimetti, F.; Dolo, V.; et al. PCSK9 Confers Inflammatory Properties to Extracellular Vesicles Released by Vascular Smooth Muscle Cells. *Int. J. Mol. Sci.* **2022**, *23*, 13065, doi:10.3390/ijms232113065.
141. Cafora, M.; Brix, A.; Forti, F.; Loberto, N.; Aureli, M.; Briani, F.; Pistocchi, A. Phages as immunomodulators and their promising use as anti-inflammatory agents in a cftr loss-of-function zebrafish model. *J. Cyst. Fibros.* **2020**, doi:10.1016/j.jcf.2020.11.017.
142. Ellett, F.; Lieschke, G.J. Computational quantification of fluorescent leukocyte numbers in zebrafish embryos. In *Methods in Enzymology*; 2012.
143. Livak, K.J.; Schmittgen, T.D. Analysis of relative gene expression data using real-time quantitative PCR and the 2(-Delta Delta C(T)) Method. *Methods* **2001**, *25*, 402–8, doi:10.1006/meth.2001.1262.
144. Rojas, A.M.; Shiau, C.E. Brain-localized and intravenous microinjections in the Larval Zebrafish to assess innate immune response. *Bio-protocol* **2021**, doi:10.21769/BioProtoc.3978.
145. Cafora, M.; Deflorian, G.; Forti, F.; Ferrari, L.; Binelli, G.; Briani, F.; Ghisotti, D.; Pistocchi, A. Phage therapy against Pseudomonas aeruginosa infections in a cystic fibrosis zebrafish model. *Sci. Rep.* **2019**, doi:10.1038/s41598-018-37636-x.
146. Fiordelisi, A.; Piscitelli, P.; Trimarco, B.; Coscioni, E.; Iaccarino, G.; Sorriento, D. The mechanisms of air pollution and particulate matter in cardiovascular diseases. *Heart Fail. Rev.* 2017.
147. Anderson, J.O.; Thundiyil, J.G.; Stolbach, A. Clearing the Air: A Review of the Effects of Particulate Matter Air Pollution on Human Health. *J. Med. Toxicol.* 2012.
148. EEA *Air quality in Europe — 2019 report*; 2019;
149. De Grove, K.C.; Provoost, S.; Brusselle, G.G.; Joos, G.F.; Maes, T. Insights in particulate matter-induced allergic airway inflammation: Focus on the epithelium. *Clin. Exp. Allergy* 2018.
150. Yang, X.; Zhang, Y.; Zhan, X.; Xu, X.; Li, S.; Xu, X.; Ying, S.; Chen, Z. Particulate matter exposure is highly correlated to pediatric asthma exacerbation. *Aging (Albany. NY).* **2021**, doi:10.18632/aging.203281.
151. Muñoz-Planillo, R.; Kuffa, P.; Martínez-Colón, G.; Smith, B.L.; Rajendiran, T.M.; Núñez, G. K+ Efflux Is the Common Trigger of NLRP3 Inflammasome Activation by Bacterial Toxins and Particulate Matter. *Immunity* **2013**, doi:10.1016/j.immuni.2013.05.016.
152. Pickles, R.J.; DeVincenzo, J.P. Respiratory syncytial virus (RSV) and its propensity for causing bronchiolitis. *J. Pathol.* **2015**, doi:10.1002/path.4462.
153. Vázquez, Y.; González, L.; Noguera, L.; González, P.A.; Riedel, C.A.; Bertrand, P.; Bueno, S.M. Cytokines in the respiratory airway as biomarkers of severity and prognosis for respiratory syncytial virus infection: An update. *Front. Immunol.* 2019.
154. Bigi, A.; Ghermandi, G. Trends and variability of atmospheric PM2.5 and PM10-2.5 concentration in the Po Valley, Italy. *Atmos. Chem. Phys.* **2016**, doi:10.5194/acp-16-15777-2016.

155. Longhin, E.M.; Mantecca, P.; Gualtieri, M. Fifteen years of airborne particulates in vitro toxicology in milano: Lessons and perspectives learned. *Int. J. Mol. Sci.* 2020.
156. Pietrogrande, M.C.; Demaria, G.; Colombi, C.; Cuccia, E.; Dal Santo, U. Seasonal and Spatial Variations of PM10 and PM2.5 Oxidative Potential in Five Urban and Rural Sites across Lombardia Region, Italy. *Int. J. Environ. Res. Public Health* **2022**, *19*, 7778, doi:10.3390/ijerph19137778.
157. Bekki, K.; Ito, T.; Yoshida, Y.; He, C.; Arashidani, K.; He, M.; Sun, G.; Zeng, Y.; Sone, H.; Kunugita, N.; et al. PM2.5 collected in China causes inflammatory and oxidative stress responses in macrophages through the multiple pathways. *Environ. Toxicol. Pharmacol.* **2016**, doi:10.1016/j.etap.2016.06.022.
158. Viertel, T.M.; Ritter, K.; Horz, H.-P. Viruses versus bacteria--novel approaches to phage therapy as a tool against multidrug-resistant pathogens. *J. Antimicrob. Chemother.* **2014**, *69*, 2326–2336, doi:10.1093/jac/dku173.
159. Dai, Y.L.; Jiang, Y.F.; Lu, Y.A.; Yu, J.B.; Kang, M.C.; Jeon, Y.J. Fucoxanthin-rich fraction from Sargassum fusiformis alleviates particulate matter-induced inflammation in vitro and in vivo. *Toxicol. Reports* **2021**, doi:10.1016/j.toxrep.2021.02.005.
160. Zhu, H.; Wu, Y.; Kuang, X.; Liu, H.; Guo, Z.; Qian, J.; Wang, D.; Wang, M.; Chu, H.; Gong, W.; et al. Effect of PM2.5 exposure on circulating fibrinogen and IL-6 levels: A systematic review and meta-analysis. *Chemosphere* 2021.
161. Mozzoni, P.; Iodice, S.; Persico, N.; Ferrari, L.; Pinelli, S.; Corradi, M.; Rossi, S.; Miragoli, M.; Bergamaschi, E.; Bollati, V.; et al. Maternal air pollution exposure during the first trimester of pregnancy and markers of inflammation and endothelial dysfunction. *Environ. Res.* **2022**, *212*, 113216, doi:10.1016/j.envres.2022.113216.
162. Capistrano, S.J.; Zakarya, R.; Chen, H.; Oliver, B.G. Biomass smoke exposure enhances rhinovirus-induced inflammation in primary lung fibroblasts. *Int. J. Mol. Sci.* **2016**, doi:10.3390/ijms17091403.
163. Rota, F.; Ferrari, L.; Hoxha, M.; Favero, C.; Antonioli, R.; Pergoli, L.; Greco, M.F.; Mariani, J.; Lazzari, L.; Bollati, V. Blood-derived extracellular vesicles isolated from healthy donors exposed to air pollution modulate in vitro endothelial cells behavior. *Sci. Rep.* **2020**, doi:10.1038/s41598-020-77097-9.
164. Németh, T.; Mócsai, A. Feedback Amplification of Neutrophil Function. *Trends Immunol.* 2016.
165. Kim, J.B.; Prunicki, M.; Haddad, F.; Dant, C.; Sampath, V.; Patel, R.; Smith, E.; Akdis, C.; Balmes, J.; Snyder, M.P.; et al. Cumulative lifetime burden of cardiovascular disease from early exposure to air pollution. *J. Am. Heart Assoc.* 2020.
166. Lim, H.; Kwon, H.J.; Lim, J.A.; Choi, J.H.; Ha, M.; Hwang, S.S.; Choi, W.J. Short-term effect of fine particulate matter on children's hospital admissions and emergency department visits for asthma: A systematic review and meta-analysis. *J. Prev. Med. Public Heal.* 2016.
167. Milani, G.P.; Cafora, M.; Favero, C.; Luganini, A.; Carugno, M.; Lenzi, E.; Pistocchi, A.; Pinatel, E.; Pariota, L.; Ferrari, L.; et al. PM2 .5, PM10 and bronchiolitis severity: A cohort study. *Pediatr. Allergy Immunol.* **2022**, *33*, doi:10.1111/pai.13853.
168. Silva, M.T. When two is better than one: macrophages and neutrophils work in concert in innate immunity as complementary and cooperative partners of a myeloid phagocyte system. *J. Leukoc. Biol.* **2010**, doi:10.1189/jlb.0809549.
169. Benard, E.L.; van der Sar, A.M.; Ellett, F.; Lieschke, G.J.; Spaink, H.P.; Meijer, A.H. Infection of zebrafish embryos with intracellular bacterial pathogens. *J. Vis. Exp.* **2012**, doi:10.3791/3781.
170. Nguyen-Chi, M.; Phan, Q.T.; Gonzalez, C.; Dubremetz, J.F.; Levraud, J.P.; Lutfalla, G. Transient infection of the zebrafish notochord with E. coli induces chronic inflammation. *DMM Dis. Model. Mech.* **2014**, doi:10.1242/dmm.014498.
171. Sheshachalam, A.; Srivastava, N.; Mitchell, T.; Lacy, P.; Eitzen, G. Granule protein processing and regulated secretion in neutrophils. *Front. Immunol.* 2014.
172. Segal, A.W. How neutrophils kill microbes. *Annu. Rev. Immunol.* 2005.
173. Wellenius, G.A.; Boyle, L.D.; Wilker, E.H.; Sorond, F.A.; Coull, B.A.; Koutrakis, P.; Mittleman, M.A.; Lipsitz, L.A. Ambient fine particulate matter alters cerebral hemodynamics in the elderly. *Stroke* **2013**, doi:10.1161/STROKEAHA.111.000395.
174. Neophytou, A.M.; Hart, J.E.; Cavallari, J.M.; Smith, T.J.; Dockery, D.W.; Coull, B.A.; Garshick, E.;

Laden, F. Traffic-related exposures and biomarkers of systemic inflammation, endothelial activation and oxidative stress: A panel study in the US trucking industry. *Environ. Heal. A Glob. Access Sci. Source* **2013**, doi:10.1186/1476-069X-12-105.
175. Milani, G.P.; Plebani, A.M.; Arturi, E.; Brusa, D.; Esposito, S.; Dell'Era, L.; Laicini, E.A.; Consonni, D.; Agostoni, C.; Fossali, E.F. Using a high-flow nasal cannula provided superior results to low-flow oxygen delivery in moderate to severe bronchiolitis. *Acta Paediatr. Int. J. Paediatr.* **2016**, doi:10.1111/apa.13444.
176. Milani, G.P.; Rocchi, A.; Teatini, T.; Bianchetti, M.G.; Amelio, G.; Mirra, N.; Grava, A.; Agostoni, C.; Fossali, E.F. Hyponatremia in infants with new onset moderate-severe bronchiolitis: A cross-sectional study. *Respir. Med.* **2017**, doi:10.1016/j.rmed.2017.10.028.
177. Mazzoni, M.B.; Milani, G.P.; Bernardi, S.; Odone, L.; Rocchi, A.; D'Angelo, E.A.; Alberzoni, M.; Agostoni, C.; Bianchetti, M.G.; Fossali, E.F. Hyponatremia in infants with communityacquired infections on hospital admission. *PLoS One* **2019**, doi:10.1371/journal.pone.0219299.
178. Masella, A.P.; Bartram, A.K.; Truszkowski, J.M.; Brown, D.G.; Neufeld, J.D. PANDAseq: Paired-end assembler for illumina sequences. *BMC Bioinformatics* **2012**, doi:10.1186/1471-2105-13-31.
179. Caporaso, J.G.; Fierer, N.; Peña, A.G.; Goodrich, J.K.; Gordon, J.I.; Huttley, G.A.; Kelley, S.T.; Knights, D.; McDonald, D.; Muegge, B.D.; et al. QIIME allows analysis of high-throughput community sequencing data. *Nat. Methods* **2010**.
180. Wang, Q.; Garrity, G.M.; Tiedje, J.M.; Cole, J.R. Naïve Bayesian classifier for rapid assignment of rRNA sequences into the new bacterial taxonomy. *Appl. Environ. Microbiol.* **2007**, doi:10.1128/AEM.00062-07.
181. Lozupone, C.; Lladser, M.E.; Knights, D.; Stombaugh, J.; Knight, R. UniFrac: An effective distance metric for microbial community comparison. *ISME J.* 2011.
182. Altschul, S.F.; Gish, W.; Miller, W.; Myers, E.W.; Lipman, D.J. Basic local alignment search tool. *J. Mol. Biol.* **1990**, doi:10.1016/S0022-2836(05)80360-2.
183. Jo, E.J.; Lee, W.S.; Jo, H.Y.; Kim, C.H.; Eom, J.S.; Mok, J.H.; Kim, M.H.; Lee, K.; Kim, K.U.; Lee, M.K.; et al. Effects of particulate matter on respiratory disease and the impact of meteorological factors in Busan, Korea. *Respir. Med.* **2017**, doi:10.1016/j.rmed.2017.02.010.
184. Setti, L.; Passarini, F.; De Gennaro, G.; Barbieri, P.; Licen, S.; Perrone, M.G.; Piazzalunga, A.; Borelli, M.; Palmisani, J.; DI Gilio, A.; et al. Potential role of particulate matter in the spreading of COVID-19 in Northern Italy: First observational study based on initial epidemic diffusion. *BMJ Open* **2020**, doi:10.1136/bmjopen-2020-039338.
185. Feng, C.; Li, J.; Sun, W.; Zhang, Y.; Wang, Q. Impact of ambient fine particulate matter (PM2.5) exposure on the risk of influenza-like-illness: A time-series analysis in Beijing, China. *Environ. Heal. A Glob. Access Sci. Source* **2016**, doi:10.1186/s12940-016-0115-2.
186. Eiland, L.S. Respiratory Syncytial Virus: Diagnosis, Treatment and Prevention. *J. Pediatr. Pharmacol. Ther.* **2009**, doi:10.5863/1551-6776-14.2.75.
187. Pichon, M.; Lina, B.; Josset, L. Impact of the respiratory microbiome on host responses to respiratory viral infection. *Vaccines* 2017.
188. Lynch, J.P.; Sikder, M.A.A.; Curren, B.F.; Werder, R.B.; Simpson, J.; Cuív, P.; Dennis, P.G.; Everard, M.L.; Phipps, S. The influence of the microbiome on early-life severe viral lower respiratory infections and asthma-Food for thought? *Front. Immunol.* 2017.
189. Cho, I.; Blaser, M.J. The human microbiome: At the interface of health and disease. *Nat. Rev. Genet.* 2012.
190. Heinrich, A.; Haarmann, H.; Zahradnik, S.; Frenzel, K.; Schreiber, F.; Klassert, T.E.; Heyl, K.A.; Endres, A.S.; Schmidtke, M.; Hofmann, J.; et al. Moraxella catarrhalis decreases antiviral innate immune responses by down-regulation of TLR3 via inhibition of p53 in human bronchial epithelial cells. *FASEB J.* **2016**, doi:10.1096/fj.201500172R.
191. Teo, S.M.; Mok, D.; Pham, K.; Kusel, M.; Serralha, M.; Troy, N.; Holt, B.J.; Hales, B.J.; Walker, M.L.; Hollams, E.; et al. The infant nasopharyngeal microbiome impacts severity of lower respiratory infection and risk of asthma development. *Cell Host Microbe* **2015**, doi:10.1016/j.chom.2015.03.008.
192. Schaar, V.; De Vries, S.P.W.; Perez Vidakovics, M.L.A.; Bootsma, H.J.; Larsson, L.; Hermans, P.W.M.;

Bjartell, A.; Mörgelin, M.; Riesbeck, K. Multicomponent Moraxella catarrhalis outer membrane vesicles induce an inflammatory response and are internalized by human epithelial cells. *Cell. Microbiol.* **2011**, doi:10.1111/j.1462-5822.2010.01546.x.

193. Ederveen, T.H.A.; Ferwerda, G.; Ahout, I.M.; Vissers, M.; de Groot, R.; Boekhorst, J.; Timmerman, H.M.; Huynen, M.A.; van Hijum, S.A.F.T.; de Jonge, M.I. Haemophilus is overrepresented in the nasopharynx of infants hospitalized with RSV infection and associated with increased viral load and enhanced mucosal CXCL8 responses. *Microbiome* **2018**, doi:10.1186/s40168-017-0395-y.
194. Biesbroek, G.; Tsivtsivadze, E.; Sanders, E.A.M.; Montijn, R.; Veenhoven, R.H.; Keijser, B.J.F.; Bogaert, D. Early respiratory microbiota composition determines bacterial succession patterns and respiratory health in children. *Am. J. Respir. Crit. Care Med.* **2014**, doi:10.1164/rccm.201407-1240OC.
195. Kloepfer, K.M.; Lee, W.M.; Pappas, T.E.; Kang, T.J.; Vrtis, R.F.; Evans, M.D.; Gangnon, R.E.; Bochkov, Y.A.; Jackson, D.J.; Lemanske, R.F.; et al. Detection of pathogenic bacteria during rhinovirus infection is associated with increased respiratory symptoms and asthma exacerbations. *J. Allergy Clin. Immunol.* **2014**, doi:10.1016/j.jaci.2014.02.030.
196. Oh, J.; Conlan, S.; Polley, E.C.; Segre, J.A.; Kong, H.H. Shifts in human skin and nares microbiota of healthy children and adults. *Genome Med.* **2012**, doi:10.1186/gm378.
197. Erb-Downward, J.R.; Thompson, D.L.; Han, M.K.; Freeman, C.M.; McCloskey, L.; Schmidt, L.A.; Young, V.B.; Toews, G.B.; Curtis, J.L.; Sundaram, B.; et al. Analysis of the lung microbiome in the "healthy" smoker and in COPD. *PLoS One* **2011**, doi:10.1371/journal.pone.0016384.
198. Biswas, K.; Hoggard, M.; Jain, R.; Taylor, M.W.; Douglas, R.G. The nasal microbiota in health and disease: Variation within and between subjects. *Front. Microbiol.* **2015**, doi:10.3389/fmicb.2015.00134.
199. Brugger, S.D.; Eslami, S.M.; Pettigrew, M.M.; Escapa, I.F.; Henke, M.T.; Kong, Y.; Lemon, K.P. Dolosigranulum pigrum Cooperation and Competition in Human Nasal Microbiota. *mSphere* **2020**, doi:10.1128/msphere.00852-20.
200. Sonawane, A.R.; Tian, L.; Chu, C.Y.; Qiu, X.; Wang, L.; Holden-Wiltse, J.; Grier, A.; Gill, S.R.; Caserta, M.T.; Falsey, A.R.; et al. Microbiome-Transcriptome Interactions Related to Severity of Respiratory Syncytial Virus Infection. *Sci. Rep.* **2019**, doi:10.1038/s41598-019-50217-w.
201. Cafora, M.; Hoxha, M.; Cantone, L.; Bollati, V.; Pistocchi, A.; Ferrari, L. Assessment of innate immune response activation following the injection of extracellular vesicles isolated from human cell cultures in zebrafish embryos. In *Methods in Enzymology*; 2020 ISBN 9780128206621.
202. Thery, C.; Lavieu, G.; Martin-Jaular, L.; Mathieu, M.; Tkach, M.; Zivkovic, A.M.; Zocco, D. Minimal information for studies of extracellular vesicles 2018 (MISEV2018): a position statement of the International Society for Extracellular Vesicles and update of the MISEV2014 guidelines. *J. Extracell. vesicles* **2018**.
203. Cantone L, H.M. and B. V Characterization of microvesicles using the MACSQuant Analyzer.
204. Mathew, L.K.; Sengupta, S.; Kawakami, A.; Andreasen, E.A.; Löhr, C. V.; Loynes, C.A.; Renshaw, S.A.; Peterson, R.T.; Tanguay, R.L. Unraveling tissue regeneration pathways using chemical genetics. *J. Biol. Chem.* **2007**, doi:10.1074/jbc.M706640200.
205. Zhang, Y.; Bai, X.-T.; Zhu, K.-Y.; Jin, Y.; Deng, M.; Le, H.-Y.; Fu, Y.-F.; Chen, Y.; Zhu, J.; Look, A.T.; et al. In Vivo Interstitial Migration of Primitive Macrophages Mediated by JNK-Matrix Metalloproteinase 13 Signaling in Response to Acute Injury. *J. Immunol.* **2008**, doi:10.4049/jimmunol.181.3.2155.
206. Ferrari, L.; Cafora, M.; Rota, F.; Hoxha, M.; Iodice, S.; Tarantini, L.; Dolci, M.; Delbue, S.; Pistocchi, A.; Bollati, V. Extracellular vesicles released by colorectal cancer cell lines modulate innate immune response in zebrafish model: The possible role of human endogenous retroviruses. *Int. J. Mol. Sci.* **2019**, doi:10.3390/ijms20153669.
207. Macchi, C.; Ferri, N.; Sirtori, C.R.; Corsini, A.; Banach, M.; Ruscica, M. Proprotein Convertase Subtilisin/Kexin Type 9. *Am. J. Pathol.* **2021**, doi:10.1016/j.ajpath.2021.04.016.
208. Raimondo, S.; Naselli, F.; Fontana, S.; Monteleone, F.; Lo Dico, A.; Saieva, L.; Zito, G.; Flugy, A.; Manno, M.; Di Bella, M.A.; et al. Citrus limon-derived nanovesicles inhibit cancer cell proliferation and suppress CML xenograft growth by inducing TRAIL-mediated cell death. *Oncotarget* **2015**,

doi:10.18632/oncotarget.4004.
209. Agrawal, A.; Murphy, T.F. Haemophilus influenzae infections in the H. influenzae type b conjugate vaccine era. *J. Clin. Microbiol.* 2011.
210. Klimentová, J.; Stulík, J. Methods of isolation and purification of outer membrane vesicles from gram-negative bacteria. *Microbiol. Res.* 2015.